UCRL 9598

UNIVERSITY OF CALIFORNIA

Ernest O. Lawrence Radiation Laboratory

CONTROLLED THERMONUCLEAR RESEARCH QUARTERLY REPORT

December 1960 through February 1961

LIVERMORE AND
BERKELEY, CALIFORNIA

DISCLAIMER

This document was prepared as an account of work sponsored by the United States Government. While this document is believed to contain correct information, neither the United States Government nor any agency thereof, nor the Regents of the University of California, nor any of their employees, makes any warranty, express or implied, or assumes any legal responsibility for the accuracy, completeness, or usefulness of any information, apparatus, product, or process disclosed, or represents that its use would not infringe privately owned rights. Reference herein to any specific commercial product, process, or service by its trade name, trademark, manufacturer, or otherwise, does not necessarily constitute or imply its endorsement, recommendation, or favoring by the United States Government or any agency thereof, or the Regents of the University of California. The views and opinions of authors expressed herein do not necessarily state or reflect those of the United States Government or any agency thereof or the Regents of the University of California.

Research and Development

UCRL-9598
UC-20 Controlled Thermonuclear Processes
TID-4500(16th Ed.)

UNIVERSITY OF CALIFORNIA
Lawrence Radiation Laboratory
Berkeley and Livermore, California

Contract No. W-7405-eng-48

CONTROLLED THERMONUCLEAR RESEARCH QUARTERLY REPORT

December 1960 through February 1961

March 15, 1961

Printed in USA. Price $2.00. Available from the
Office of Technical Services
U. S. Department of Commerce
Washington 25, D.C.

CONTROLLED THERMONUCLEAR RESEARCH QUARTERLY REPORT

December 1960 through February 1961

Contents

I. PYROTRON (MAGNETIC MIRROR PROGRAM)

1. Introduction and Summary (Post) 7
2. High-Compression Experiments (Coensgen) 8
3. Effect of Metallic Coating on Confinement of Plasma in Table Top (Perkins) 9
4. Table Top Diagnostics. I. (Ellis and Carlson) 14
5. Table Top Diagnostics. II. (Passell) 15
6. Table Top Diagnostics. III. (Mattingly) 17
7. Theoretical Considerations (ALICE) (Futch, Heckrotte, Killeen, and Damm) 17
8. ALICE Diagnostics (Foote and Damm) 19
9. Beam Neutralization (Damm and Futch) 19
10. Vacuum and Surface Studies (Hunt, Damm, and Popp) . . . 20
11. Grid Source Development (Gordon) 23
12. P-4 (Steady-State Plasma) System (Barr, Gardner, Hall and Oleson) 24

II. ASTRON PROGRAM

1. Introduction (Christofilos) 26
2. Astron Gas Target Electric-Conductivity Measurement (Reagan) 26

III. LIVERMORE PINCH PROGRAM (Birdsall, Colgate, Furth, Halliday, Hartman, and Spoerlein)

1. Summary 31
2. Electron-Beam Pinch 31
3. Levitron Diagnostic Spectroscope 33
4. Levitron 33
5. Conical Pinch Accelerator 35
6. Collisionless Plasma Shock (Experimental) 35

---

*Preceding Quarterly Reports: UCRL-9500, UCRL-9393.

7. Collisionless Plasma Shock (Theoretical) 35
8. High-Field Research 37
9. Instability Theory 37
10. Supernova Calculations 40
11. Space-Charge Waves and Plasma Diagnostics (Trivelpiece) . 40

IV. BERKELEY PLASMA RESEARCH

1. Sheet Pinch Studies (Anderson) 42
2. Homopolar Program (Halbach, Paxson, and Veron) 44
3. Hydromagnetic Wave and Cyclotron Heating (Cooper, DeSilva, and Wilcox) 48
4. Some Effects of Finite Conductivity in Hothouse I (Northrop) 51
5. Plasma Physics and Microwave Diagnostics (Hopkins, Paulikas, Pyle, Rugge, and Stearns) 57
6. Prebreakdown Crossed-Field Study (Bernstein and Kunkel) . 59

V. THEORETICAL AND BASIC EXPERIMENTAL PLASMA PHYSICS

1. A Computation for Studying the Formation of the Astron E Layer (Killeen) 62
2. Stability of Infinitely Thin Electron Layers (Neil) 62
3. Instability of a Resistive Sheet Pinch (Furth and Killeen) . . 63
4. Scattering Losses from Magnetic Mirror Machines (BenDaniel) 63
5. The Magnetic Compression of a Partially Ionized Gas (Geesaman and Killeen) 64
6. Rearrangement Collisions (Mittleman) 64
7. Calculation of the Diffusion of the Vacuum Magnetic Field of an Electron Beam into a Plasma (Heckrotte, Hester, and Hiskes) 65
8. Theory of an Electrostatic Probe in a Plasma (Hall and Geesaman) 67
9. Magnetic Shocks (Zwick) 68
10. Beam Loading of a Radio-Frequency Cavity (Neil) 70
11. Electric Dissociation Calculations (Hiskes) 70
12. Adiabatic Motion Near the Center of a Magnetic Mirror (Hetherington and Woods) 71
13. Containment of Positrons in the Cusp Geometry (Gibson, Jordan, and Lauer) 71
14. Atomic and Molecular Beam Research (Baker, Brink, Chambers, and McFarland) 74

VI. ENGINEERING AND TECHNOLOGICAL DEVELOPMENT

1. Ultrahigh-Vacuum Development (Milleron and Levenson) 76

2. Mechanical Engineering Development (Batzer) 78

3. Electrical Engineering Development (Smith) 84

VII. TALKS AND PUBLICATIONS 97

CONTROLLED THERMONUCLEAR RESEARCH QUARTERLY REPORT*

December 1960 through February 1961

Lawrence Radiation Laboratory
University of California
Berkeley and Livermore, California

March 15, 1961

I. PYROTRON (MAGNETIC MIRROR) PROGRAM

1. INTRODUCTION AND SUMMARY

Richard F. Post

Almost the entire quarter was devoted to preparations for new phases of operation in the three major experiments (Toy Top III, Table Top and ALICE).

Major construction was completed and first attempts were made at operating Toy Top III with three stages. Neutrons could again be produced in the second stage, but plasma transfer to the third stage has not yet been accomplished.

The Table Top facility is being rebuilt (Table Top III) with two major objectives in mind: (a) Extension of measurable confinement times to 1 second, and (b) Achievement of ion temperatures much higher than the electron temperature. Objective (a) is to be accomplished by increasing the L/R time constant of the coil system, through redesign and, eventually, through refrigeration to liquid nitrogen temperatures. Objective (b) is to be accomplished by replacing the plasma injector system with one similar to that used in Toy Top III. In the new Table Top, it should be possible to observe the confined plasma for periods of several collision-relaxation times (if it remains stable).

In the developments preparatory to the ALICE (high-energy neutral injection) experiment, a well-collimated intense beam (320 ma) of 20-kev protons was produced. Neutralization experiments are now under way to determine what fraction of this beam can be converted into neutrals for injection into the ALICE chamber. Encouraging preliminary performance of the differential and evaporative pumping chambers which act to isolate the main ALICE chamber from the neutralizer and ion source was obtained. Under static conditions, a pressure of 2×10^{-10} mm Hg was achieved in the last of the three chambers (the one which "mocked up" the ALICE chamber). Under dynamic conditions it will be required that the pressure at this point remain below about 1 to 2×10^{-9} mm Hg.

*This work done under the auspices of the U. S. Atomic Energy Commission.

A significant piece of experimental work accomplished during the quarter was the partial elucidation of the effect of a metallic coating on plasma containment in Table Top. A correlation was established between the densities of the trapped and compressed plasma and the presence or absence of a metallic coating on the inner surface of the vacuum chamber. The correlation was established by examining the behavior of the velocity-space instability[1] that can be induced in the Table Top plasma, as a function of the total amount of injected plasma. The evidence indicates that the absence of a metallic coating reduces, but does not destroy, the effectiveness of initial trapping of plasma. This does not, however, constitute proof of a hydromagnetically "stabilizing" effect of such a coating,[2] as other effects, such as asymmetric electrostatic fields which are possible without the coating, could produce the same result.

With respect to our perennial paradox, "Why is the 'flute' hydromagnetic instability not observed in our experiments?", the following remarks can be made. The hypothesis that the hydromagnetic stability of the plasma in our experiments arises from "tying" the field lines in metallic conductors does not entirely jibe with the totality of our present evidence. It seems likely that the explanation must be sought in other directions. It is the author's opinion that the explanation may possibly be found in the interplay between particle drift motions (which tend to destroy flutes) and the nature of the sea of statistical fluctuations from which the flutes must grow. In systems of high symmetry, such as the ones we use, it appears from preliminary theoretical calculations that the Fourier amplitudes of the potentially unstable modes of the plasma system are of "measure zero" with respect to the normal fluctuations. In our experimental situations, where the field-gradient-induced drift motions impose on any azimuthally varying perturbation an inherent decay time (a time not much longer than the time constant of the instabilities themselves), flute instabilities might never be initiated. This conjecture, as well as others that have been made to explain the absence of flute instability, can presumably be subjected to experimental test.

2. HIGH-COMPRESSION EXPERIMENTS

Frederic H. Coensgen

The period from December 1, 1960 to February 28, 1961 has been largely devoted to construction and preliminary operation of the complete three-stage Toy Top III. At this time, all the major construction has been completed; however, minor changes are continually being made as weak points appear and as improved components (vaccum switches, for example) become available.

During the check-out runs, it was possible to re-establish the conditions of last October. It was found that the neutron production from the first two stages is essentially the same as reported earlier. However, it has been

[1] R. F. Post and W. A. Perkins, Phys. Rev. Letters 6, 85 (1961).

[2] R. F. Post, R. E. Ellis, F. C. Ford, and M. N. Rosenbluth, Phys. Rev. Letters 4, 166 (1960).

impossible to transfer plasma to the ion analyzer or to a probe beyond the 4-in. vacuum section. The probe data indicate that no plasma is transferred into the 4-in. section. In three-stage operation there was no detectable neutron production in the 4-in. chamber although the production rate in the 9-in. section remained unchanged. From the data we have at this time there appears to be an alignment problem. Probes that can be inserted through the 4-in. section into the 9-in. section are being constructed. With these probes it should be possible to trace the plasma motion and determine those factors which influence this motion.

3. EFFECT OF METALLIC COATING ON CONFINEMENT OF PLASMA IN TABLE TOP

Walton A. Perkins

Some effects on plasma confinement of the presence or absence of thin stainless steel coating on the inner walls of the glass vacuum system of Table Top have been investigated. Escaping plasma electrons are monitored by scintillators protruding radially and axially into the vacuum chamber and an x-ray detector. When there is no metallic coating on the gas vacuum chamber a velocity-space plasma instability[1] can be induced under certain conditions of density and compression ratio. With a metallic coating the instability is greatly reduced, as can be seen from Fig. 1. The radial-probe signal is an indication of the enhanced transport of particles across the field lines, and therefore signals the presence of the instability. As can be seen from the top radial-probe traces, the initial flux of plasma across the confining field is markedly reduced by the metallic coating. Furthermore, it occurs only during the compression period of 0.5 msec. The lower set of radial-probe traces shows that the slow component occurs much later in the presence of the metallic coating.

In these experiments the x-ray detector is apparently recording both the x rays caused by electrons striking the radial scintillation probe and the bremsstrahlung from the plasma. With the metallic coating the electron flux striking the radial probe is greatly reduced so that the initial spike disappears from the x-ray detector signal, leaving only the signal from the plasma bremsstrahlung. The signal from the 12.5-cm-diameter end-probe scintillator, which intercepts all the end flux, exhibits the least change, showing with coating an increase by a factor of about 2, but no significant change in its time behavior.

The variation with radius of the end energy flux was measured with a 0.3-cm-diam plastic scintillator. The pulse heights at 0.5 msec for the uncoated and coated systems are shown in Fig. 2. This indicated that a higher initial density was obtained with the metallic-coated system. The higher initial density meant that collisions could smooth out the anisotropic velocity distribution and thereby inhibit the instability. This, we believe, is the key to the effects observed.

---

[1] R. F. Post and W. A. Perkins, Phys. Rev. Letters, 6, 85 (1961).

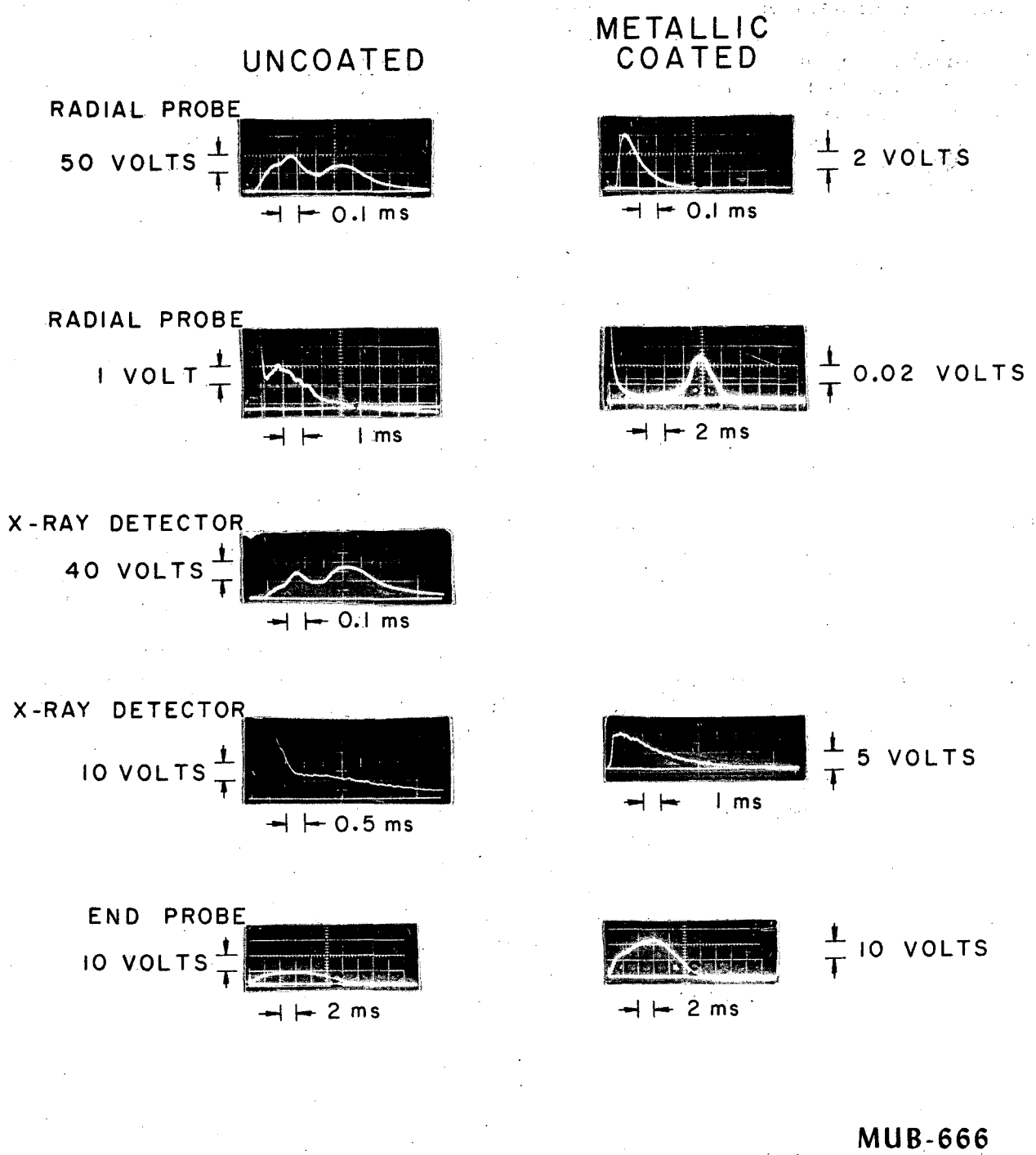

Fig. 1. Signals from radial probe, x-ray detector, and end probe for an uncoated and a metallic-coated chamber.

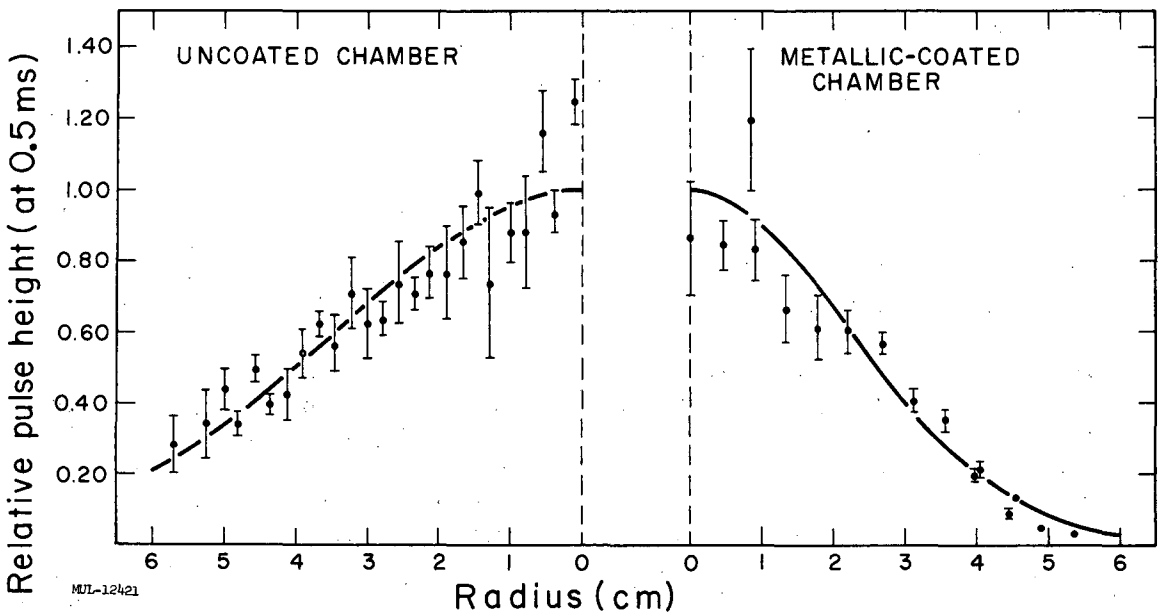

MU-23476

Fig. 2. End-escaping flux as a function of radius for an initial magnetic field of 0.0 gauss for uncoated and metallic-coated chamber. The curve is a Gaussian fit to the experimental points.

Indeed when the amount of injected plasma was decreased the radial-probe signal increased in magnitude and returned to a time behavior characteristic of no metallic coating. The radially escaping energy flux as a function of relative injected plasma density is shown in Fig. 3. The plasma is stable at very low density because its β is below the critical β. At very high density, collisions decrease the anisotropic velocity distribution and thereby the instability. With the coating, the plasma density after compression is higher for the same injected-plasma density, so that the instability (which requires an intermediate compressed-plasma density) occurs at a lower injected-plasma density.

The question now arises: Why is the initial plasma density (after compression) lower with an uncoated system than with a metallic-coated system?

It has been suggested[2] that a metallic coating would tie down the field lines in a mirror machine and thereby inhibit the flute instability. Here the flute instability could lower the initial density for the uncoated system, for which the field lines are presumably not tied.

Another possible explanation is that plasma strikes the insulated walls (uncoated system) during injection and an asymmetric charge distribution builds up, causing an asymmetric electric field. Such an electric field could cause a radial transport which would lower the trapped density. With a metallic conductor on the walls no large asymmetric charge distributions can build up. Furthermore, with a metallic coating, the induced electric field distribution associated with the compression field is forced to be axially symmetric, having only a uniform E_θ component at the walls. This means that the initial motion of the injected plasma caused by the compression must also be axially symmetric. Initial axial symmetry may be important for plasma stability during compression.

New Table Top

The Table Top mirror machine is being rebuilt. In the past a plasma was produced that was characterized by high electron temperature (approx 25 kev) and low ion temperature (less than 1 kev). Extensive measurements of the electron component were made to determine the plasma temperature, density, stability, and confinement region. Table Top is being rebuilt so that similar studies can be made with a hot-ion plasma (approx 2 kev) and cold-electron plasma (approx 0.2 kev). Particular emphasis will be placed on stability and confinement studies. Attempts to observe the growth of ambipolar potentials will be made.

By using knowledge gained in other sections of the mirror machine group (Toy Top and ALICE), we hope to build an effective trapping field and improve the vacuum by a factor of 10^3.

A complete description of the new Table Top machine will be given in the next quarterly report.

---

[2] R. F. Post, R. E. Ellis, F. C. Ford, and M. N. Rosenbluth, Phys. Rev. Letters 4, 166 (1960).

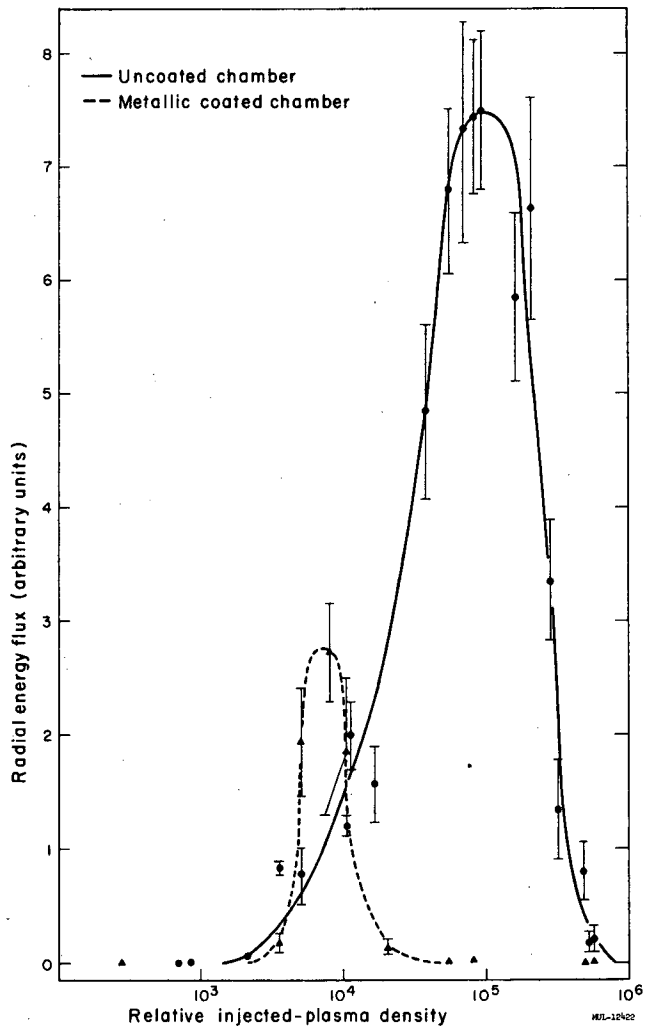

MU-23477

Fig. 3. Radially escaping energy flux as a function of relative injected-plasma density for an uncoated and a metallic-coated chamber.

4. TABLE TOP DIAGNOSTICS. I

Robert E. Ellis and Norris W. Carlson

Scintillator Probe Calibration

The scintillation efficiency of an aluminum-coated plastic fluor was tested further, to determine whether deviations from the curve of oscilloscope signal per unit current versus electron residual energy, as shown in the preceding quarterly report,[1] would occur at beam currents considerably higher than reported there. With a beam of 0.4 μa of electrons (as compared to the highest beam current--0.04 μa--used previously), an essentially linear relation of signal per unit current to residual beam energy was obtained, as before. This curve was displaced somewhat to higher energies, however. Upon rerunning the 0.04-μa data, we found a similar displacement from previous results. Our conclusion was that the probe fluor surface had been subjected to some contaminant (assumed to be diffusion pump oil vapor). Similar deterioration of signal has been observed before, apparently not primarily associated with the large number of pulses received by the fluor in the testing process, but rather with formation of a contaminant layer deposited over a considerable period of time. Several thousand pulses at a continuous rate of one pulse per second do not produce a deterioration in signal, whereas a similar number of pulses spread out over several weeks or months may cause a reduction of as much as 50% in the probe signal for given beam current and energy conditions. It appears, therefore, that the scintillator probes of the type described in several previous reports may be relied upon to give repeatable results, with the proviso that during a program of several thousand pulses of approx 1 msec duration, or equivalent beam exposure in an oil-vapor-pumped vacuum system, recalibration at appropriate intervals and fluor replacement be undertaken.

A test of the 21-channel scintillator probe[1] with the electron beam indicates that it performs very satisfactorily in signal output. In the present design, no change is required except that the small lucite light pipes (approx 1/8 in. in diameter and 4 in. long) that connect the flexible glass fiber light pipes to the plastic fluors should be light-insulated from each other to a higher degree. Most desirably, the lucite rods should be aluminum-vapor-plated after being properly shaped. Cross talk between channels was observed to vary from a small fraction of 1% to as high as about 1% when the beam was directed on one channel and the signal observed in another. Obviously, rather large values of cross talk would be obtained in the present case if all channels were simultaneously irradiated. There is no evident reason why sufficient elimination of cross talk is not possible with the present probe, or complete avoidance of this problem by rebuilding and vapor plating as mentioned above.

Accel-Decel Electrostatic Particle Energy Analyzer

Because of difficulties in producing and maintaining (against breakage and corrosion) the rather delicate four-pronged orthogonal-field probe

[1] R. E. Ellis and Norris W. Carlson, in Controlled Thermonuclear Research Quarterly Report, UCRL-9500, Dec. 1960, p. 9.

required for the electrolytic tank tests of the analyzer electrode model, such tests have not yet been completed. A probe has been produced recently in our shops, but further tests on the model have been interrupted by higher-priority work at the analog computer facility.

An electron gun, with necessary controls for pulsed beam operation, has now been completed and installed on the analyzer for the purpose of testing the operation of the analyzer, as well as calibration for electron detection. A deuterium gas ion source of the type used on the Cockcroft-Walton accelerator has also been obtained for a similar calibration for ions. It has not yet been installed.

A modification of plastic fluor and light piper, mounted in the rear (accelerating) electrode, has resulted in improved signal-to-noise ratio for ion detection, as determined by analyzing the ions from a titanium deuteride spark source. It is hoped that further advantage may be obtained by extending this modification. The difficulty arises from having to stand off 100 kev across the light piper. Thus far it has been necessary to make a small gap in the lucite light pipe, and to vapor plate an aluminum grid on the surface exposed to high voltage, so as to prevent high field gradients across the lucite. The uncoated section of lucite is then "hidden" from the voltage in a metal exit tube. The idea is to increase the solid angle for light collection for the fluor signal while not changing the amount of light entering the collector from the spark-source plasma generator.

5. TABLE TOP DIAGNOSTICS. II

Thomas O. Passell*

The Table Top mirror machine is being rebuilt. Hence, this quarter was devoted primarily to planning experiments for the rebuilt machine. The new system differs from the previous device in two primary ways.

(a) The time scale of the magnetic compression fields is now 8 msec to peak field, with a 1/e decay time of 200 msec compared with 0.5 msec and 9 msec previously.

(b) System base vacuum has been changed from the 10^{-6} mm Hg range to the 10^{-9} mm Hg range.

The extension in time allows the use of mechanical shutters to resolve the time behavior of system parameters. It appears that the integrating calorimeters used successfully on the previous system can give the time behavior of escaping plasma energy when used in conjunction with a mechanical shutter on the rebuilt system. Hence, three possible shutters have been developed to varying stages of performance:

(a) A simple 4:1 lever with a paddle (containing a 2.5-cm-diam hole) on the long end and activated at the short end by an air cylinder with a 2-cm stroke.

---

*Stanford Research Institute, Menlo Park, California.

(b) A leaf shutter taken from a Fairchild aerial reconnaissance camera, rebuilt with nonmagnetic and vacuum-worthy materials--giving an 8.9-cm shutter opening.

(c) A window-shade shutter identical in principle with that on a Graflex camera, having a rectangular aperture 6 × 8 cm.

The lever-arm shutter has been mocked up and operated to observe its reproducibility. After the "on" switch is pressed, an initial delay of 25 ± 2 msec is followed by a 5-msec open time. The 2-cm motion will be transmitted into the vacuum system via a bellows seal.

The leaf shutter now has a teflon body replacing its original brass casting. If the teflon survives a vacuum-worthiness test, the moving-leaves mechanism will be rebuilt of thin stainless steel sheet.

A window-shade-type shutter from a standard Graflex camera has been obtained for possible copying with vacuum-worthy materials.

A flange ring, to be sandwiched between the main-mirror-region vacuum chamber and the burial chamber pump in the rebuilt Table Top, has been fabricated to accommodate any one of the above shutters, plus as many as four separate diagnostic outputs.

Calorimetry in connection with the mechanical shutter is expected to give

(a) The containment time of plasma as a function of parameters that should influence stability and hence containment time.

(b) The spatial distribution of plasma energy as a function of radius.

(c) The approximate value of β achieved during compression.

Another aspect of the longer time scale will be the possibility of full development of ambipolar potentials.[1] As with the previous system, the present plan is to observe the transmission as a function of kinetic energy of a pulsed beam of positive ions (Li^+) aimed along the longitudinal axis. Some of the operation problems will be ironed out by the initial use of an electron beam.

Development of the lithium ion gun was somewhat retarded by the recent announcement[2] that platinum reacts chemically (with some violence) with lithium. Hence, the use of platinum-base alloys as the porous effuser-ionizer elements in the lithium ion gun no longer appears so promising. It may be that the lower current densities and shorter operating life of the bare β^- eucryptite lithium mineral may have to be tolerated.

---

[1] R. F. Post, in Controlled Thermonuclear Research Quarterly Report, UCRL-9393, Sept. 1960, p. 23.

[2] Chemical and Engineering News, January 30, 1961, p. 42.

6. TABLE TOP DIAGNOSTICS. III

James T. Mattingly

Rejuvenation of Electron Multipliers

A vacuum system in which all possible sources of contamination are avoided has been assembled, embodying a 70-liter Vac Sorb fore pump and a 5-liter VacIon high-vacuum pump. This very clean system will be the environment for testing electron multipliers supplied by the manufacturer (RCA). Those electron multipliers having a high gain ($> 10^6$) will be used on Table Top in diagnostic experiments.

The shortest time for pumping from atmospheric pressure to 10^{-6} mm Hg is about 50 minutes. To lower the pumpdown time, the 5-liter pump will have to be replaced by a larger-capacity high-vacuum pump.

7. THEORETICAL CONSIDERATIONS (ALICE)

Archer H. Futch, Jr., Warren Heckrotte, John Killeen, and Charles C. Damm

Spatially dependent build-up equations for ALICE and the numerical solutions for an approximate form of these equations have been discussed in preceding progress reports. The approximate form of these equations was obtained by assuming that the ion density was isotropic at every point in the plasma. The numerical solution indicated an enhanced build-up by virtue of the charge exchange of the trapped ions with the neutral beam. An attempt was made by one of us to verify this result by analytical methods.[1] However, the resulting equations were too difficult to solve analytically. Even general conclusions were difficult to extract for cases of practical interest.

As a result of the analytical treatment, it was found possible to express the build-up equation in a form that could be solved numerically without making the approximation that the ion density is isotropic. The time-dependent equation is expressed in terms of the density of ion centers, D(R), by

$$\frac{dD(R)}{dt} = J\sigma_t^n n_0 \lambda_1(R) + \frac{J}{\pi}\left(\frac{\sigma_j^i v_r}{v_0} + \frac{\sigma_{cx}^A v_r}{v_0}\right)\int_{\phi_1(R)}^{\phi_2(R)} n(R,\phi)d\phi$$

$$- J\left(\frac{\sigma_{cx}^A v_r}{v_0}\right)\lambda_2(R)D(R) - n_0(\sigma_{cx}^M v)D(R)$$

$$- \frac{2(\sigma_s v)D(R)}{\pi}\int_{R-\rho}^{R+\rho} \frac{n(r)r\,dr}{\left[4R^2r^2 - (R^2+r^2-\rho^2)^2\right]^{1/2}} \quad . \qquad (1)$$

[1] Warren Heckrotte, in Controlled Thermonuclear Research Quarterly Report, UCRL-9106, March 1960, p. 74.

The ion density n(r) is related to the density of centers, D(R), by the equation

$$n(R, \phi) = n(r) = \int_{r-\rho}^{r+\rho} \frac{2D(R')\, R'\, dR'}{\pi[4R'^2 r^2 - (R'^2 + r^2 - \rho^2)^2]^{1/2}} , \quad (2)$$

and r is related to R by the relation

$$r^2 = \rho^2 + R^2 + 2\, R\rho \cos\phi, \quad (3)$$

where ϕ is angle between R and a line perpendicular to the neutral beam. Additional notation used in the foregoing equations is:

σ_t^n = cross section for trapping of the energetic neutral atoms by collisions with background gas molecules,

$\frac{\sigma_t^i v_r}{v_0}$ = velocity-averaged cross section for trapping of the energetic neutral atoms by collisions with previously trapped ions,

σ_{cx}^M = cross section for charge exchange of a trapped ion with background gas molecules,

$\frac{\sigma_{cx}^A v_r}{v_0}$ = velocity-averaged cross section for trapping of the energetic neutral atoms by collisions with previously trapped ions,

σ_s = cross section for Coulomb scattering into the mirror loss cone,

v = velocity of energetic trapped ions,

ρ = radius of ion orbit in the magnetic field,

n_0 = neutral gas density,

and λ_1, λ_2, ϕ_1 and ϕ_2 are functions of R only for a particular geometry.

Preliminary solutions of these equations indicate that the charge exchange of the trapped ions with the neutral beam does not lead to the significant enhancement of the build-up that was found previously. The solutions exhibit exponential growth. However, the resulting ion density taking this process into account is approximately the same as when this process is ignored. The precise evaluation of the effect, since it is small, awaits on increasing the accuracy of the numerical procedures.

Consideration has also been given to the effect of electrons on the trapping of ions and the subsequent build-up rate of the plasma. The cross section for ionization of neutral atoms by electrons, when averaged over a Maxwellian distribution, is almost flat for electrons in the energy range of 50 to 1000 ev. Hence, once the electrons have increased in energy to 50 kev, we may approximate their trapping rate in the build-up equations by a

constant cross section. By averaging measured cross sections[2] for ionization by electrons over a Maxwellian velocity distribution, we obtain a value for this cross section of about 2.5×10^{-16} cm^2. Estimates indicate that the electron should have increased in energy approximately 10^8 ions/cc. Therefore, the electrons should contribute to the trapping rate over a significant part of the build-up period. This effect will be taken into account in the future calculations.

8. ALICE DIAGNOSTICS

James H. Foote and Charles C. Damm

A secondary-emission detector has been designed for use in ALICE. It will measure the energetic D^0 (or H^0) flux that results when trapped D^+ (or H^+) ions charge-exchange and leave the trapping region. Although this detector is primarily designed to determine the variation of the escaping D^0 intensity with time, for which no absolute calibration is necessary, we plan to measure the number of secondary electrons emitted by the detector plate for each incident D^0 atom. This calibration will be made with the D^0 beam produced by the apparatus used in the water-vapor neutralization experiment of Charles Damm and Archer Futch. We will thus be able to check the general operation and associated electronics of the detector, and also obtain information that will help determine the absolute D^0 flux leaving the ALICE chamber (and hence, the trapped D^+ intensity).

9. BEAM NEUTRALIZATION

Charles C. Damm and Archer H. Futch

Hydrogen Neutralizer

The differential pumping system between the hydrogen neutralizer and the plasma chamber has been assembled (including a simulated plasma chamber), and initial evacuation to base pressure has been accomplished. Without bakeout, but with titanium and molybdenum evaporations as planned, base pressures in the three chambers are approximately 6×10^{-9}, 4×10^{-9}, and 2×10^{-10} mm Hg. Ionization-gauge calibration work is planned in order to verify the accuracy of these readings. The base pressures indicated are certainly within the range of interest for the ALICE trapping experiment, but the complete evaluation must await the assembly of the neutralizing section and the introduction of the neutralizing gas. The assembly of the neutralizing section is estimated to be 85% complete.

Water Vapor Neutralizer

The proton source used for the water neutralization experiments is now operating reliably at accelerating voltages up to 14 kv. Target beam intensities are steady and of the order of 10 μa, which is sufficient for reasonably

[2] W. L. Fite and R. T. Brackmann, Phys. Rev. 112, 1141 (1958).

precise thermal detection. Measurements of the relative beam intensities were made by a thermocouple determination of the target equilibrium temperature. Target construction was modified to decrease the thermal equilibration time. The baffle system used for pumping the water vapor has also been improved so that the vapor distribution remains constant for an indefinite period.

These improvements have enabled us to determine the equilibrium (or thick-target) H^0 fraction for a proton beam in water vapor. The points obtained at various energies are plotted in Fig. 4, each point being an average of several readings. An uncertainty of ± 5% should be assigned to these points at this time.

All the points are somewhat lower than the preliminary data in the preceding quarterly report indicated. The earlier data were obtained from electrical measurements, and part of the discrepancy can be removed by correcting for the H^- component. Additional electrical measurements are planned to investigate any remaining discrepancy. The ion source has been slightly remodeled for operation at energies up to 20 kev, and all data will be extended to this level.

10. VACUUM AND SURFACE STUDIES

Angus L. Hunt, Charles C. Damm, and Earl C. Popp

Hydrogen Evolution After Evaporation of Molybedenum In an Unbaked System

The preceding quarterly report included mass-spectrometric data on the evolution of gaseous components during the evaporation of molybdenum in an unbaked vacuum system. This work has been extended to the collection of data on the evolution of gas after evaporation by improving the apparatus. A lower noise level, due to battery operation of the mass-spectrometer sweep circuit, has resulted in increased pressure sensitivity and resolution. The hydrogen pressure sensitivity is now about 4×10^{-10} mm Hg per scale division.

After molybdenum gettering, the pressure remains near 1×10^{-9} mm Hg for many hours. The pressure in the system then rises slowly. In our system, the mass spectrometer shows that this pressure rise is due to a single component, hydrogen. The partial pressures of all other gases remain constant within the sensitivity limits of the mass spectrometer. Figure 5 shows the approximately linear relationship found between the hydrogen peak height and the pressure as determined by one of the two ionization gauges within the system.

There seems no doubt of the linearity of the relationship between the partial pressure of hydrogen and the pressure in this system, although the experimental points show some scatter due to instrumental instability.

Probably the molybdenum film is continuously gettering hydrogen in our particular system, and when it becomes saturated with respect to

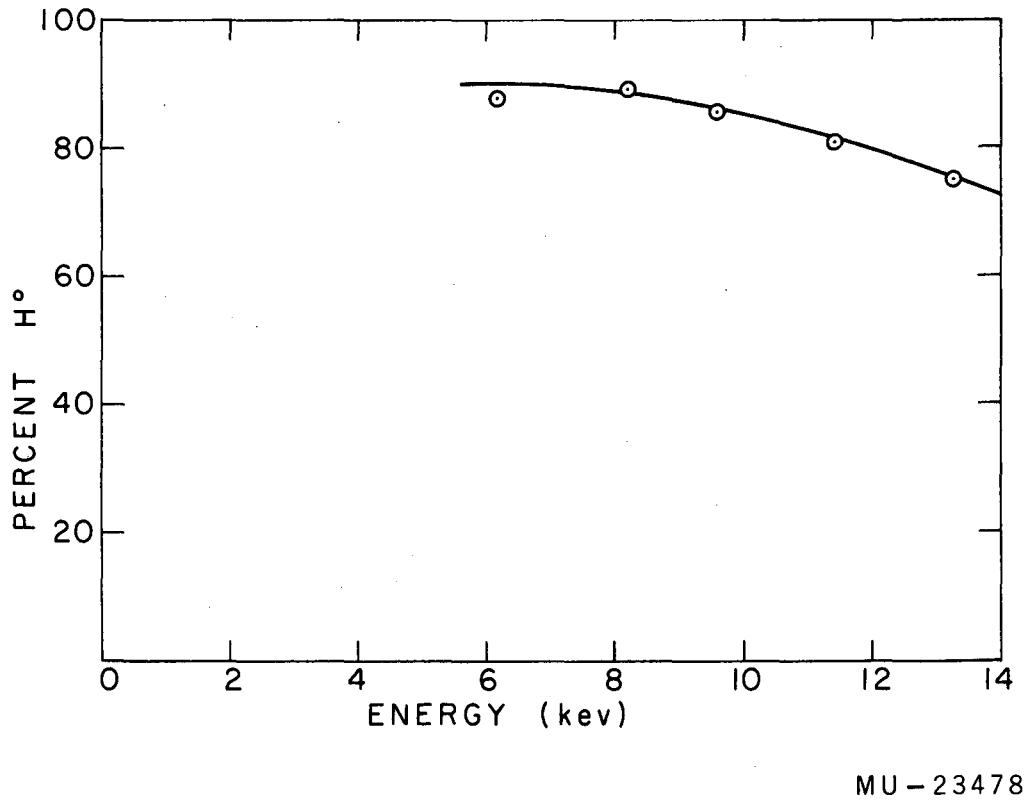

Fig. 4. Per cent H^0 in a hydrogen beam equilibrated in water vapor.

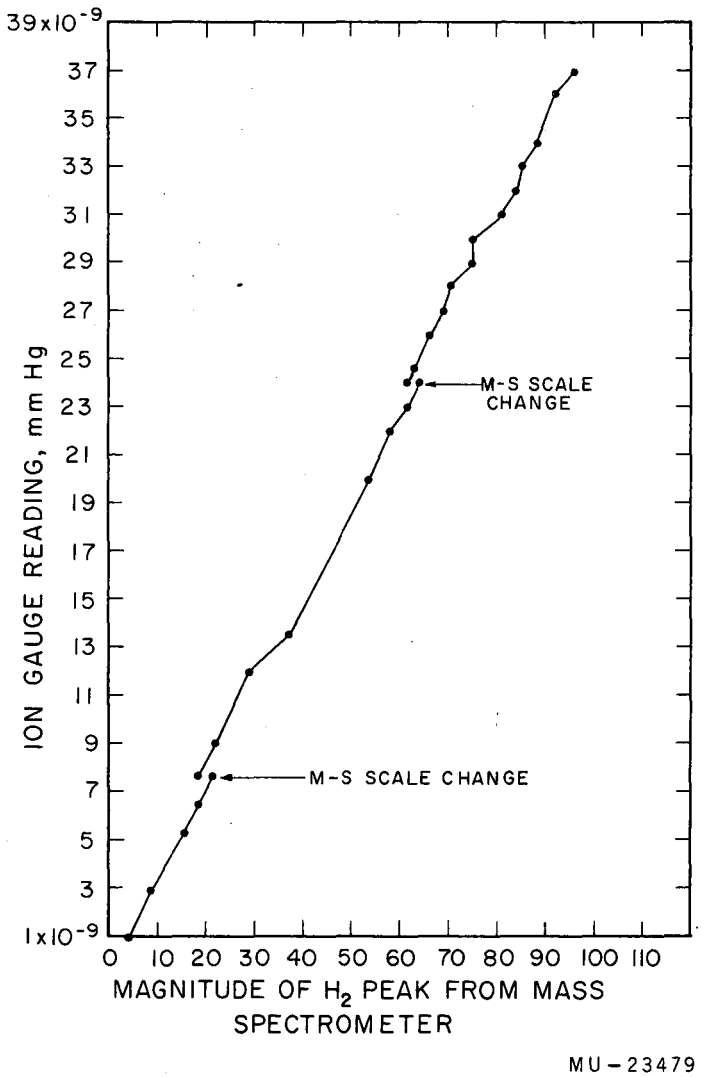

Fig. 5. Relation between hydrogen peak and ionization-gauge reading during the aging of a molybdenum deposit.

hydrogen the hydrogen partial pressure rises. Otherwise, it is difficult to understand why a rapidly gettered component such as hydrogen should be desorbed as the molybdenum film is aged.

Two sources for the hydrogen are possible. The hydrogen may be the result of cracking of fore pump oil or diffusion pump oil within the diffusion pump, or the molybdenum film may be a dehydrogenation catalyst producing hydrogen from the higher-molecular-weight hydrocarbons. The most likely source of hydrogen would seem to be thermal cracking within the diffusion pump. Conventional traps can provide no protection from this source of hydrogen contamination.

Evaporated Tungsten as a Getter

To ascertain the relative merit of evaporating a more refractory metal than molybdenum for gettering of residual gases, a layer of tungsten was evaporated over a molybdenum deposit. The large thermal load on the walls of the vacuum tank during the tungsten evaporation did not produce any deterioration in the vacuum conditions in the molybdenum-gettered system. Application of 3700 watts to the tungsten filament for 1.5 minutes did not prevent the base pressure from reaching 4×10^{-10} mm Hg within less than 3 min after power was removed from the filament. At this power level the radiative load on the walls was about 0.5 watt/cm^2. No improvement in the base pressure was obtained by evaporation of 0.96 g of tungsten. The rate of pressure rise in the system, when valved from the VacIon pump, was sensibly zero both before and after the evaporation of tungsten. Since even slightly lower pressures were obtained by subsequent evaporation of molybdenum over the tungsten deposit, tungsten does not appear to be superior to molybdenum as a general getter of residual gas.

It was found that the tungsten filament, when operated at about 2000°C, reduced the ionization gauge readings. Apparently, thermionic electrons from the tungsten filament reach the ionization gauge collector, for the gauge effect was eliminated by biasing the evaporating filament positive with respect to the grounded tank walls. The required biasing potential difference between the filament and the vacuum chamber walls increased with the temperature of the filament. The maximum thermionic emission current was not more than 5 μa. This effect can be expected to introduce gauge errors in any experimental geometry in which the gauge is in line with any electron source. For example, this effect would produce gauge errors if surfaces in line with the gauge were bombarded by high-energy particles providing sources of secondary electrons.

11. GRID SOURCE DEVELOPMENT

Frank Gordon

Improvement in arc chamber geometry has brought the proton beam on the 1×3-1/4-in. target 3 feet from the source up to 320 ma with a total high-voltage power-supply drain of 650 ma.

A high-voltage regulator is now being used which regulates ripple in the accelerating voltage supply to approximately ± 2 v rms in 20 kv. The

supply is also regulated for line voltage fluctuations and output loading. Ultimately, the regulation system will be used as part of a feedback loop to keep the beam on target during the ALICE injection cycle. The source magnet supply was switched over from a temporary Perkins supply to an M. G. set. This wanders excessively now, but presently will be regulated well within tolerance.

The ion source now seems to be mechanically and electrically acceptable. Improvements, especially in the electron drain system, are contemplated, but future emphasis will be toward optimizing neutralized (atomic hydrogen) beam to a target at least 10 ft from the source.

12. P-4 (STEADY-STATE PLASMA) SYSTEM

William L. Barr, Andrew L. Gardner, Laurence S. Hall, and Norman L. Oleson*

Probe Measurements

Tests have been made to assess the perturbing effect of the floating tungsten shield which surrounds the stem of the cylindrical Langmuir probe most used in the P-4 plasma. A solid rod was used to represent the effect of an additional shield symmetrically positioned at the other end of the active portion of the probe. This technique was applied only in the outer portions of the plasma, where a stationary probe could be used without being melted. The added "dummy" shield had the following effects on the measurements of plasma parameters:

Electron temperature	not significantly changed
Plasma potential	not significantly changed
Ion density (assumed to be proportional to the asymptotic value of $-dI^2/dV$ at large negative values of probe voltage.	the measured value was decreased by 20% or less when the "dummy" shield was present. the effect was greatest when the probe was nearest the plasma axis.

The heating of the rotating probe has been further reduced by allowing the probe to cool (at floating potential) for two or three revolutions after having collected current for one revolution. This permits the voltage to be scanned past the inflection point in the voltage-current characteristic curve and allows an approximate determination of the plasma potential.

Boron nitride has been used and shows promise as an insulator for use in probe work with the P-4 plasma. Its machinability and high-temperature characteristics are its principal advantages.

Work on the "Theory of Electrostatic Probes" is reported elsewhere in this quarterly report (see the Theoretical section). A report "On the Application of Bohm's Criterion for the Formation of a Sheath" (UCRL-9401) will appear as a Letter to the Editor of Physics of Fluids in March.

---

*U. S. Naval Postgraduate School, Monterey, California.

Ion Analysis

Some initial work has been done toward measuring the ratio of He^{+} to He^{++} present in the P-4 plasma. The plan is to use the rotating-probe mechanism to move a mass-spectrograph type of structure through the plasma and magnetically separate the radially extracted ions with the existing field of about a kilogauss. The experimental feasibility of the measurement has not yet been proved.

Ion Heating

The report "Thermodynamic Cycling in Magnetic Pumping" (UCRL-6355) has been completed in draft form.

Spectroscopic Studies

The absolute intensities of several spectral lines of neutral He were measured. The results were used in conjunction with the electron temperature (determined from probe measurements) and published excitation cross sections to calculate the electron density. The average value for the electron density obtained from six spectral lines was 3×10^{12} cm^{-3}, with a mean deviation of $\pm$ 50%. This may be compared to a more accurate value of 2×10^{13} cm^{-3} obtained from previous microwave measurements.

Electron Beam Instabilities

Instrumentation for study of the interaction of an electron beam with the plasma is continuing. Charles Wharton has reported on the results to date in the Electrical Engineering Development section of this quarterly.

II. ASTRON PROGRAM

1. INTRODUCTION

Nicholas Christofilos

The effort of the Astron group is continuing primarily on the construction of the 5-Mev accelerator. A basic component, the modulator using a hydrogen thyratron to switch the pulse-forming network energizing the magnetic cores of the accelerator, is now developed. Five hundred units or modulators are required, one for each core. It is expected that the electron gun (700 kev, 200 amp) and the first accelerator unit (500 kev) will be ready for tests within six months. The completion of the accelerator is expected within approximately 10 months. In addition, two months of testing and debugging will be required before the installation will be ready for the Astron experiment.

The other components of the Astron facility are being built in parallel with the accelerator.

Owing to great interest in studying the interaction of a relativistic electron beam with a plasma, there has been some thought of expanding the Astron program to include experiments of the interaction of the 5-Mev 200-amp electron beam with plasma to study hydromagnetic and plasma (electrostatic) oscillations and instabilities.

In the theoretical field the most important activity during this quarter was the coding in the LARC of the problem of studying the formation of the E layer, including end effects. Dr. Leslie Peck* and Dr. John Killeen are working on this problem.

2. ASTRON GAS TARGET ELECTRIC-CONDUCTIVITY MEASUREMENT

Daryl D. Reagan

The hose instability of relativistic electron beam has been described by Lewis.[1] Preliminary estimates[2] indicate that this instability may be generated by the beam from the proposed Astron accelerator. The feasibility of the experiment will depend upon the properties that can be built into an ionized gas target.[2] The target must have electron density much higher than the beam density. It must be long and thin and should have low electric conductivity. Proposed parameters are: density, $10^{14}/cm^3$; length, 1 m; radius, 1 cm; and conductivity, less than 100 mho/m. This conductivity corresponds to a fully ionized hydrogen plasma having electron temperature

*Consultant to Lawrence Radiation Laboratory from Boston, Massachusetts.

[1] Harold W. Lewis, Stability of a Relativistic Beam in a Plasma, Jason Summer Study Group, 1960, Institute for Defense Analyses.

[2] R. E. Hester and D. D. Reagan, Some Remarks on the Feasibility of a Hose Instability Beam Experiment, UCID-4192, Aug. 29, 1960.

0.1 ev. The target will probably be housed in a glass or quartz tube about 1 in. i. d. At the time for the beginning of the beam pulse, the plasma will have no currents or magnetic field.

This note outlines a direct method of measuring the conductivity of such a plasma that is simpler than the conventional microwave techniques, and is less ambiguous in its interpretation. Suppose one starts with infinitely long cylindrical plasma of radius r_0 and suddenly applies a uniform axial magnetic field, B_0. The magnetic field will diffuse into the discharge according to the equation

$$\nabla^2 B_z = \mu_0 \sigma \dot{B}_z \quad \text{for} \quad r < r_0, \tag{1}$$

the axially symmetric solution to which is

$$B_z = B_0 \left[1 - \sum_{n=1}^{\infty} a_n J_0 \left(\lambda_n \frac{r}{r_0} \right) e^{-\lambda_n^2 t / r_0^2 \sigma \mu_0} \right], \tag{2}$$

where λ_n is the nth zero of $J_0(\lambda)$, the zero-order Bessel function, σ is the plasma conductivity, $\mu_0 = 4\pi \times 10^{-7}$ farads/m, t is the time, and $a_n = 2/\lambda_n J_1(\lambda_n)$. The a_n's form an alternating series the terms of which diminish slowly with n. In the practical case, however, the magnetic field will be applied in a finite time interval, so that higher terms will not be excited to appreciable amplitude. Figure 6 shows the shape of the B_z field at various times worked out for a hydrogen plasma 3 in. in diameter and having conductivity 10^3 mho/m. This example corresponds to the conditions in the experiment designed to test the method.

In the preliminary experiment the plasma is produced by a current pulse (approx 10 kv, approx 5 ka) which flows axially in the gas (approx 100 μ pressure) in a 3-in. -diam 12-in. -long pyrex pipe (see Fig. 7). After the plasma-producing pulse subsides, a delay of the order 10 to 100 μsec permits the currents and magnetic fields to decay and the ionized gas to cool somewhat. Then a rectangular pulse of current is applied to a single-turn primary wrapped around the middle of the pyrex pipe. The magnetic field change is measured by two secondaries, one outside the pyrex pipe and one inside. The inside coil is protected by glass tubing.

The inside coil measures the rate of change of B near the axis, while the outside coil measures the rate of change of total flux. It is hoped eventually to achieve signal-to-noise ratio sufficient to measure the plasma conductivity with the outer coil alone, by measuring the asymptotic decay period of the pulse. This is a direct measure of the parameter $r_0^2 \sigma \mu_0 / \lambda_1^2$, from which an average value, σ, of plasma conductivity can be calculated directly.

We have done experiments which demonstrate the feasibility of the method of resistance measurement. We have just completed a low-Z pulser that increases the energy dissipated in the discharge from about 1 joule to the order of 100 joules.

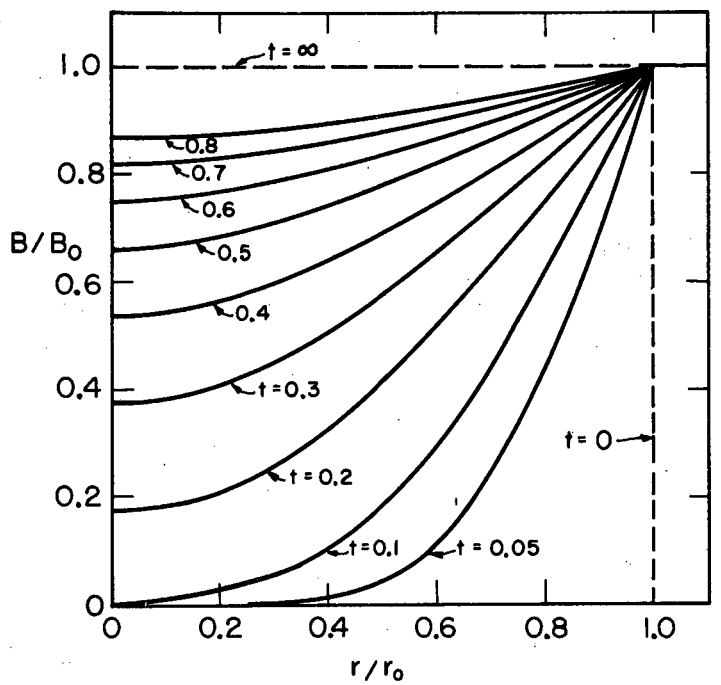

MU-23480

Fig. 6. Magnetic field as a function of radius for several times. Time t is μsec after initiation of measuring pulse. These curves were calculated for uniform conductivity and for $B^2/8\pi nkt \rightarrow 0$.

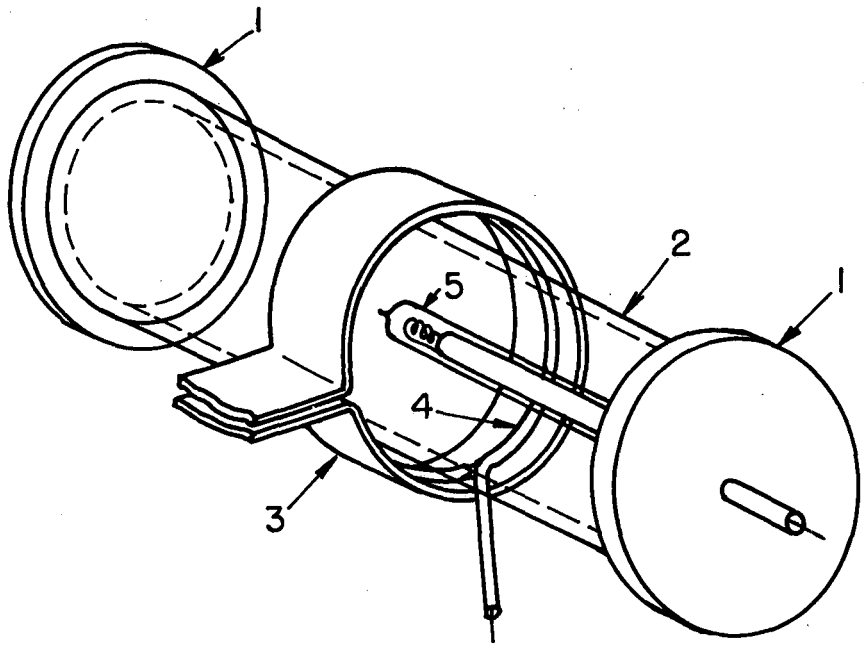

MU-23481

Fig. 7. Apparatus to test the scheme: The discharge is formed between brass plates (1) in a 3×12-in. pyrex industrial pipe (2). The probing B field is produced by a current pulse in the primary strap (3). The changes in B are measured by the voltages produced across the secondary coils (4) and (5). The "inside" coil (5) is protected by a glass sheath.

We require microwave apparatus to measure the electron density and conductivity of our discharge. This equipment is being assembled. When this equipment is working we can test the resistance-measuring technique quantitatively.

III. LIVERMORE PINCH PROGRAM

Dale H. Birdsall, Stirling A. Colgate, Harold P. Furth,
Fred O. Halliday, Charles W. Hartman, and Ross L. Spoerlein

1. SUMMARY

The electron-beam pinch apparatus has been used to demonstrate perfect containment of particles on flux surfaces in the "inverse stabilized pinch," and random leakage of particles during the turbulent phase of an ordinary "stabilized pinch" of comparable current density.

A vacuum of better than 2×10^{-7} mm can now be achieved in the inner region of the Levitron, even when the liner is heated to 425 °C. Mounting of the field windings is nearly complete.

The effect of initial neutral-gas gradients has been studied in the conical-pinch accelerator. Hydromagnetic oscillations have been excited with the accelerated plasma. A new electrostatic plasma accelerator has been designed.

The machine calculation on interpenetrating plasma streams is showing the anticipated shock-formation features.

A fundamental article on magnetic metal forming is being published.

A broad family of velocity-space instabilities, related to the Bennett pinch condition, has been recognized. This study has helped to interpret several previously known instability types, such as the "mirror instability," and has led to the discovery of a number of new instabilities.

The unstable hydrodynamic collapse of a supernova star has been followed with an improved code.

A study has been made of the effect of plasma space-charge waves on microwave diagnostics.

2. ELECTRON-BEAM PINCH

The electron-beam linear pinch experiment has been converted to operation with a hard core. As in previous hard-core pinch studies,[1] the "inverse stabilized pinch" (see Fig. 8) is found to have much more reproducible magnetic-probe traces than a conventional "stabilized pinch" of comparable current density. One would expect, therefore, that the containment of energetic particles is correspondingly better for the inverse stabilized pinch. This expectation is completely borne out by the electron-beam results (see Fig. 8). With the ordinary stabilized pinch, the electron-beam trace becomes highly erratic after 3.5 μsec (when the probe traces begin to become irreproducible). After 5.5 μsec it is impossible to transmit the beam to the phosphor. With the inverse stabilized pinch, the beam can be transmitted throughout the cycle and traces out a regular circular flux surface. The slight distortion and the gaps in the trace on Fig. 8 are due to the presence

[1] S. A. Colgate and H. P. Furth, Phys. Fluids 3, 982 (1960).

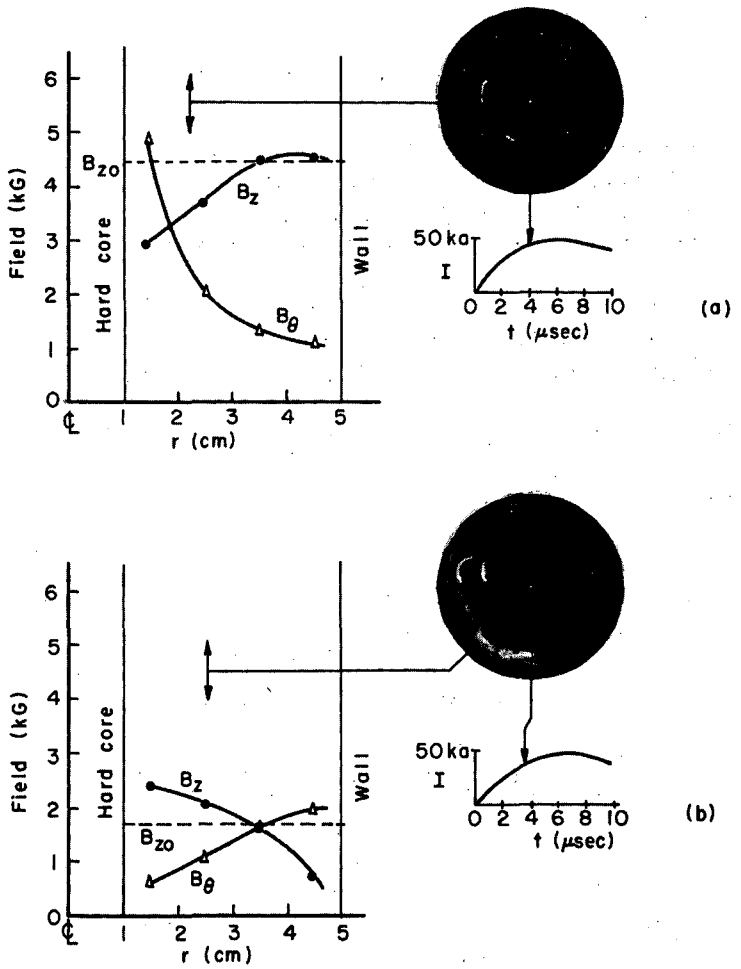

MU-23498

Fig. 8. Comparison of electron-beam traces in (a) the inverse stabilized pinch and (b) the stabilized pinch. Timing and location of the electron beam are indicated on accompanying graphs.

of six radial spokes which feed the current to the hard core at the beam-input end. These results have reenforced our expectation that the Levitron will permit significantly better containment of hot particles than has been possible in ordinary toroidal pinches.

As in the stabilized-pinch experiments described in our preceding quarterly report, the beam traces shown in Fig. 8 are considerably longer than what one would expect from the rate of interdiffusion of magnetic fields during the "beam-on" time of 0.1 μsec. A series of experiments has been made with a view to resolving this mystery. The beam was passed through the hard-core vacuum field, and was found to produce extended traces even in a (time-wise) constant magnetic field. The length of these traces was proportional to the pitch of the magnetic field lines, and amounted to as much as a complete turn for a helical magnetic field making five turns along the length of the tube. The possibility that a motion in time of the beam trace was responsible for the traces was further excluded by varying the "on" time of the beam: no effect was observed. To explain a static smear, one tends to look to nonadiabatic effects and particle drifts. The strongest of these effects is the azimuthal drift due to the radial centrifugal force and the B_z field, but this turns out too small by an order of magnitude. In addition, variation of the absolute magnetic field strength or the particle energy is found to have little effect on the beam trace. The present view is, therefore, that ordinary "optical distortion" is responsible. The most promising explanation is that the finite radial extent of the beam places different electrons on flux surfaces having different pitch, and therefore a distortion of the original spot into an azimuthal streak takes place. Experiments varying the initial spot size have confirmed that this must be the major source of the observed beam spread.

3. LEVITRON DIAGNOSTIC SPECTROSCOPE

A diagnostic tool for observing the optical radiation from the Levitron has been designed and is being fabricated and calibrated. It consists of a modified Jarrell-Ash monochromator which will allow time-resolved scanning of up to four wave lengths simultaneously with oscilloscope outputs. Fundamentally it will observe λ = 4861 A, 2297 A, and any two wave lengths in the range from about 4000 to 5000 A.

4. LEVITRON

The Levitron is constructed with an annular rough vacuum space surrounding a stainless steel liner. Using rf heating of approximately 20 kw, we have succeeded in heating the stainless steel liner to 425 °C, at the same time maintaining a rough vacuum of 10 μ in the annular space. The relative leak rate between the annular volume and the liner volume was small enough so that a ratio in pressure of 3×10^{-6} could be maintained between the two volumes. This leak rate is low enough so that with rf heating a good vacuum should have been achieved in the liner volume.

However, a persistent leak in the trapped volume of the core prevented achievement of a good vacuum in the liner space. After the core had been

drilled and plugged, the leak from the core volume still persisted, so that separate pumping on the core was required in order to achieve a good vacuum within the liner space. When the core was unplugged, the liner heated, and a titanium filament then used within the liner space, a vacuum of better than 2×10^{-7} mm was achieved.

Because of the long thermal time constant of heating the core by radiation from the heated liner, the core never came up to the full bakeout temperature. Consequently, it is expected that a very much better vacuum can be achieved once the core is directly heated. The heating of the core can be achieved only when the Levitron is in place on the iron transformer so that there is good coupling to 60-cycle power. On completion of a separate heating and pumping operation on the core, in order to remove all contaminants within the core volume, it is expected that the Levitron will be able to operate with the core open to the main liner volume. Therefore, the preliminary achievement of 2×10^{-7} mm vacuum in the liner with the unbaked core volume directly connected to the liner volume was felt to constitute a sufficiently good performance to justify proceeding with the coil winding.

At this date 90% of the θ-coil windings and 70% of the z-coil windings are completed. Following the completion of the coils, the Levitron will be mounted within the transformer iron and connections made to the condenser bank. Initial measurements will be made without levitation; the support rods of the core will be left in place, and the magnetic aperture will be measured with an electron beam. The probable time before an electron beam on a magnetic surface will intersect a support rod is sufficiently long to permit a reasonably accurate mapping of a flux surface (a hundred turns).

These initial measurements should give an indication of the accuracy of the coil winding and of the effective magnetic aperture of the machine. The electron gun to be used for these measurements has been completed and observed to give 10^{-7} coulomb of charge in 2×10^{-7} sec for voltage as high as 70 to 80 kv.

5. CONICAL PINCH ACCELERATOR

The large neutral-gas-density gradients in the pinch chamber at discharge time, which were reported in the previous quarter, have been reduced to factors of 2 by installation of a more slowly opening pulsed gas valve (0.75-msec open time). Most of this quarter has been spent diagnosing the gas valves and pinch-plasma output under the new conditions.

The dominant effects of changing the initial gas distribution towards greater uniformity have been to increase the density of accelerated plasma and reduce the average ion energy. Further study and optimization of acceleration will be postponed pending an experimental shock study.

The accelerated-plasma characteristics for primary pinch pressure from 30 to 140 μ D_2 are: density, 10^{15} to 8×10^{15} D^+/cc; directed ion energy, 1 kv to 100 v; ion temperature, 10 to 20 ev.

An interesting confirmation of plasma density (previously measured with a piezoelectric probe) has been obtained by observation of the frequency of high-Q radial hydromagnetic oscillations in the accelerated plasma, when projected into the axial B field in the drift region. The frequency of oscillation is observed to be proportional to magnetic field from about 1 to 4.2 kG.

6. COLLISIONLESS PLASMA SHOCK (EXPERIMENTAL)

The conical pinch output has been fired into a drift region containing neutral deuterium at 1 to 50 μ. Observation of hydromagnetic oscillations indicates efficient ionization of the background gas by the energetic electrons of the moving plasma. The observed deceleration of the plasma appears to be roughly accounted for by ionization and electron-heating energy losses. Measurements of the electron temperature are in progress.

The dynamical friction of electron-ion collisions, when a fully ionized stationary plasma is substituted for the neutral background, should also produce an observable deceleration. Estimated electron heating should raise the electron temperature above the critical limit imposed on ion-ion and ion-electron wave growth by small-amplitude theory[1] ($T_e/T_i \gtrsim 3.5$).

7. COLLISIONLESS PLASMA SHOCK (THEORETICAL)

Shock calculations have been carried out for interpenetration of five ion-plasma periods of initially cold streams ($v_t/v_0 = 0.1$). The mass ratio is 10. After several electron-plasma periods, waves at wave length $\approx v_0/f_{pe}$ develop and saturate at potentials comparable to the electron streaming energy. After several ion-plasma periods, modes of wave length $\approx v_0/f_{pi}$ appear.

Figure 9 shows an instantaneous potential distribution at $t = 5/f_{pi}$. The shock front is located at position 0.75, unshocked plasma is streaming into the shock region from the right at streaming velocity v_0, a reflecting plane is located at $x = 0$, and the potential is constrained to be zero at $x = 0$. The scale heights shown indicate waves have developed potentials comparable with the ion streaming energy. All fields appear to fluctuate at about f_{pe}. Interaction of the incoming ion stream within four ion-plasma wave lengths is strong enough to randomize about 30% of the ion streaming energy. Reduction of the integration time step by a factor of 2 leaves the picture substantially unchanged.

Longer calculations will be made with an improvement in cross-over corrections to include the effects of multiple cross-overs occurring within a time step.

---

[1] T. E. Stringer (Atomic Energy Research Establishment, Harwell), private communication.

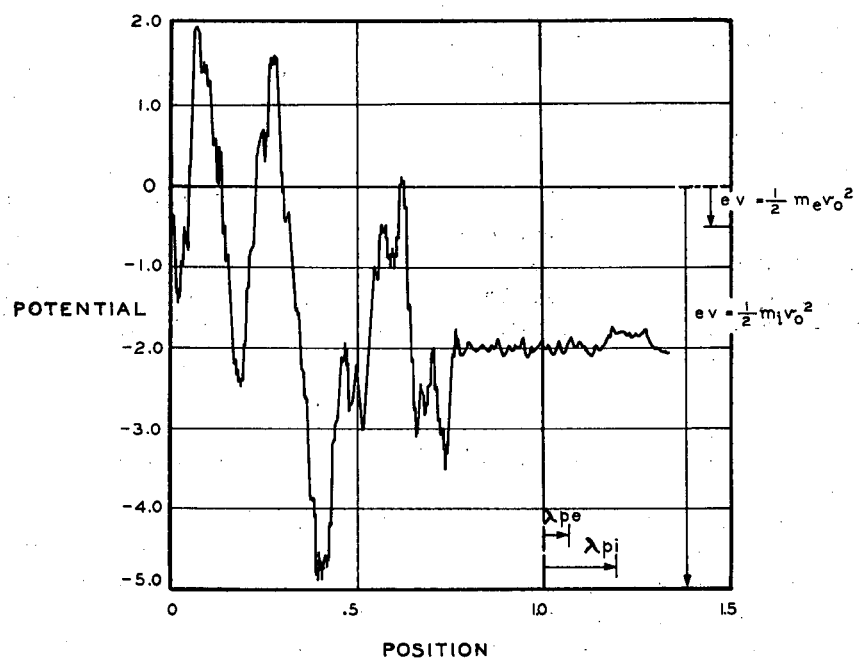

MU-23482

Fig. 9. Instantaneous potential distribution at $t = 5/f_{pi}$, as obtained in the collisionless plasma shock calculation.

8. HIGH-FIELD RESEARCH

The experimental program on magnetic metal forming has been completed, and a summary article on the results, as well as on the basic theory of the technique, has been written.[1]

The 200-kilogauss high-energy beam-analyzing magnet has been completed and is being tested.

Following a suggestion by Clyde Taylor, we are studying the feasibility of extending critical field studies[2] on superconducting Nb_3Sn above 100 kilogauss in a pulsed field. The incompleteness of the Meissner effect at high fields makes the maintenance of superconductivity difficult, unless the sample is exceedingly thin. The problem is that, owing to the field penetration, eddy currents are induced in the nonsuperconducting parts of the sample, with resultant temperature rise. This remark also suggests that superconductors of the Nb_3Sn type will tend to be limited to those thermonuclear applications in which magnetic fields are either steady or change at less than a cycle per sec.

---

[1] D. H. Birdsall, F. C. Ford, H. P. Furth, and R. E. Riley, Metal Forming by Magnetic-Field Pressure (UCRL-6303, Jan. 1961, to be published in American Machinist, March 20, 1961).

[2] J. E. Kuuzler et al., Phys. Rev. Letters 6, 89 (1961).

9. INSTABILITY THEORY

The stability analysis for relativistic sheet pinches, which was described in the preceding quarterly report, has given rise to recognition of a general type of velocity-space instability, which is indigenous to a wide variety of plasma-containment geometries.

The instability can arise in a neutral plasma where there is a counterstreaming either of unlike particles (flow of plasma current), or of like particles (thermal anisotropy). The instability consists of the bunching of current into "pinches" running in the direction of the original current flow or that of maximum thermal velocity. The stability conditions obtained in the limit of null growth rate are always roughly equivalent to the Bennett condition for the formation of an ordinary pinch,

$$2 N k T < I^2, \tag{1}$$

where N is the density per unit length of the pinch. This condition can be rewritten as

$$N r_c (v_0/v_1)^2, \tag{2}$$

where r_c is the classical electron or ion radius (depending on which kind of particle produces the plasma pressure) and v_0 and v_1 are the velocity of current flow and the thermal velocity respectively. In the instability analyses, the quantity N that characterizes the incipient "pinches" depends on

the plasma density and on the square of the instability wave length (or the wave length times some geometric dimension). Accordingly, the longest wave lengths are always the most difficult to stabilize against. The growth rates of this type of instability are measured in terms of the ion or electron plasma frequency. In the case of the instability due to current flow, the plasma frequency of the more massive type of particle applies, even when the current is carried by the less massive particles. This is because a perturbation in real density occurs, and charge-separation electric fields couple the two kinds of particle. In the case of the instability due to thermal anisotropy, there is no perturbation of density in real space, only in velocity space; hence the two particle types are decoupled to first order and either plasma frequency (or both) may apply, depending on which kind of particle is responsible for the anisotropy.

These general remarks are illustrated by the following examples. A thin sheet pinch is subject to breakup into "streamers," with the stability condition (in the limit $\omega \to 0$)

$$(v_0/v_1)^2 \, r_c \, n \, \delta \, \lambda < 1, \tag{3}$$

where n is the volume density, δ is the pinch thickness, and λ the instability wave length. This applies to ordinary sheet pinches, where the drift velocity v_0 is smaller than thermal velocity, and also to relativistic sheet pinches, provided that r_c is reduced by the factor $1/\gamma$. This type of instability, followed by ordinary hydromagnetic instabilities of each streamer, is probably responsible for neutron production in reverse-field theta pinches.

These results can be modified to apply to current-flow situations where the current is carried by ions, as in high-energy injection machines. In that case and for $\lambda \to \infty$, Eq. (3) becomes

$$\left(\frac{v_0}{v_1}\right)^2 2\pi \, n \, r_c \, \delta \, R\left(1 - \frac{R^2}{b^2}\right) < 1, \tag{4}$$

where R is the radius of the ion layer and b is the radius of a conducting outer cylinder. (Geometric factor calculated by V. K. Neil, who has also done the case of finite wave length.) Equation (4) can be rewritten as

$$\left(1 - \frac{R^2}{b^2}\right)\frac{1}{4}\left(\frac{v_0}{v_1}\right) \beta < 1, \tag{5}$$

where β refers to the ratio of the centrifugal pressure to the energy density of the containing field. Equation (5) is evidently very close to the condition,

$$(v_0/v_1)^2 \, \beta < 1, \tag{6}$$

which Newcomb and Post[1] have calculated for the "mirror instability" in a uniform plasma of small gyro-radius.

The familiar mirror instability itself is a manifestation of the instability mode that we are considering, but since no net current flows in the zero-order configuration, this belongs to our second category, of instabilities arising from thermal anisotropy.

The simplest thermal-anistropy problem involves an infinite uniform plasma without magnetic fields. The stability condition is

$$\left[\left(\frac{v_0}{v_1}\right)^2 - 1\right] \frac{1}{\pi} r_c n \lambda^2 < 1, \tag{7}$$

where v_0 and v_1 now refer to the two thermal velocities. This type of instability has already been reported by Weibel[2] and Fried,[3] who call it a "mechanism for instability of transverse plasma waves." The recognition that Eq. ( ) is essentially equivalent to Bennett's condition, and that we are talking here about the formation of pinches, permits us to predict the non-linear behavior of the system. We can also see that this instability is not confined to electron-velocity anisotropies, but could also occur, for instance, when two neutral streams of plasma interpenetrate.

The thermal-anisotropy instability in the infinite medium can be suppressed by addition of a magnetic field in the direction of maximum thermal velocity, if this field is strong enough so that the gyro-radii are small compared with λ. Thus this type of instability disappears in the hydromagnetic approximation.

When the thermal velocity is comparable in two directions, but low in the third (as with the mirror instability), then, in the absence of an initial magnetic field, sheet pinches will form in planes orthogonal to the direction of low thermal velocity.

A fine application of the thermal-anisotropy instability is furnished by a spherical electrostatic containment scheme[4] that has recently enjoyed some publicity. Here the electron velocity is maximal in the radial direction, the instability modes correspond to Legendre polynomials, and the lowest-order stability condition is

$$\left(\frac{v_0}{v_1}\right)^2 \frac{\eta}{8\pi R} r_e < 1, \tag{8}$$

where η is the total number of particles, and R is the radius of the sphere.

---

[1] R. F. Post, Velocity-Space Instabilities in the Mirror Machine, UCRL-6079, August 1960.

[2] E. S. Weibel, Phys. Rev. Letters 2, 83 (1959).

[3] B. D. Fried, Phys. Fluids 2, 337 (1959).

[4] W. C. Elmore, J. L. Tuck, and K. M. Watson, Phys. Fluids 2, 239 (1959).

10. SUPERNOVA CALCULATIONS

The computation of unstable hydrodynamic collapse of the supernova star has been followed with an improved equation of state for the material of the star above the temperature of 1 Mev. These high temperatures achieved in the collapse of a supernova star break up the helium into neutrons and protons and cause a large change in the specific heat of the material of a star. This additional reduction in the internal energy of the material drives the collapse of the star to smaller radii and more extreme temperatures and densities (Fig. 10). The peak temperatures at which reflection occurs are in the neighborhood of 3 Mev and densities 10^{13} g/cm^3. The reflected shock appears to be of the proper strength to give the observed ejection of stellar material (i. e., the explosion of a star), and at the same time corresponds to the shock required for the generation of the cosmic ray spectrum.

11. SPACE-CHARGE WAVES AND PLASMA DIAGNOSTICS

Alvin W. Trivelpiece*

Upon review of the properties of the characteristic modes of propagation on an axially magnetized cylindrical plasma column, it can be shown that in some cases these modes can give rise to errors in the measurement of the properties of a plasma by conventional microwave transmission methods of plasma diagnostics, where it has been tacitly assumed that the plasma is very large compared with the wave length of the diagnostics signal. Analysis of the specific case of electric vector parallel to the axis of a plasma column illustrates the essential features of the coupling of a diagnostics signal to the space-charge wave modes.

*Electrical Engineering Department, University of California, Berkeley; Consultant to Lawrence Radiation Laboratory.

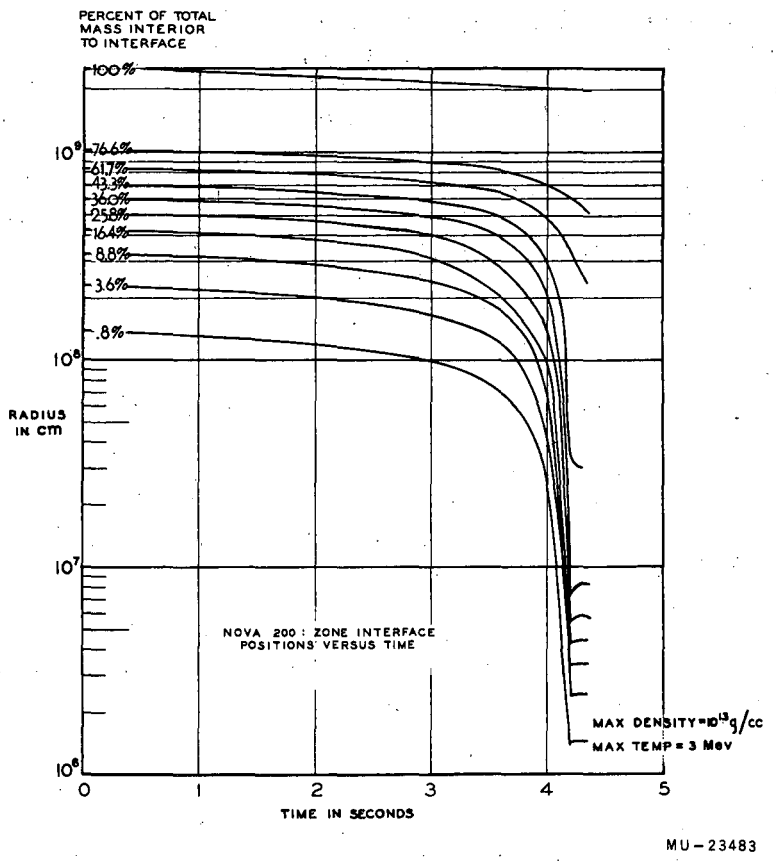

Fig. 10. Supernova collapse.

IV. BERKELEY PLASMA RESEARCH

1. SHEET PINCH STUDIES

Oscar A. Anderson

The stability of the Triax has been a controversial subject since the program began. However, the present theoretical predictions are that neither the ordinary hydrodynamic instability nor resistive ripping should develop during the time scale of the discharge. Indeed, neither of these is ordinarily observed in the experiments. Instead, there are other effects: sometimes, a gradual diffusion of the pinch boundaries, and less often, what seems to be a sudden secondary discharge or flare. One of the first examples of the flare effect may be seen in a streak photograph published in March 1960.[1] In this case the flare occurred 3 μsec after the main discharge started and was located near the wall. Because it is very likely to be related to the general problem of confinement, the flare effect has been given close attention during the past quarter.

This study was made with the new 6-by-10 Triax, operated with 250 μ of D_2 on the 200-μf bank at 15 kv. Under these conditions, approximately one-fourth of the streak photographs showed a flare before peak current. The over-all spectrum was photographed by J. M. Stone, who identified the most prominent lines. These included λ 4150 (Al^{++}) and λ 4481.3 (Mg^{+}) as well as other lines from elements contained in the insulators. The timewise behavior of these impurity lines, and also the D^{β} line, was then observed with a Jarrel-Ash monochromator. The D^{β} intensity was found to peak at the time of the first pinch, and then to decrease quickly to a steady value. The impurity lines, such as Mg^{+}, generally were absent up to about 2 or 3 μsec and then sometimes showed a sudden increase.

In order to correlate all this information, an optical system was arranged that divided the pinch light between the streak camera and two monochromators, with very little parallax. One monochromator was set on an impurity line, while the other usually monitored the continuum. For each discharge the three records were compared, with the aid of time markers. It was found that the appearance of a flare in the streak photograph always coincided with the onset of impurity light, as shown in Fig. 11, but that there was no corrsponding jump in the continuum or in D^{β}. (The first three pictures in Fig. 11 were selected to show various positions in which the flare may appear; in the fourth there is no flare.)

The evidence is that the main discharge contains mostly deuterium, while the secondary discharge (flare) contains mostly wall impurities. The problem is to discover how and why this happens. It is not yet known whether the emission and breakdown of impurities occurs in a small or a large region of the tube. A fairly large over-all area may be involved, since there is usually an increase of about 1 kv in the tube voltage at the time of the flare. Better information may be gained with the aid of stereoscopic streak photography, as discussed in an earlier Quarterly, UCRL-9243. An improved stereoscopic system is being designed by J. M. Stone. This system, when in operation, will help to decide between the various explanations proposed for the flare effect.

[1] Oscar A. Anderson, in Controlled Thermonuclear Quarterly Report, UCRL-9106, March 1960, p. 52.

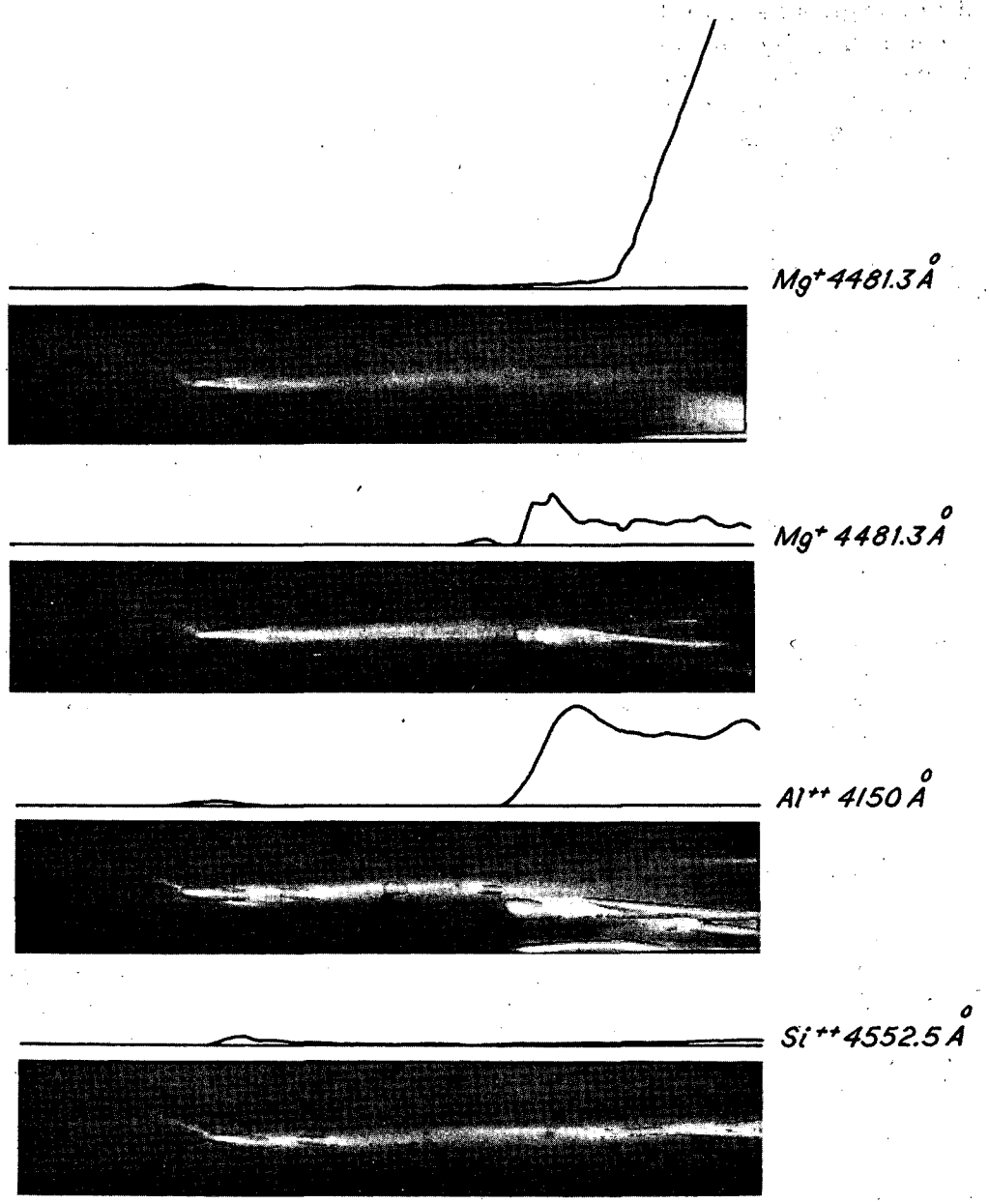

ZN-2762

Fig. 11. Flare effect in 6-by-10 Triax (sweep time, 4 μsec).

Meanwhile, a program of reducing pinch contamination is in progress. One of several possible approaches is to study the relationship between pinch initial conditions (determined by preheating method) and the severity of wall bombardment.[2] In previous work with the preheat cycle, a rather fast discharge was found necessary to avoid irregular cathode effects.[3] More recently, by use of the 6-by-10 Triax, the effect of varying the relative timing between the preheat and main discharges was observed. As is seen in Fig. 12, the general appearance of the pinch changes with the timing, and at 5.3 μsec, for example, the pinch is especially narrow. More data will be taken to see whether wall impurities are involved.

A second approach to the contamination problem is to reduce undesirable aftereffects of the pinch discharge. Normally the condenser bank output current rings for several cycles, even though only the first half-cycle is of interest. To reduce unnecessary wall bombardment caused by the extra current, damping resistors were added to the bank. Unfortunately, after a few discharges the low-pressure switches no longer operated properly (the switch insulators need a great deal of current to keep themselves clean[4]), and the resistors had to be removed. When the 6-by-10 Triax is operated at higher levels this will no longer be a problem, and this experiment will be repeated.

The third way of reducing contamination will be to improve the vacuum system. To replace the simple fore pump arrangement previously used, a complete new system (based on a PMC-1440 diffusion pump) has been designed. This will be able to handle the large amounts of deuterium involved in Triax discharges without backstreaming. The system has been built and is ready to install.

2. HOMOPOLAR PROGRAM

Klaus Halbach, G. Donald Paxson, and Didier Veron*

Owing to a further cleanup in Homopolar IV and a change in operating conditions, we obtained the first satisfactory results during this past quarter. In the present mode of operation the negative terminal of a charged capacitor bank (1.6 μf, 60 kv, 3 to 10 ohms in series) is connected to the center electrode all the time. About 2 msec after the magnetic field is turned on, the puff valve releases from 20 to 50 μliters of D_2, and about 2.5 msec later, at the peak value of the magnetic field (20 kgauss), the gas in the machine breaks down.

---

[2] Stirling A. Colgate, Initial Conditions for the Dynamic Pinch, UCRL-4895, May 1957.

[3] Oscar A. Anderson, in Controlled Thermonuclear Quarterly Report, UCRL-9393, September 1960, p. 37.

[4] William R. Baker, Rev. Sci. Instr. 30, 700 (1959).

*Visitor from Centre d'Études Nucléaires de Fontenay-aux-Roses, France.

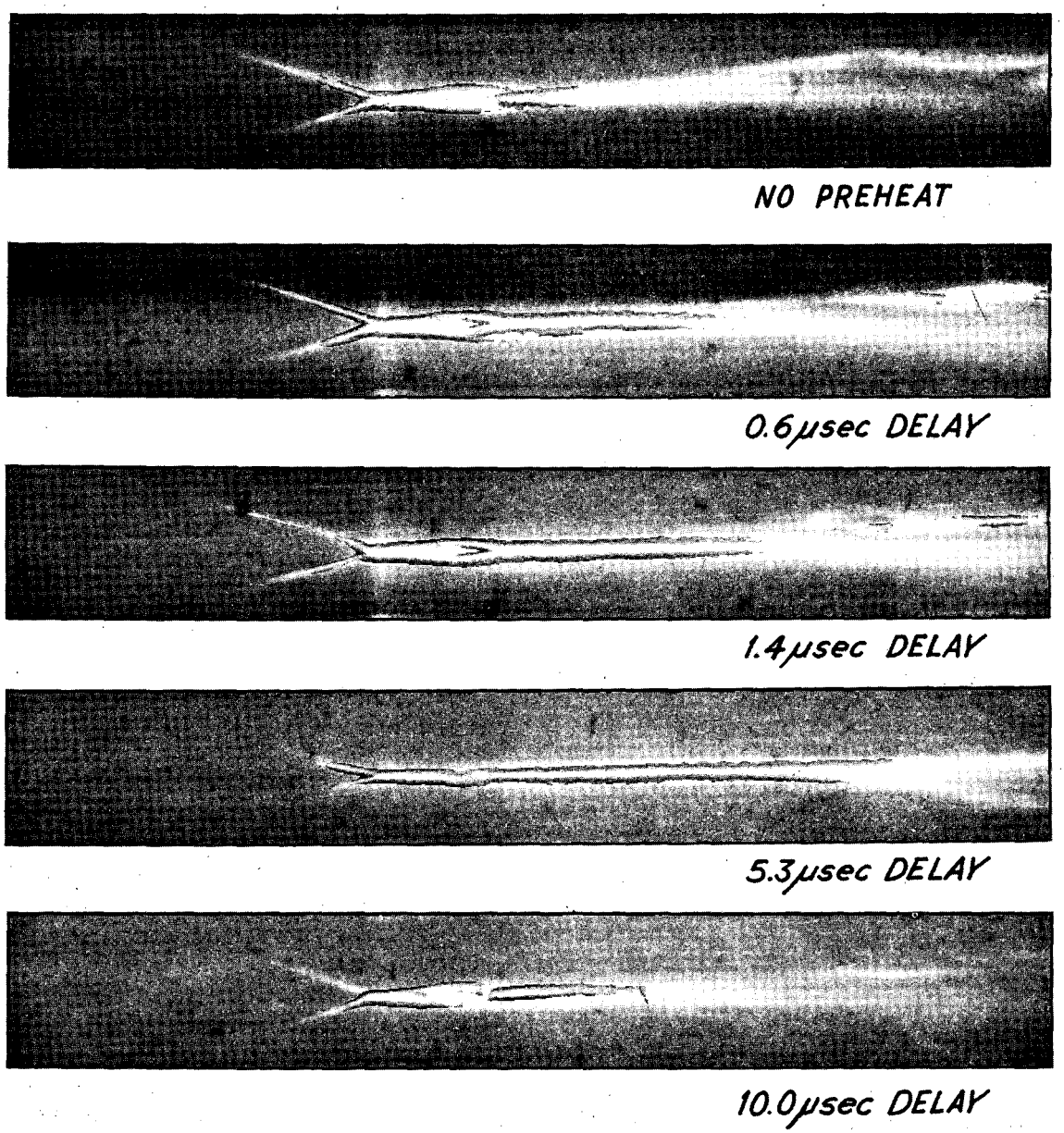

ZN-2763

Fig. 12. 6-by-10 Triax operated with various delays between preheat and main discharges. (Deuterium pressure, 500 μ, sweep time, 5 μsec.)

To check whether a true plasma rotation is associated with the measured back voltage, we applied a crowbar about 2 μsec after the initial breakdown. In Fig. 13 typical current, charge, and voltage traces of such an experiment are reproduced (voltage 2 μsec delayed with respect to current and charge).

If a charge Q passes through Homopolar IV, the angular momentum M delivered to the plasma by this charge is

$$M = Q\,B \cdot \pi(r_2^{\,2} - r_1^{\,2})/2\,\pi,$$

where B is the axial magnetic field and r_1 and r_2 are the radius of the inner and outer electrodes, respectively. Using this relation in analyzing the charge and current traces and taking into account that after the first half crowbar cycle the plasma has some rotation in the opposite direction, we can conclude that about 90% of the angular momentum imparted to the plasma by the charging current can be recovered at the time the crowbar is applied, indicating that the plasma is really rotating.

In order to estimate the actual back voltage we assume a 1/r dependence of the rotational velocity and uniform density in the radial direction. Using the amount of gas released by the puff valve for the mass of the rotating plasma, we obtain 21 kv for the back voltage. If we use, as another extreme, the amount of gas we find in the machine after the discharge, we obtain 9 kv. We believe that the former number comes closer to the real value than the latter, since the change of the ringing frequency indicates that most of the gas release by the walls takes place after crowbarring of the machine. Using 20 kv as the effective back voltage, we obtain 3.6×10^5 m/sec and 1.2×10^5 m/sec rotational velocity close to the center and outer electrodes, respectively. It should be noted that these velocities are about 10 times the velocity ceiling encountered in Homopolar I, II, and III and, to our knowledge, all other rotating-plasma machines. We attribute this to the fact that, even though about 2.5 msec elapsed between the opening of the puff valve and breakdown of the gas in the machine, the neutral gas still could not reach the insulators or surfaces not parallel to the magnetic field.

The rotational velocities mentioned above correspond to 1440 ev and 160 ev energy of the deuterons. Since the back voltage never goes down to low values before crowbar time, we expect approximately equal energies in Larmor motion of the deuterons. Both the rotational and Larmor energies are tentatively confirmed by preliminary Doppler-shift measurements with a monochromator. This together with the fact that the ion density should be of the order of 10^{14} cm^{-3} suggests that a search for neutrons is appropriate. An estimate of the neutron production in this machine gives the result that we should detect neutrons for back voltages higher than 40 kv, depending of course somewhat on the detection equipment. Unfortunately we cannot obtain higher back voltages than 30 to 35 kv at present, since the magnetic field we can produce with our present equipment is not strong enough to support the centrifugal force associated with higher rotational velocities.

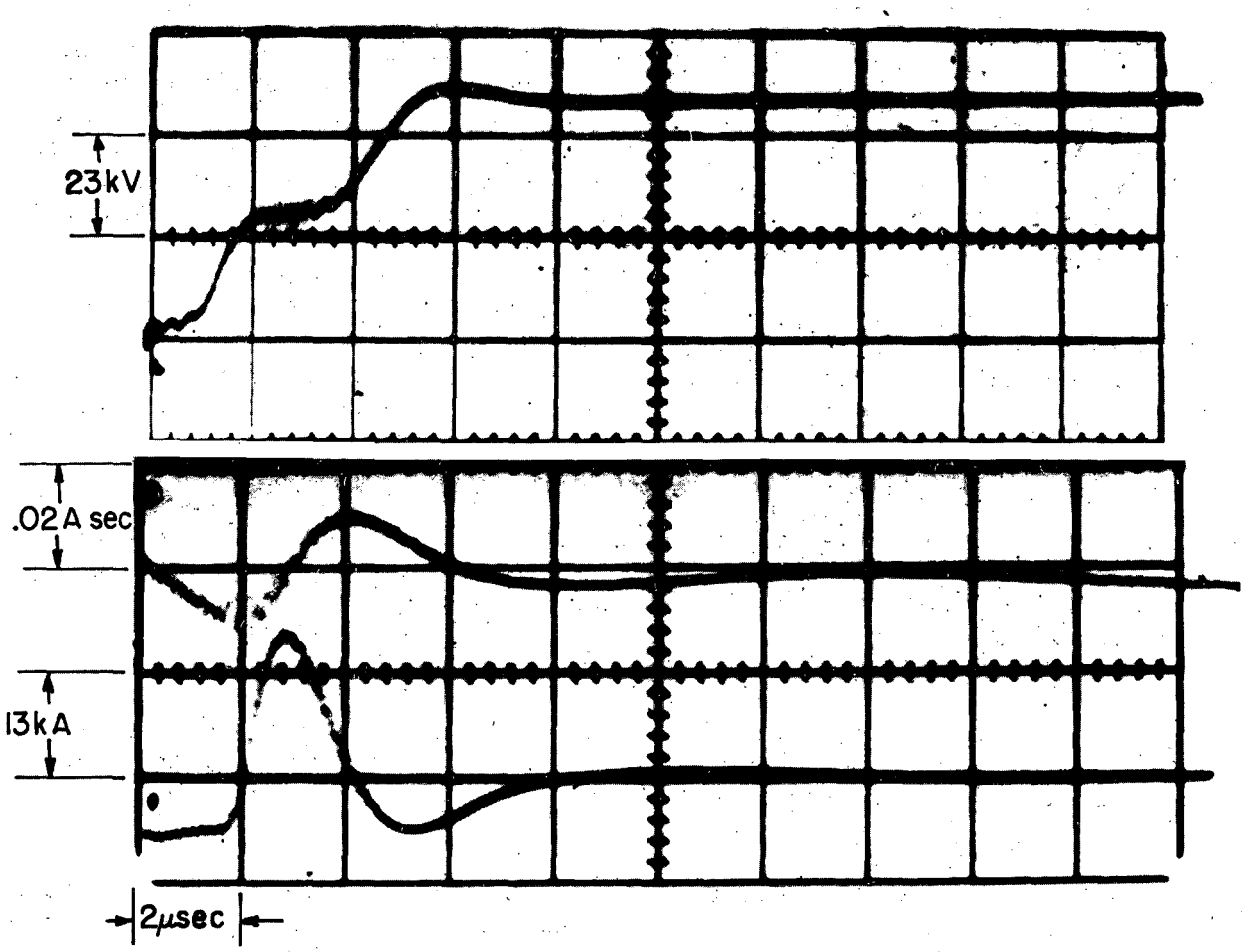

ZN-2761

Fig. 13. From top to bottom, voltage, charge, and current traces.

3. HYDROMAGNETIC WAVE AND CYCLOTRON HEATING

Hothouse I

William S. Cooper III, Alan W. DeSilva, and John M. Wilcox

Resistivity Measurement

We have experimentally measured the "parallel" resistivity of the hydrogen plasma in the Hothouse I experiment as a function of time under typical operating conditions (initial hydrogen pressure, 100 μ of Hg; magnetic field, 16,000 gauss). The electron temperature was then derived from the resistivity measurements. The resistivity was measured directly by observing the potential drop produced by a known current in the plasma.

To perform this experiment the insulator at the receiving end of the tube was provided with an electrode of the same diameter as that at the driving end, and the plasma was then prepared as described previously. After the ionizing current was crowbarred, a small probing current was induced between the two electrodes. This current is confined to a cylinder along the axis of the tube defined by the diameter of the electrodes, since any radial currents would accelerate the plasma azimuthally, setting up back emf's that oppose such current flow. Since there will of necessity be a small potential gradient along the axis of the tube (indeed, this is what we are measuring), there will also be a small amount of plasma rotation. The radial current required to maintain this rotation against viscous losses constitutes a leakage current. Measurements were made under conditions such that this was a small effect.

The probing current should be small enough so that the energy deposited in the plasma during the measurement does not change the average energy of the plasma. In practice this perturbation energy was less than 10% of the plasma thermal energy.

Wave observations have indicated that near the tube walls, an insulating boundary layer tends to form which isolates the plasma electrically from the wall. This boundary layer is presumably due to a local drop in the electron temperature, and hence conductivity, near the wall. Such a boundary layer at an electrode would add a spurious resistance to that of the main body of plasma, resulting in a high value for the calculated resistivity. Thus the measurement sets an upper limit to resistivity and a lower limit to temperature.

The attenuation for hydromagnetic waves of the type produced in this experiment is principally determined by $\eta_{\parallel}$,[1] which is the part of the resistivity tensor that is measured by the above method. The resistivity was determined as a function of time by turning on the probing current at various times after crowbar. The results of this measurement are plotted in Fig. 14, where the indicated temperature is calculated from Spitzer's formula for $\eta_{\parallel}$. We have also plotted the temperature as determined by damping of Alfvén waves. The agreement around 50 μsec, when wave experiments are normally

[1] L. Spitzer, The Physics of Fully Ionized Gases (Interscience Publishers Inc., New York, 1956).

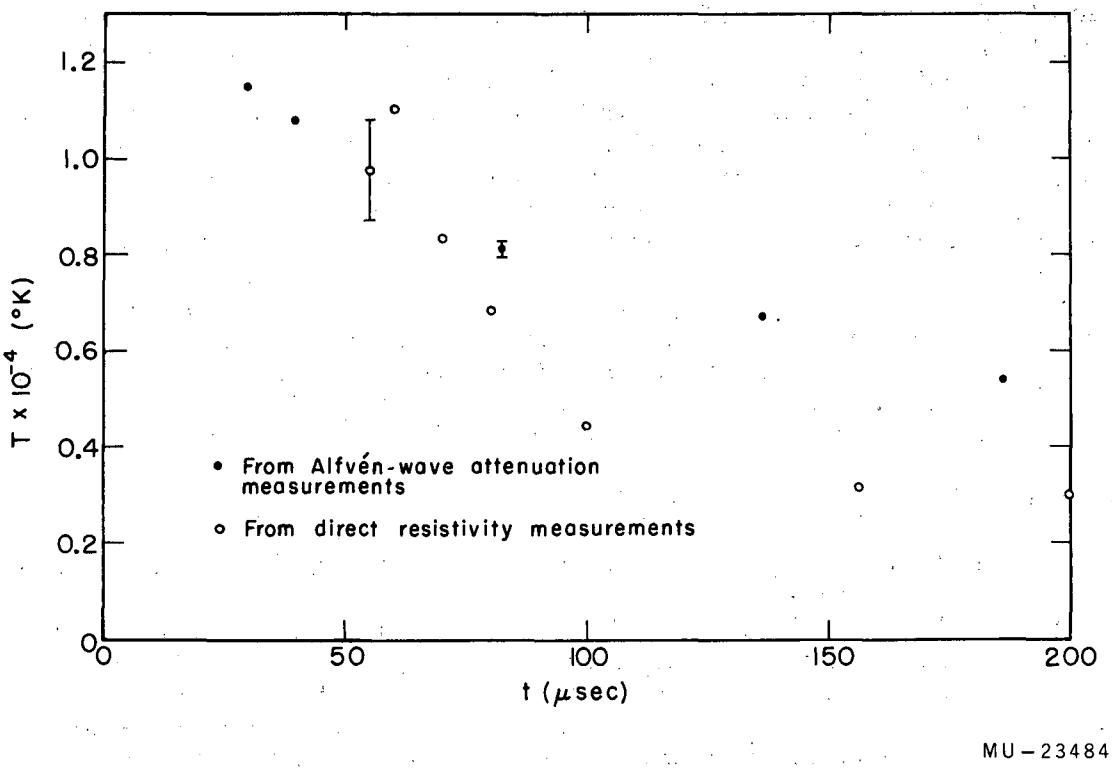

Fig. 14. Plasma temperature vs time, from both Alfvén-wave attenuation measurements and direct resistivity measurements. Sample standard deviations are shown for two points.

performed, is very good, with an indicated temperature of 12,000 ^{o}K. The temperature as determined by the direct resistivity measurement drops more rapidly in time, probably reflecting a local increase in resistivity in the plasma close to the electrodes due to cooling by thermal conduction.

Impurity Levels

We have also estimated the level of impurities in the plasma. Analysis of emission spectrum of the discharge in the visible region reveals, in addition to the strong lines of the hydrogen Balmer series, lines characteristic of Si, Si^{+}, Si^{++}, Si^{+++}, O, O^{+}, C^{+}, and Na. An estimate of the absolute number density of impurity atoms within the discharge region may be made by comparison of observed impurity line intensities (using a monochromator) before and after introduction of a known amount of impurity gas. Methane (CH_4) and oxygen (O_2) were used to estimate the impurity levels of carbon and oxygen, respectively. It was found that the observed line intensities could be explained by the presence of partial pressures of 0.2 μ of carbon and 0.4 μ of oxygen. Oxygen presumably comes from minute leaks, outgassing, bottled gas impurity, and insulator materials. Since silicon would come only from insulator material (no silicon oils are used in the vacuum pumps), it is assumed that the level for oxygen represents also an upper limit for silicon. Translating these figures into mass densities, we obtain an estimate of the impurity mass density of 1.1×10^{-9} g/cm^3.

Effect on Alfvén-Wave Velocity Measurements

Thus if we use hydrogen mass densities above 10^{-8} g/cm^3, which corresponds to pressures above 100 μ of H_2, the density perturbation due to impurities should be less than 11%. The mass density enters the formula for the Alfvén-wave velocity as a square root, and so the change in velocity due to impurities at 100 μ of H_2 is of the order of 5%. These calculations assume a uniform distribution of impurity atoms throughout the discharge region. In reality, the impurities seem to originate at the walls, and estimates of diffusion times for these atoms into the central plasma region indicate that they could not penetrate significantly far in the time available. The base pressure in the tube is 0.02 μ. If we assume that this residual gas is air, then we can calculate that the density perturbation to 100 μ of H_2 is only about 0.15%.

Hydrogen itself may represent an impurity, since gas which is absorbed on the walls of the tube may be released in the ionization process, increasing the density of the plasma. That the spectroscopically measured ion densities agree so well with the particle density of gas initially put in the tube indicates that this process is probably not important. We conclude, then, that the presence of impurities in the plasma influences the plasma mass density by only a few per cent from that calculated from a knowledge of the initial hydrogen pressure.

Ion Cyclotron Resonance

Peter R. Forman, Gordon W. Hamilton, and John M. Wilcox

The oscillators were tested at medium power in push-pull. The loading of the two oscillators was found to be unbalanced because of the necessity of

unequal lengths of transmission lines for push-pull loading. The unbalanced loading could not be corrected by changing grid drives, so we decided to modify the oscillators to run them in parallel rather than push-pull.

The oscillator grids were connected through a small resistance to make them oscillate in parallel. A variable inductance, consisting of a variable-length shorting stub, was inserted in parallel with the plasma load to adjust the load voltage for efficient operation. After adjustments, the oscillators were run at their full power of about 450 kw each.

For safety purposes a "crowbar" consisting of five ignitrons in series was connected across each oscillator pulse line. If sparking or excessive current occurs in the oscillator, a signal from a pulse discriminator actuates the ignitron crowbars through a 5C22 and a pulse transformer.

At low oscillator powers, the plasma presents a load for only a few hundred microseconds after firing the pre-ionizing slow bank. At higher oscillator powers, the plasma load lasts throughout the 3-msec pulse. However, the propagated wave is uneven and highly attenuated. Optical observations of the deuterium β light indicate that the light is prolonged by the rf, compared with the slow bank alone. More light is emitted under conditions of a magnetic beach than with a uniform magnetic field, but Doppler broadening is unmeasurable.

It has been decided to increase the magnetic field at the center of the chamber and to install outer electrodes at both ends of the cylindrical chamber so that the effective shape of the chamber will conform to the shape of the magnetic field lines.

4. SOME EFFECTS OF FINITE CONDUCTIVITY IN HOTHOUSE I

T. G. Northrop

Two effects of finite conductivity have been calculated for the Hothouse I experiment (Alfvén waves in a cylinder). The first is the phase difference between the applied current and voltage. The second is the difference to be expected between the observed velocity of propagation of a pulse and the Alfvén velocity. If the plasma conductivity were infinite, the current and voltage of a sinusoidal wave would be in phase at the input end, and the observed velocity of a pulse would be the Alfvén velocity. The somewhat idealized geometry used for the calculation is shown in Fig. 15.

Fields and currents in the wave are as follows.[1]

<u>The perturbation magnetic field:</u>

$$b_\theta(r, z, t) = \sum_{n=1}^{\infty} b_n J_1(k_{cn} r) e^{-z/L_n} \cos(k_n z - \omega t);$$

[1] Alan W. DeSilva, William S. Cooper III, and John M. Wilcox, Alfvén Wave Reflections and Propagation Modes, UCRL-9496, Feb. 1961.

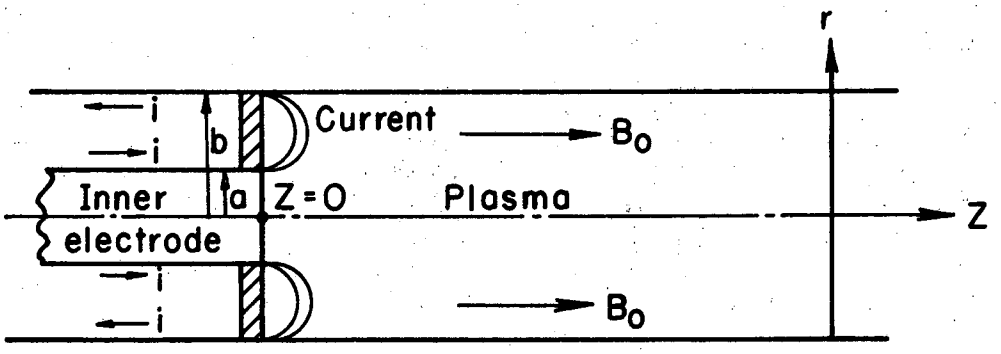

MU-23485

Fig. 15. Geometry of the Alfvén-wave experiment.

The radial and longitudinal current densities:

$$j_r(r, z, t) = \frac{1}{\mu_0} \sum b_n J_1(k_{cn} r)\, e^{-z/L_n} \left[k_n \sin(k_n z - \omega t) + \frac{1}{L_n} \cos(k_n z - \omega t) \right],$$

$$j_z(r, z, t) = \frac{1}{\mu_0} \sum b_n k_{cn} J_0(k_{cn} r) e^{-z/L_n} \cos(k_n z - \omega t);$$

The plasma velocity:

$$v_\theta(r, z, t) = -\frac{V^2}{\omega B_0} \sum b_n J_1(k_{cn} r) e^{-z/L_n} \left[k_n \cos(k_n z - \omega t) - \frac{1}{L_n} \sin(k_n z - \omega t) \right];$$

The radial electric field:

$$E_r(r, z, t) = \sum b_n J_1(k_{cn} r)\, e^{-z/L_n} \left[\left(\frac{k_n}{\mu_0 \sigma} - \frac{V^2}{\omega L_n} \right) \sin(k_n z - \omega t) + \left(\frac{1}{\mu_0 \sigma L_n} - \frac{V^2 k_n}{\omega} \right) \cos(k_n z - \omega t) \right];$$

where V = Alfvén velocity = $(B_0^2/\mu_0 \rho)^{1/2}$. The Ohm's law used is $\vec{j} = \sigma(\vec{E} + \vec{v} \times \vec{B})$. Thus Hall current, electron inertia, and electron pressure have been neglected.

The experimental fact that j_r vanishes at the outer wall has been used in the above equations. The k_{cn} are therefore quantities such that bk_{cn} are zeroes of J_1. The quantities k_n and $1/L_n$ are the real and imaginary parts of

$$\left(\frac{i\omega^2/V^2 - \alpha k_{cn}^2}{\alpha + i} \right)^{1/2},$$

where α is $\omega/\mu_0 \sigma V^2$. For infinite conductivity α vanishes and $k_n = \omega/V$, $1/L_n = 0$.

The object is to superpose the modes (denoted by the index n) in such a way as to match known boundary conditions. The radiation problem is thereby solved. The boundary conditions at $z = 0$ determine the b_n. In the coaxial line b_θ must go as $1/r$ for $a < r < b$ (see Fig. 15). Because of the continuity of the tangential component of the magnetic field across the insulator, b_θ must also have a $1/r$ dependence in the plasma at $z = 0$ between $r = a$ and $r = b$. The other condition to be fulfilled is that E_r vanish at $z = 0$ for $0 < r < a$. This is because E_r must vanish in the conducting center electrode, and the tangential component of the electric field is continuous across an interface.

By means of a formal expansion in α (which is nonconvergent, but probably asymptotic), the quantities b_n, $b_\theta(r, 0, t)$, and $E_r(r, 0, t)$ can be determined to first order in α. From the equations given above it can be seen that at $z = 0$, b_θ varies as $\cos \omega t$, while E_r is of the form $E_s(r) \sin \omega t + E_c(r) \cos \omega t$, where

$$E_s(r) = -\sum b_n J_1 (k_{cn} r) \left(\frac{k_n}{\mu_0 \sigma} - \frac{V^2}{\omega L_n} \right)$$

and

$$E_c(r) = \sum b_n J_1 (k_{cn} r) \left(\frac{1}{\mu_0 \sigma L_n} - \frac{V^2 k_n}{\omega} \right) .$$

Thus for $\sigma = \infty$, E_r and b_θ are in phase. But for $\sigma \neq \infty$, there will be a phase difference. To first order in α one finds

$$E_s(r) = -\frac{\alpha V a_0}{r} ,$$

$$E_c(r) = \frac{V a_0}{r} ,$$

$$E_r(r, 0, t) = \frac{V a_0}{r} \left(- \frac{\alpha}{2} \sin \omega t + \cos \omega t \right),$$

where a_0/r is the amplitude of $b_\theta(r, 0)$; i.e., $b_\theta(r, 0, t) = a_0/r \cos \omega t$ (for $r > a$). Because $b_\theta(r, 0, t)$ is in phase with the applied current, and because $\int_a^b E(r, 0, t) dr$ is the applied voltage, the current lags the voltage by $\alpha/2$ radians. A plasma with finite conductivity appears inductive to the input circuit. In the experiment $\alpha \approx 0.01$, so the phase lag $\approx 1/4$ deg, which would be unobserved in the present experiments.

The first-order (in α) effect of resistivity on the rate of propagation of a pulse has also been calculated, without making the assumption that only a small band of frequencies is present. If a current pulse is sent between inner and outer electrodes, many frequency components are present, and the fields are superpositions of them. For example,

$$b_\theta(r, z, t) = \int_0^\infty d\omega\, A(\omega) \sum_n b_n J_1(k_{cn} r) \exp(-z/L_n) \cos\left[k_n z - \omega t + \phi(\omega)\right].$$

Here $A(\omega)$ and $\phi(\omega)$ are determined from the shape of the current pulse. Let it be somewhat as shown in Fig. 16. The quantities k_n and $1/L_n$ are functions of ω. At a given radius and z, $b_\theta(r, z, t)$ will have a maximum as a function of t. At a larger z, the maximum arrives at a later time. The difference in z divided by the time difference is the experimentally observed "velocity." Since k_n/ω is a function of ω, the velocity of each frequency component is different, and one expects the usual group velocity effect. However, it happens that $k_n = \omega/V + 0(a^2)$, so that this usual effect is of order a^2 and negligible. But $1/L_n = a(1/L_n)_1 + 0(a^3)$; i.e., k_n contains only even powers of a, while $1/L_n$ contains only odd powers. As a consequence the primary [i.e., $0(a)$] effect of the resistivity is that different frequencies damp at different rates but travel with the same velocity. This changes the shape of the pulse with time, hence affects the position of the maximum.

The result of the analysis shows that the observed velocity would be

$$V(1 + Ia),$$

where

$$I = \int_0^\infty \omega^2\, d\omega \int_{-\infty}^\infty \frac{i(t)}{i''(t_0)} \sin\omega(t - t_0)\, dt,$$

and

$$i''(t_0) = \left.\frac{d^2 i}{dt^2}\right|_{t=t_0}.$$

If $i(t)$ is symmetric about t_0, I vanishes. Then the difference between the observed velocity and V is $0(a^2)$ and is the usual group velocity effect.

There is another velocity that might be observed. Suppose at a given time the position of the peak of b_θ as a function of z were observed. At a later time let the z of the peak again be located. These two measurements define a different velocity, which is the true velocity of the peak of the pulse. It turns out to be $V(1 + Ia/2)$.

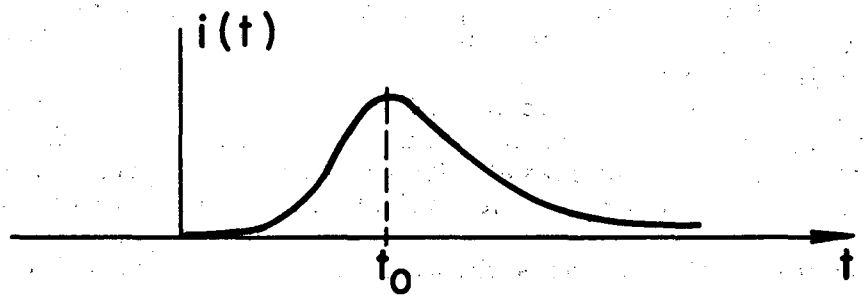

MU-23486

Fig. 16. Current pulse between electrodes as a function of time.

5. PLASMA PHYSICS AND MICROWAVE DIAGNOSTICS

Donald B. Hopkins, George A. Paulikas,* Robert V. Pyle,
Henry F. Rugge, and J. Warren Stearns

Microwave Diagnostics

Goubau transmission lines made from 10- and 15-mil anodized aluminum wire are being used to measure the density of plasmas in weak discharges (10^{10} to 10^{12} electrons/cm^3); see Fig. 17. The G line is parallel to the axis of the tube and is incorporated in one leg of an 8-mm microwave interferometer. Auxiliary experiments show that 90% of the energy is within 5 mm of the wire. The plasma perturbation produced by the fine wire can be inferred from changes in the axial electric field. The limits of the technique will be investigated by raising the discharge current.

Enhanced-Diffusion Experiment

The dc and quasi-dc experiments have been completed and a final report is in preparation. An experiment is in progress to investigate the growth of the instability when the driving current of the discharge alternates at approximately the frequency of the instability.

Dissociation of Molecular Ions by Magnetic Fields

Hiskes has shown that several types of molecular ions can be dissociated by electric fields of the order of 10^6 volts/cm or less, if the ions are in high vibrational states.[1] An equivalent Lorentz force should also produce the same effects. Recently Riviere and Sweetman have experimentally demonstrated the breakup of H_2^+ ions by electric fields.[2] An experiment is in progress to examine the breakup of H_2^+, H_3^+, and perhaps other ions in magnetic fields, using 10-Mev/nucleon ions from the heavy-ion linear accelerator. This phenomenon may possibly provide a technique for injecting and trapping a beam in a highly evacuated confining geometry.

---

*National Science Foundation Fellow.

[1] John R. Hiskes, Dissociation of Molecular Ions by Electric Fields, UCRL-9182 (Rev.), Nov. 1960.

[2] A. C. Riviere and D. R. Sweetman, Phys. Rev. Letters 5, 560 (1960).

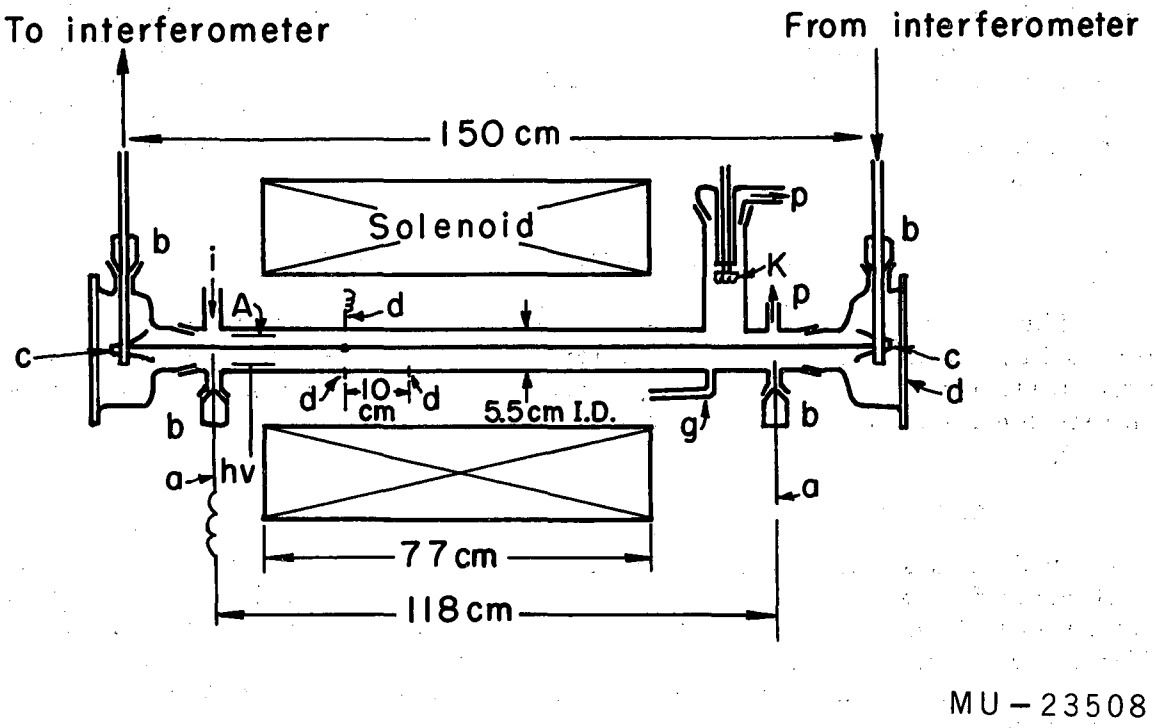

Fig. 17. Goubau-line interferometer: A, anode; K, cathode, a, movable electrostatic probe with collecting area at —●— ; b, sliding Wilson seals; c, Goubau launcher and receiver horns; d, electrostatic probes; i, gas inlet; p, pumpout; g, pressure gauge.

6. PREBREAKDOWN CROSSED-FIELD STUDY

Melvin J. Bernstein and Wulf B. Kunkel

The measurements of the ionization coefficient α/p in H_2 across a strong magnetic field[1] have been completed. Measured values of α/p lay between 0.04 and 2.5 cm^{-1} $(mm\ Hg)^{-1}$. Smaller values had too large an error and larger values with this system produced excessive ionization or breakdown. Figure 18 shows a typical set of curves for measuring α/p, where ln i is plotted as a function of gap separation. Two values of i were measured at most gap separations, denoted by d, in order to check reproducibility. Figure 19 shows the results plotted along with the predicted theoretical curves. The theoretical equation (Blevin and Haydon[2]) states

$$\alpha/p = 5.4\sqrt{1+\omega^2\tau^2}\ \exp\left[-139(p/E)\sqrt{1+\omega^2\tau^2}\right],$$

where ω = cyclotron frequency, $1/\tau$ = average collision frequency, p = pressure of gas in mm, E = electric field in V/cm. As suggested by the authors of the theory, the value for the collision frequency was adjusted to produce the best fit with the experimental points. By trial and error this collision frequency was found to be $1/p\tau = \nu_c/p = (3.1 \pm 0.1) \times 10^9\ sec^{-1}$ $(mm\ Hg)^{-1}$. These measurements were made at 20°C.

This value for the collision frequency is very much smaller than those deduced by other methods.[3] This large discrepancy comes from deviations in the theory. The theory assumed a constant collision frequency and only elastic collisions. A qualitative analysis for the effect of the actual cross section of H_2 and of inelastic collisions shows that α/p should be smaller than predicted by theory is good only for yielding an expression for α/p in the range 0.15 to 3.0. It probably holds for much larger values, but no verification has been made.

At present, experiments in the same geometry are being developed to measure directly the drift velocity of electrons in hydrogen under the influence of an electric field crossed with a strong magnetic field.

---

[1] Melvin J. Bernstein, in Controlled Thermonuclear Research Quarterly Report, UCRL-9243, June 1960, p. 76; in Controlled Thermonuclear Research Quarterly Report, UCRL-9393, Sept. 1960, p. 56.

[2] Blevin and Haydon, Australian J. Phys. 11, 18 (1958).

[3] S. C. Brown, Basic Data of Plasma Physics (John Wiley and Sons, Inc., New York, 1959).

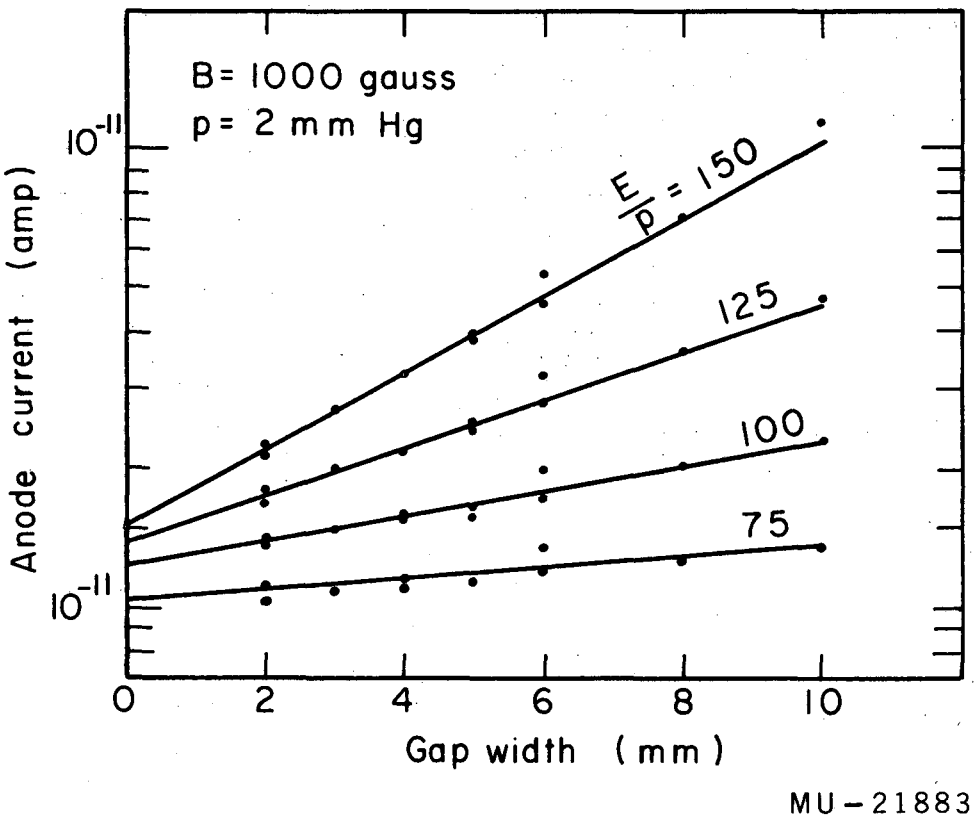

Fig. 18. Typical set of data plotting ln i vs d, from which α/p is computed.

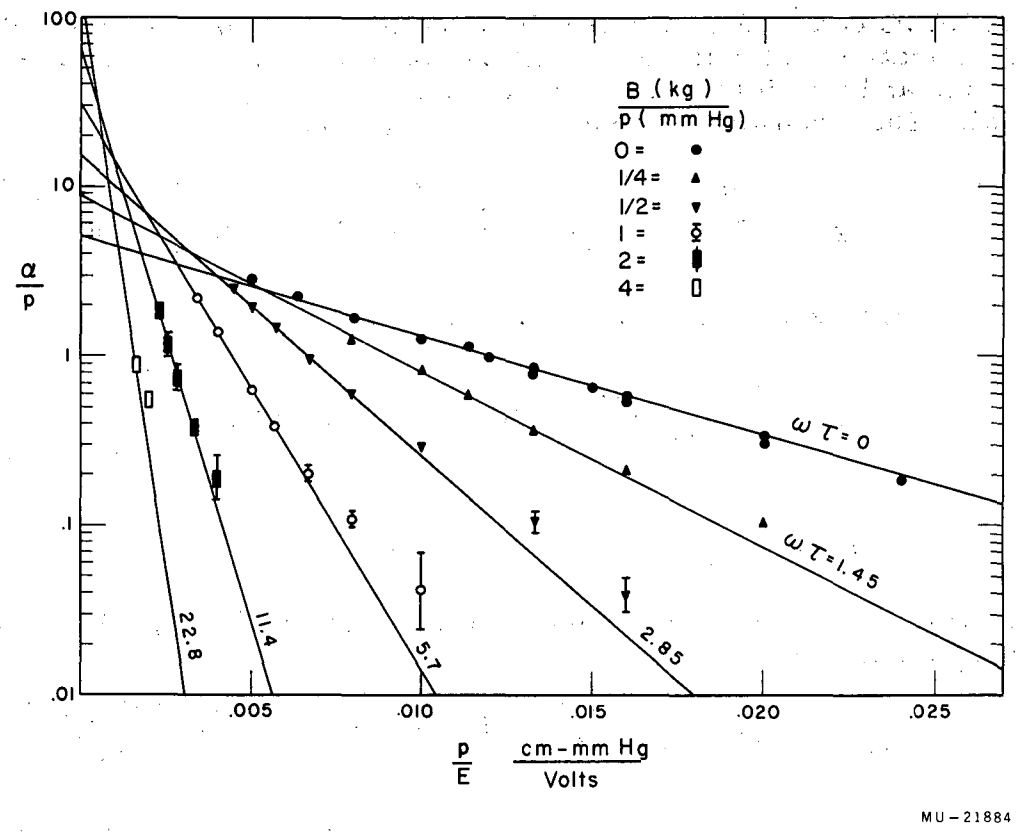

Fig. 19. Experimental values of α/p plotted vs p/E along with theoretical curves of α/p. With these coordinates the theoretical curves are straight lines.

V. THEORETICAL AND BASIC EXPERIMENTAL PLASMA PHYSICS

1. A COMPUTATION FOR STUDYING THE FORMATION OF THE ASTRON E LAYER

John Killeen

A LARC code called LAYER is being prepared to study the self-consistent formation and build-up of the Astron E layer. Cylindrical symmetry is assumed and the field can be specified by one component of the vector potential. The equation to be solved for $A_\theta(r, z, t)$ is

$$\frac{1}{c^2} \frac{\partial^2 A_\theta}{\partial t^2} - \frac{\partial^2 A_\theta}{\partial z^2} - \frac{\partial}{\partial r}\left[\frac{1}{r} \frac{\partial}{\partial r} (rA_\theta)\right] = j_\theta,$$

where $j_\theta(r, z, t)$ is the current density given by

$$j_\theta = \frac{2ep_\theta}{r} \iint \gamma^{-1} \rho(r, z, p_r, p_z, t)\, dp_z\, dp_r,$$

$$\gamma = (1 + p_z^2 + p_r^2 + p_\theta^2)^{1/2} .$$

The function ρ is the electron distribution in phase space, which satisfies Liouville's equation,

$$\frac{\gamma}{c} \frac{\partial \rho}{\partial t} + p_z \frac{\partial \rho}{\partial z} + p_r \frac{\partial \rho}{\partial r} + qp_\theta \frac{\partial A_\theta}{\partial z} \frac{\partial \rho}{\partial p_z} + \frac{p_\theta}{r}\left(p_\theta + q \frac{\partial (rA_\theta)}{\partial r}\right) \frac{\partial \rho}{\partial p_r} = 0.$$

The difference equations corresponding to the above set of partial differential equations has been derived. The relevant equations have been coded for the LARC, and the program is now being debugged.

2. STABILITY OF INFINITELY THIN ELECTRON LAYERS

V. Kelvin Neil

Investigation of the instability described in the preceding quarterly report has continued. At the time of the preceding report there remained a question of the accuracy of the criterion for stability as applied to Astron. A more refined calculation has been made which indicates that the previous numerical results were indeed correct. If the electrons move in the azimuthal direction and have an angular spread in velocity, this angular spread must be some 45 deg to prevent bunching in the axial direction. The temperature of the neutralizing ions was neglected in the calculation, but it can be shown that a value of the ion temperature likely to be achieved in practice will have a negligible stabilizing effect. It is not clear just what the electron velocity distribution in Astron will be, but it appears possible that a very large spread in axial velocity may be present, perhaps of the order of magnitude of that required for stability. The more precise treatment of this problem is being prepared for publication.

3. INSTABILITY OF A RESISTIVE SHEET PINCH

Harold P. Furth and John Killeen

The effect of finite conductivity on the stability of a sheet pinch is being investigated. An analysis is made of a model using an incompressible fluid of infinite extent, with a sheetlike region of finite, isotropic conductivity representing the pinch. The procedure is to assume perturbations in the magnetic field and plasma velocity, which in the infinite-conductivity approximation should lead to stable hydromagnetic oscillations, and to calculate their resistive relaxation. We obtain a pair of partial differential equations for the first-order perturbations in the magnetic field and plasma velocity.[1] The differential equations are solved by replacing them by a pair of implicit difference equations. The solution of the difference equations is effected by an IBM 709 code called RIPPLE which has been completed and is being used. Unstable relaxations are found for wave lengths large compared with the thickness of the sheet pinch.

[1] Harold P. Furth and John Killeen, Resistive Relaxation of a Perturbed Sheet Pinch in Controlled Thermonuclear Research Quarterly Report, UCRL-9500, p. 76.

4. SCATTERING LOSSES FROM MAGNETIC MIRROR MACHINES

David J. BenDaniel*

A report has been prepared, David J. BenDaniel, A Theory of Scattering Loss from a Magnetic Mirror System, UCRL-6236, March 1961. This report collects and summarizes the theory and some of the numerical results previously reported.[1]

The attempt of this work was to develop an approximate theoretical description of the scattering losses from a magnetic mirror machine, which would be more amenable to numerical calculations than the numerical calculations of the Fokker-Planck equation such as carried out by Roberts.[2, 3]

The principal approximation is the assumption of the separability of the distribution function into a product of functions of speed and angle. The development finally leads to equations describing the various features of physical interest. The results correct previous calculations of a similar nature,[4] which indicated mirror losses, for a mirror ratio of about 3.3, greater than found herein by a factor of about two. The present results thus check and verify to a good approximation the numerical results of Roberts.[2, 3]

*Now at General Electric Company, Research Laboratory, Schenectady, N. Y.

[1] Controlled Thermonuclear Research Quarterly Reports, UCRL-8887, Sept. 1959, p. 83; UCRL-9002, Dec. 1959, p. 82.

[2] Controlled Thermonuclear Research Quarterly Report, UCRL-9243, June 1960, p. 100.

[3] J. Roberts and M. Carr, End Losses from a Mirror Machine, UCRL-5651T, Apr. 1960.

[4] A. Garren, R. Riddell, L. Smith, G. Bing, J. Roberts, T. Northrop, and L. Henrich, "Individual Particle Motion and the Effects of the Scattering in an Axially Symmetric Magnetic Field", UCRL-8076, March 1958.

In addition, the theory has been extended to consider "short mirror systems" as opposed to "long" or "square-well" mirror systems. Numerical results on the effect of the finite size of the mirror region on the loss rate are given.

5. THE MAGNETIC COMPRESSION OF A PARTIALLY IONIZED GAS

Donald P. Geesaman and John Killeen

The preparation of the new code, PLASMA II, which was described in the preceding quarterly report,[1] has been continued. The purpose of this code is to investigate the hydromagnetic compression of a partially ionized gas. Ohmic heating is confined to the electrons, and is determined by the electric resistivity, which may be different parallel and perpendicular to the magnetic field and is a function of the electron temperature and the degree of ionization.[2] Shock heating applies only to the ions. Heat exchange between the components is included.[2]

The effects of thermal conduction, ionization, and charge exchange are included in the equations for the ion, electron, and neutral temperatures as well as the equations of motion and equations of continuity. The relevant differential equations for a cylindrically symmetric problem have been derived and the difference equations formulated. An investigation of the inclusion of the effects of runaway electrons in the problem has also been carried out.

[1] Controlled Thermonuclear Research Quarterly Report, UCRL-9500, p. 74.

[2] J. Killeen, G. Gibson, and S. A. Colgate, Boundary Layer Formation in the Pinch, Phys. of Fluids 3, 387-394 (1960).

6. REARRANGEMENT COLLISIONS

Marvin H. Mittleman

The problem of rearrangement collisions has been considered. Previous formulations of this process suffer from the difficulty which is best described by saying that the initial and final states are not orthogonal. This results in a situation in which a constant potential (zero force) causes such a transition. A new formulation has been given (UCRL-6302, submitted to Phys. Rev.) in which this difficulty has been eliminated.[1] Transitions take place only between mutually orthogonal states.

The method is being applied to give a comprehensive treatment of proton-hydrogen scattering. At higher energies (> 25 kev) the hydrogen atomic states are used to expand the wave function. The resultant equations are being programmed for the IBM 650—at low energies the H_2^+ molecular wave functions, given by Bates et al., are used to expand the wave function. The resultant integrals are being done on the 650 and the differential equations which they enter into are being programmed for the 709.

[1] Marvin H. Mittleman, On the Formal Theory of Rearrangement Collisions (UCRL-6302, Feb. 1961), submitted to Phys. Rev.

7. CALCULATION OF THE DIFFUSION OF THE VACUUM MAGNETIC FIELD OF AN ELECTRON BEAM INTO A PLASMA

Warren Heckrotte, Ross E. Hester, and John R. Hiskes

Recently considerable theoretical effort has been devoted to the study of high-current high-energy electron beams traversing low-temperature plasmas. As a result of this interest a proposal has been made to study the hose instability[1] of a relativistic electron beam by using the Astron electron accelerator, which should provide a beam of a few hundred amperes in the range 2 to 5 Mev.

The velocity of propagation of the instability will be, to first order, equal to or less than 10^9 cm/sec. This rather slow propagation and an expected beam pulse length of 2×10^{-7} sec indicate that a plasma column of the order of 100 cm in length will be sufficient for an experiment. Therefore one experimental proposal is to pass the beam through a cylindrical column of plasma whose length is much greater than its diameter. It is expected that the plasma will be contained by a cylindrical quartz tube capped at the ends with very thin metallic foils. The plasma density will be of order 10^{13} ions/cm^3. Under these conditions one can assume that in the initial penetration of the beam into the plasma, currents are induced in the plasma body that exclude the electron beam's self-magnetic field from the plasma. The magnetic field must diffuse into the plasma before the instability can develop. Since the plasma column is very long compared with its diameter, and the time required for the beam to penetrate the plasma column is less than 10^{-9} sec, the magnetic field will diffuse radially into the plasma. Diffusion from the ends can be neglected.

Detailed calculations have been made of the diffusion times and field distributions for a cylindrical system. Figure 20 is a sketch of the model used for the calculation.

With respect to the problem of the magnetic field diffusing into the plasma, we conclude the experiment appears feasible if the conductivity of the plasma is of the order 10^{12}/sec. Specifically, for a beam diameter of 1 cm, a plasma diameter of 10 cm, and $\sigma = 10^{12}$ sec, sufficient diffusion will occur in 2×10^{-8} sec to support the instability growth.

The experimental configuration considered here is such as to minimize the role of displacement currents. We are extending our consideration to other configurations in which the displacement current may be expected to play an important role.

---

[1] Harold W. Lewis, Stability of a Relativistic Beam in a Plasma, Jason Summer Study Group, 1960, Institute for Defense Analyses.

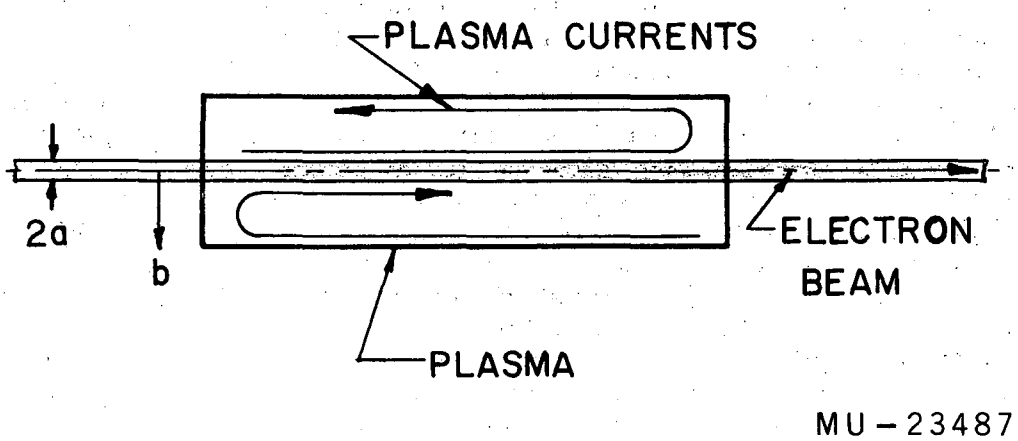

Fig. 20. Model for diffusion calculation.

8. THEORY OF AN ELECTROSTATIC PROBE IN A PLASMA

Laurence S. Hall and Donald P. Geesaman

A description of this problem and its motivation has been given earlier.[1] Briefly, Poisson's equation and the collisionless Boltzmann equation are solved simultaneously to obtain the behavior of spherical and cylindrical electrostatic probes in a plasma of infinite extent. The analysis leads to a nonlinear integro-differential equation of the form

$$\frac{1}{r^g}\frac{d}{dr}\left(r^g\frac{dV}{dr}\right) = -4\pi e\left\{Z_R n_R e^{-Z_R eV/\theta_R} + Z_A K\left[\frac{2}{r^g}\int_0^\infty d(L^g)\int_{\chi_M(L,r)}^\infty dE\,\frac{F_A(E,L)}{\sqrt{E-\chi(L,r)}} - \frac{1}{r^g}\int_0^\infty d(L^g)\int_{\chi_M(L,r_p)}^\infty dE\,\frac{F_A(E,L)}{\sqrt{E-\chi(L,r)}}\right]\right\},$$

where $g = 1, 2$ for cylindrical and spherical cases, respectively; R, A are indices for repelled and attracted particles; K is a normalization constant; $\chi(L,r) \equiv L^2/2m_A r^2 + eZ_A V$; $\chi_M(L,r) \equiv \text{Max}\ \chi(L,r^1)$, $r \leqslant r^1 < \infty$; r_p is probe radius; L is angular momentum; E is energy; n is particle density; and $F_A(E,L)$ is the distribution of inwardly directed particles, taken to be Maxwellian at infinity. The function $\chi_M(L,r)$ can be computed directly for an inward numerical integration of the equation. The function $\chi_M(L,r_p)$, however, involves a complete knowledge of V, and hence any solution must be obtained by an iterative procedure based on an approximate knowledge of V or $\chi_M(L,r_p)$. For the equation written in dimensionless form such a procedure has been programmed for the IBM 709.

The normalization and boundary conditions of the problem are

$$V(r_p) = V_p,$$

and the degenerate

$$V(r) = \frac{dV(r)}{dr} = \frac{d^2V(r)}{dr} = 0 \qquad \text{for } r \to \infty.$$

[1] Robert L. Chazin, Donald P. Geesaman, John Killeen, and Laurence S. Hall, in Controlled Thermonuclear Research Quarterly Report, UCRL-9393, Sept. 1960, p. 67.

In the initial attempts at integrating this equation the boundary conditions of vanishing potential, field, and charge density were imposed at a radius R, large compared with the sheath thickness. For R's of practical interest this proved too crude an approximation. This is not surprising, as it introduced an error of the order $1/R^g$, and the nonlinear character of this differential equation makes it pathologically sensitive to changes of boundary conditions. An improvement is possible, however, since for sufficiently large r the equation reduces to a form of Bessel's equation with an inhomogenous term. A particular integral can be found to various orders of $1/r^g$, and by using the boundary conditions for $r \to \infty$ a one-parameter family of solutions is found in this region. These solutions can be used to calculate the boundary conditions for the numerical integration of the nonlinear region. The free parameter is then adjusted to satisfy the condition at the probe.

This improvement has recently been incorporated into the calculation along with some changes designed to minimize the computational error in the region of small V. This latter step was necessary since our interest in the details of the small field penetrating beyond the sheath has committed the calculation to a difficult numerical integration across a region of small and slowly changing potential. In this region appreciable computational errors are difficult to prevent and are disastrously amplified.

9. MAGNETIC SHOCKS

Stanley A. Zwick

Approximate loop solutions for the zero-temperature magnetic pulse problem have been obtained for μ (the reciprocal of the Alfvén Mach number in the undisturbed plasma) in the range 0.06 to 0.25. (Solutions with μ greater than 0.25 were presented in an earlier report.[1]) Mathematical (convergence) difficulties, not related to the physics of the problem, have cost the present group of solutions quantitative accuracy; however, the general features of the group are as follows.

For μ less than about 0.15, the magnetic field is reversed near the loop center (x = 0). The resultant $\underline{v} \times \underline{B}$ force produces a reflex curvature of the legs of the loop, where the particle velocity is relatively high. At the top of the loop, the constant "downward" electric field predominates, as for solutions with larger μ. The resultant trajectory, for a field reversal in a small region near the loop center, would be about as indicated in Fig. 21. It may be noted that the electric field (in a frame moving with the pulse) causes the reflex curvature of the loop legs to extend somewhat beyond the region of field reversal. Similarly, it results in a slight down-bend at the loop crossing for loop solutions without magnetic field reversal if the magnetic field is nearly zero at the loop center.

Thus far, there is no indication that loop solutions cannot be found for arbitrarily small μ. Also, there is no reason to expect any change in the

[1] Stanley A. Zwick, in Controlled Thermonuclear Research Quarterly Report, UCRL-9393, Sept. 1960, p. 63.

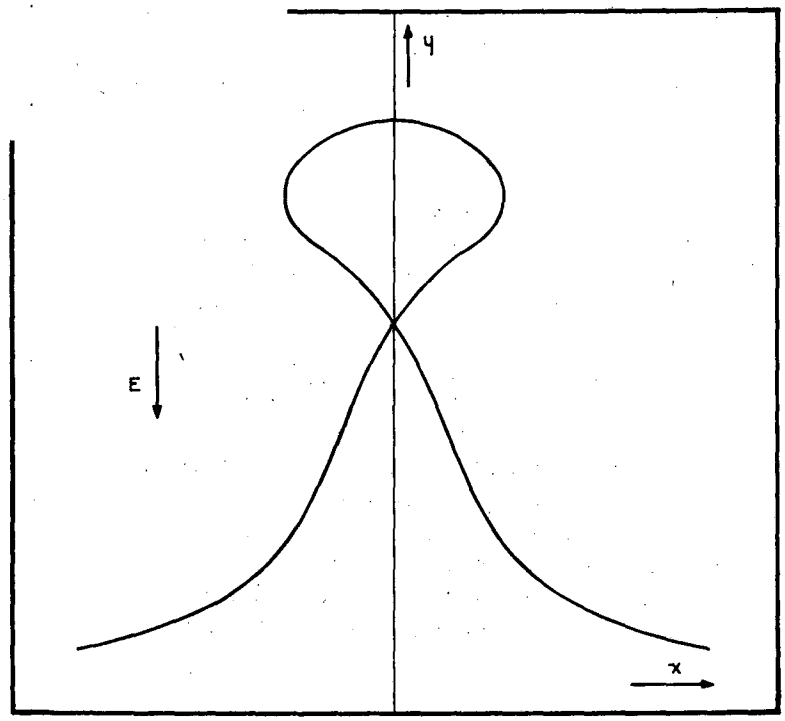

MU-23488

Fig. 21. Indicated loop trajectory with magnetic field reversal.

the domed shape of the loop top (such as the appearance of secondary loops there). Finally, for at least a class of loop solutions, it appears that the sum of the loop ordinates $y_1 + y_2 + y_3$ is constant through the loop. The reason for this is not known.

10. BEAM LOADING OF A RADIO-FREQUENCY CAVITY

V. Kelvin Neil

The interaction of a beam of particles in an accelerator with the radio-frequency cavity that provides the accelerating electric field has been discussed by V. K. Neil and A. M. Sessler, Coherent Electromagnetic Effects in High-Current Particle Accelerators. I. Interaction of a Particle Beam with an Externally Driven Radio-Frequency Cavity, UCRL-9326, July 1960. The purpose of that article was to calculate the effects of the beam on the cavity, and to obtain an expression for the required driving voltage. This calculation was self-consistent; however, the eigenfrequency of the cavity was assumed to coincide with a harmonic of the beam circulation frequency. Since that work was completed, it has been pointed out by G. K. O'Neill and W. K. H. Panofsky that the externally applied voltage required may be considerably reduced by proper tuning of the cavity. The presence of the beam effectively changes the inductance of the cavity, and if the cavity is driven at resonance, the wall currents are out of phase with the driving mechanism. It is possible to vary the inductance of the cavity to compensate for this effect and bring the wall currents back into phase with the rf generator. The generator is most effective for maintaining the cavity voltage when it is exactly in phase with the wall currents. A self-consistent calculation has been performed to determine the necessary change in the cavity inductance. In most practical cases this change is of the order of 1% or less. The power supplied to the cavity is not changed thereby, but the power loss in the driving mechanism may be substantially reduced.

11. ELECTRIC DISSOCIATION CALCULATIONS

John R. Hiskes

The electric dissociation calculations are being extended to determine the threshold fields for dissociating the successive vibrational levels of all isotopic mixtures of the hydrogen ion, HD^+, HT^+, D_2^+, DT^+, T_2^+. The vibrational eigenvalues for the uppermost levels of these ions have been calculated. The threshold fields (assuming no rotation) for each of these ions is less than 10^5 volts/cm. The antibonding potential is capable of supporting a bound state for the H_2^+, D_2^+, and T_2^+ ions. The lifetime of these states is sufficiently long that they may be present in ion beams. The threshold field for dissociating this level in H_2^+ is of order 10^4 volts/cm.

The lack of a stepwise dissociation of H_2^+ ions reported by Riviere and Sweetman[1] may be due to a superposition of contributions from different rotational states. To examine this possibility the matrix elements for H_2^+ dissociation are being evaluated for several rotational states.

[1] A. C. Riviere and D. R. Sweetman, Phys. Rev. Letters 5, 560 (1960).

The helium hydride ions are formed by the collision of a He^+ ion and an H_2 molecule, in contrast to H_2^+, which is formed by ionizing the parent neutral molecule, H_2. This formation process suggests that the uppermost vibrational levels of helium hydride are preferentially populated. On the basis of the best potential functions available, the threshold fields required for dissociating the uppermost vibrational level of the different isotopic mixtures is in the range 10^5 to 10^7 volts/cm.

12. ADIABATIC MOTION NEAR THE CENTER OF A MAGNETIC MIRROR

N. W. Hetherington and C. H. Woods

In the scheme proposed by Lauer et al., of injecting energetic charged particles into a controlled-fusion device,[1] the particles are required to execute adiabatic motion near the center (peak field) of a magnetic mirror for a brief time, and then to move longitudinally away from the peak field a distance comparable with the gyro radius before drifting once around the nominal drift circle. It is therefore of interest to investigate the motion of particles in this situation. Furthermore, the theory of diffusion in the Bumpy Torus magnetic field is intimately connected with the time which a typical particle spends near the peak of the "bumps."

A detailed analysis has been made of the adiabatic motion of a particle in the field produced by a single loop, the diameter of which is large compared with the gyro radius. The results (given in UCID-4246 under the above title) indicate that a particle can rarely be expected to drift more than a small part of the distance around the drift circle while near the plane of the loop.

[1] G. Gibson, W. C. Jordan, and E. A. Lauer, Steady Injection of a Beam of Energetic Charged Particles into the Bumpy Torus–Design of a Proposed Experiment, UCID-4241, Feb. 1961.

13. CONTAINMENT OF POSITRONS IN THE CUSP GEOMETRY

Gordon Gibson,* Willard C. Jordan,† and Eugene J. Lauer

Additional data have been obtained on the containment of positrons in a cusp geometry composed of two coaxial coils spaced one mean radius (76 cm) apart. (See preceding quarterly report, p. 94.)

The absence of long-time containment (longer than the pumpout time of approx 0.45 sec) which was observed in a preliminary experiment for particles emerging near the axis is confirmed. However, the better data reported here show that the observable containment region for particles emerging with an energy of 0.5 Mev has an inner boundary at approx 7 cm from the axis. This

* Westinghouse Electric Corp., Atomic Power Division

† Bendix Corporation

is illustrated in Fig. 22. With the counter on axis the counting rate decreases with the pumpout time of the gas. The magnetic field intensity was 1.68 kilogauss at the point where the axis intersects the plane of a coil. (See Fig. 33 in preceding quarterly report, UCRL-9500.) The inner boundary of the long-time containment region has a larger radius for 1.0-Mev particles; no long-time containment is observed with the counter's radial distance from the axis $\leq$ 10.2 cm, and the observation is difficult at 15.2 cm because of the small trapped fraction. Diffusion to the vacuum tank is important under these conditions.

The possibility, mentioned in the preceding report, that a collimation effect at the counter prevents the detection of particles near the axis has been checked and found to be nonexistent.

The effect of adding known amounts of a scattering gas (Ne) has also been investigated for 0.5$\pm$ 0.15-Mev positrons, 1.68 kG field on axis at the coil, and with the counter 15.2 cm from the axis. Over the range of pressures that could be investigated the mean containment times scale inversely with pressure, as expected when scattering is the dominant cause of loss. These observed times are listed in Table I.

Table I. Observed containment times.

Pressure of Ne (mm Hg)	Mean time (sec)
2.5×10^{-7}	2.9 ± 10%
5.0×10^{-7}	1.6
10.0×10^{-7}	0.75

Another result which is of some interest is that the two halves of the cusp are well isolated. That is, a probe inserted to the axis in the symmetry plane (B_z = 0) has no effect on the observed containment times. On the other hand, when a probe is inserted in a plane parallel to the B_z = 0 plane but closer to the counter, the counting rate is affected when the tip of the probe is < 45 cm from the axis. (Experimentally, it is easier to move the B_z = 0 plane by biasing the coil currents. The data were recorded with a bias of -10%, i.e., with approx 20% greater current in the coil nearer the counter.)

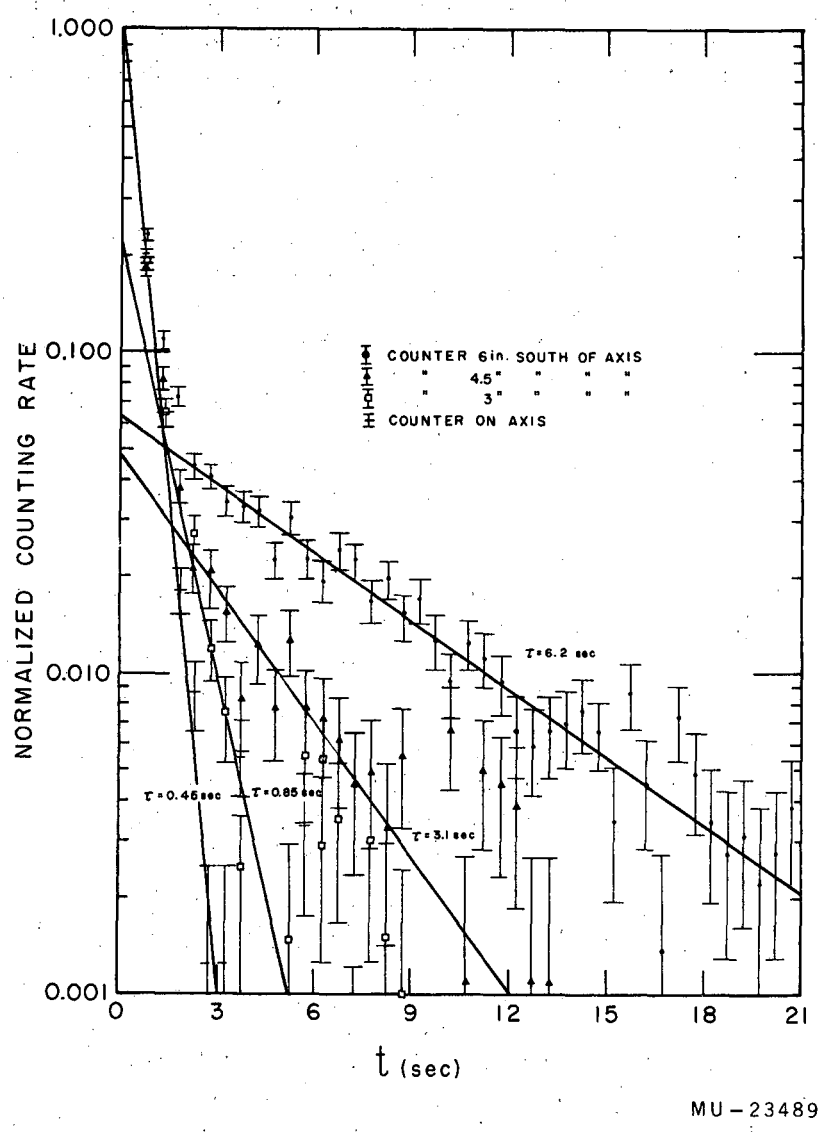

Fig. 22. Counting rate vs time after initiation of the pumpout of the radioactive gas for four different counter positions. The base pressure is 8×10^{-8} mm Hg of unknown gas. No extra scattering gas was added. The counter energy setting is 0.50 Mev. The window width (± 10%) plus the counter resolution half width results in an energy interval of 0.50 ± .15 Mev.

14. ATOMIC AND MOLECULAR BEAM RESEARCH

Forrest S. Baker, Gilbert O. Brink, Edmund S. Chambers, and Robert H. McFarland

During the month of December a proposal for expanded research in atomic and molecular physics at the Lawrence Radiation Laboratory and the University Physics Department in Berkeley was completed and presented to the Advanced Research Projects Agency. The section of the report which dealt with the experimental program at Livermore indicated the scope of interests in this area. These include:

(a) The direct measurement of the absolute cross section for ionization of potassium by electrons. This has been discussed in previous reports.

(b) The measurement of the radiationless dissociative recombination cross section for the molecular-hydrogen-ion capture of an electron. A direct measurement is not considered feasible, but an indirect one may be possible.

(c) A coincidence measurement of the production of positive and negative hydrogen ions from molecular hydrogen by electrons.

(d) An investigation of methods of populating upper states of molecular ions. Since Sweetman and Riviere have demonstrated the breakup of molecular ions by both electric and magnetic fields, a detailed investigation of the population of molecular levels may have significance in both injection into magnetic fields and molecular ion spectroscopy.

(e) A series of experiments involving the excitation and ionization cross sections of atomic and molecular hydrogen. The excitation cross section of the 2S level of atomic hydrogen will probably be among the first measured, since there is presently a conflict in the literature concerning this interaction.

Relative Electron Ionization Cross Section of Potassium

During this quarter the setup for this experiment has been essentially completed. The method of measuring the number of ions formed has been changed from measuring the current with an electrometer to ion counting with an electron multiplier. A 14-stage Cu-Be multiplier has been set up and tested for detection of positive ions. It has been found very satisfactory. An rf mass spectrometer is being completed and will be tested during the next quarter. If this detection scheme proves satisfactory it will be described in detail in a later report.

Absolute Cross Section for Electron Ionization of Potassium

The vacuum system of the beam machine is completed. A base pressure of 4×10^{-7} mm Hg has been attained. The target-button loader systems operate very satisfactorily, and this completes the construction of the basic machine structure. The interior layout of the machine is now in process of development. All electronic units for the interior components have arrived,

and cabling from the racks to the machine is completed. The 2-in. lead shielding for the machine is being fabricated and is tentatively due prior to April 22.

The counting system is nearly completed. Only the parts of the phototube assembly need yet be assembled. As soon as this is done, a complete check of the system will be conducted, employing a Ra D standard.

Installation of facilities and construction of all major units virtually has been completed in the Northeast alcove area. Those units to be used inside the 2-in. lead-shielded cave are not yet installed but are in process of design and fabrication. A 6-ft wire mesh personnel barrier now encloses the entire alcove area and is kept locked. Everything possible is being done to ensure the safety of personnel working in and near the area.

Hydrogen Ion Source

The aperture-extracted rf ion source previously described has produced 0.3 ma of hydrogen ions at 15 kv. A new source magnet has been constructed that will increase the output.

This type of supply requires a separate focusing system. Two different systems are being developed, both using a flat-plate high-voltage insulator. A short-magnetic-lens model held 40 kv without breakdown, but the magnet was not strong enough. An Einzel lens design was scaled from a larger model developed at ORNL. So far, sparking at the insulator has prevented an adequate test.

The vacuum system for the energy selector, employing the Varian magnet, is ready for installation.

Additional Instrumentation

A vacuum system capable of 10^{-10} mm background pressures is presently being constructed for use in measurements involving high-purity and low-volume gas-handling capability. A retarding-potential experiment is planned, and a reaction chamber built for this system to obtain information concerning low-energy electron interactions with hydrogen.

Acquisition of optical equipment has been started leading toward the absolute measurement of excitation intensities.

VI. ENGINEERING AND TECHNOLOGICAL DEVELOPMENT

1. ULTRAHIGH-VACUUM DEVELOPMENT

Norman Milleron and Leonard L. Levenson

Introduction

Pursuing our goal of optimizing diffusion pump systems, we worked on

(a) perfecting a new heater for oil,
(b) design of a top jet for a diffusion pump,
(c) a contamination analyzer,
(d) conductance measurements,
(e) design of a large bakable valve,
(f) properties of trap materials.

A New Heater for Oil

Levenson has improved the heater design we reported in the preceding quarterly.[1] The nichrome strip 0.001 in. thick and 1 in. wide is corrugated by feeding the strip through rollers made from pinion-gear stock. The strip is then rolled into a spiral with glass tape separating the spiral turns. A 2-3/4-in.-diam heater, operating at 1100 watts and 15 amperes, has been running in Monsanto oil for 3 weeks without failure.

One of the problems of oil pumps is the cracking of the oil fluid. Catalytic cracking of oil on metal surfaces is being investigated.

A disaster test of the new type of heater has been designed. The heater, partically immersed in oil, will be run at full power in a vacuum chamber. At instant atmospheric air is allowed to flow in on the heater, the power to the heater will be switched off. The air will then be evacuated from the chamber. This cycle will be repeated at least 100 times to observe the effect on the oil and the heater.

Design of a Top Jet for a Diffusion Pump

Consideration of the top jet of a diffusion pump is one of the key questions we are examining. Using one of our new heaters and Convoil 20 oil, we measured a vapor jet temperature of 290 °C. This superheated oil vapor was passed through a top jet similar in design to the heater itself. A distinct collimating action was seen. This collimation was due to the parallel flues formed by the corrugations in the nichrome strip inserted in the top jet. A conical form of this kind of jet is being investigated.

This version of a new top jet together with the new boiler design may result in large pumps with heights numerically less than their diameters.

[1] Norman Milleron and Leonard L. Levenson, in Controlled Thermonuclear Research Quarterly Report, UCRL-9500, Dec. 1960, p. 87.

Contamination Analyzer

A modified mass spectrometer tube was delivered by the Consolidated Systems Corp. Unfortunately, this modified tube had to be returned for repairs, owing to damage in shipment. The repaired tube has been received, but it has not been tested in use.

Conductance Measurements

The data reported[2] on measurements of molecular-flow conductance were expanded. To date, all data have been taken with CO_2 gas. Modification of the present apparatus is being made to permit use of other gases, such as argon and nitrogen.

Large Bakable Valve Design

A hydraulically pressurized actuator for a 16-in.-diam valve is still under test. Data are being accumulated on the life expectancy (number of openings and closings) of the actuator as a function of pressure.

Properties of Trap Materials

Apparatus has been constructed for the examination of the oil vapor trapping properties of various materials. A nude ionization gage in a small volume (about 3 liters) is isolated by a trapping surface from a CVC type PMC-1440 oil diffusion pump. The trap is of an optically opaque geometry, lined with the material to be tested. The test material is in granular or pellet form. The grains are held to the walls of the trap by stainless steel mesh, in a manner already described.[3] After the trap and the volume above it are baked out, oil contained in a side arm below the trap is vaporized at a controlled rate. All oil molecules must collide at least once with the trap walls. The rate at which the pressure rises in the trapped volume is a measure of the capacity of a given material to trap a given diffusion pump oil. Since tens of cc's of oil can be evaporated in a few hours, the effect of oil from the water-baffled diffusion pump is negligible. This apparatus has just been baked out. No data are available.

---

[2] Leonard L. Levenson, Norman Milleron, and Donald H. Davis, Optimization of Molecular Flow Conductance, UCRL-6014, Aug. 1960.

[3] Norman Milleron and Leonard L. Levenson, Discussion of Optimization of Large Oil-Pumped Ultrahigh-Vacuum Systems, UCRL-5597, Sept. 1960.

2. MECHANICAL ENGINEERING DEVELOPMENT

Thomas H. Batzer

Multiple Magnetic Compression

James F. Ryan and John R. Benapfl

Design studies are in progress for 5× and 10× scale-up of Toy Top III as proposed earlier.[1] The dimensions, location, and power requirements have been calculated for the dc magnet coils in the five-step field of 10×. The over-all design parameters for the metal vacuum vessels of 10× have been calculated to include wall thickness, stiffening ring sections, spacing, and weights. Metal vessels will probably be used in the first-stage injection tank and in all stages of the diagnostic section. Nonconducting vessels of 40-in. and 90-in. diameters are needed to allow placing the pulsed field coils outside the vacuum tanks. Inquiries are being made on the fabrication of large vessels from stoneware, vitrified pipe, or other commercial ceramics.

Tests are being made on the outgassing rate of epoxy fiberglass cylinders. It would be a convenient material for large nonconducting vacuum vessels. The tests to date have been made on a cylinder of fiberglass-reinforced epoxy. The cylinder was made vacuumtight by centrifugally casting a 1/16-in. layer of epoxy resin on the interior and ends of the cylinder. The vessel is approximately 9 in. in diameter, with a volume of 8 liters. The base pressure of this vessel, which includes five 9-in. Hycar O rings and two 1-in. Hycar O rings, is about 5×10^{-7} mm Hg. The pumping speed on the vessel is between 50 and 75 liters per second. The outgassing rate of the cylinder, assuming all the gas comes from the cylinder and none from the O rings, is 2×10^{-8} mm-liter/sec/cm^2. A cylinder 2 ft in diameter and 30 in. long is being fabricated to make further tests on different materials, such as high-temperature epoxies and silicone-resin liners.

Building layouts have been made for the 5× and 10× experiments. Since heavy shielding about 7 ft thick is needed, it does not seem feasible to place this experiment in Building 180. Plan and elevation views have been made of a 42,000-ft^2 building to house the 10× experiment. It provides a main pit, 40 ft wide by 164 ft long and 8 ft deep, with shielding walls 7 ft thick by 30 ft high. It also includes a capacitor-bank wing of 340,000 ft^3 plus a shop and office wing. The cost is estimated at $1,621,000.

Low-Energy Neutral-Beam Experiment

William S. Neef, Jr., William T. Crothers, and Eugene T. Bradley

The beam-tube pumping tests are in progress. The first of two pump boxes which form the ends of the reaction chamber were baked out to 450°C several times, and the pinch gaskets performed satisfactorily. It was necessary to narrow the annular area, which prevents oxidation of the seal, to 0.060 in. to reduce the bolt load requirements. The base pressure of the box after bakeout was 6×10^{-10} mm Hg. This box with its 10-in. bakable valve, trap, and diffusion pump is being assembled for performance testing prior to installation in the pulsed priming source test.

[1] F. Coensgen, W. Cummins, and A. Sherman, Proposed Multi-Stage Compression Facilities, UCID-4219, Nov. 1960.

The 6-in. bakable valve is being fabricated, as are all the parts of the beam tube connecting the main reaction chamber with the burial chamber. The design of the reaction chamber end flanges was modified in accordance with the bakeout-test results on the internally bolted flange of the pump box.

The layout for installation of a field-measuring probe in the source is nearly complete. The button-target components for beam scanning are finished and are in the final stages of assembly. The design of the reaction-chamber pressure probe is complete. The purpose of the pressure probe is to allow for continuous mass analysis and pressure measurement of the gas in the reaction chamber. Another diagnostic tool being designed for use on the ALICE reaction chamber is the secondary-emission detector. It is a bakable unit designed to fit one of the diagnostic ports. Its purpose is to detect fast neutrals coming off the plasma in the reaction chamber. All the parts of the beam burial chamber are in fabrication with the exception of the target plate, which is being designed.

A full half-mirror magnet coil, four sections, was completed and tests started. Field measurements made at 500 amp with the coils at 80 ^{o}K confirmed the calculations for field configuration and strength. In order to map field strength further from the magnets and to approach the internal design field of 45,000 gauss, higher-current tests were run within the power limits of a single 300-kw Perkins power supply. During this test a coil failure occurred, which has been carefully studied and established as the opening of a brazed joint at one of the current tabs carrying current from one coil pancake to the next. The open circuit and the resultant arc occurred at a current level of 1,200 amp. Some secondary damage to all coil sections resulted from this accident, but all coils are repairable and the delay in coil test should be no more than 6 weeks. A redesign of the cross-over tabs has been completed, and all tabs on all coils will be replaced.

Some delay in the fabrication of ALICE coils resulted from the move of the Coil Shop from Building 124 to the new Coil Shop in Building 181 during February.

Astron

Charles A. Hurley, James F. Ryan, and James E. Blades

A second trial assembly of the core stack for the 720-kv electron gun has been made with the wider insulating strips and redesigned primary straps. Measurements to locate the secondary sheets were made and used to design the connections between the secondary sheets and accelerating column. These connections are now out for fabrication; however, Electrical Engineering recently made a test which showed the necessity for decoupling sheets between the magnetic cores. The additional height required by these decoupling sheets may require changes in the connectors.

Two subassemblies of the accelerating column, being made by Coors Porcelain Company, were found vacuumtight but badly warped and out of tolerance. It is obvious that to meet the tolerances, finish machining will be necessary. This requires new electrodes or change of existing electrodes for subsequent assemblies. In the interest of expediency it was suggested

that Coors weld additional copper to the i.d. of each lens electrode. It appears that Coors can deliver a vacuumtight and dimensionally correct assembly by May 1.

The gun grid assembly and the design of the new primary strap connections are complete. All the necessary piping for the Freon cooling apparatus, the vacuum system, and cooling water has been designed and released to Plant Services. Miscellaneous parts, such as tracks for the main chamber and heat-exchanger boxes for the refrigerated cold traps, have been let for bid.

General Electric has produced four ceramic-column-module welding test sections for the induction accelerator. One was welded by General Electric to confirm the feasibility of the design. The rest of the test pieces are for training our welder. General Electric is proceeding to produce the main order of 30 ceramic column modules for the induction accelerator. The eight-core prototype accelerator is partly assembled, and awaits pulsing equipment to be installed by Electronic Engineering. A full-scale 48-core accelerator unit, less electronic parts, has been ordered.

The E layer tank of the Astron main chamber has been completed. On order is the injection-tank inflector. Bids are in for the 43-inch main field coils; General Electric is the low bidder.

The status of the modifications to Building 157 is as follows: The concrete shielding walls are complete and the two cranes required within them have been installed. The contract for steel work to support the gun and accelerator inside the shielding wall has been let to Moore Drydock Company, and work is in progress with a completion date of March 28, 1961. Work has been started by Mechanical Engineering on a steel structure for supporting the pulse-forming network cable for the accelerator and gun. Plant Engineering will do the required structural design. June 15 has been set as the tentative completion date.

Atomic-Beam Cross-Section Experiment

A reactor capsule cutter to operate inside a hot cave has been designed and is approximately 90% detailed. The new driving mechanism for the rotating section of the analyzing chamber has been designed and installed.

The teflon cap seals for the rotating section were installed and found not satisfactory. A pressure of 9×10^{-7} mm Hg was reached in the static condition, and when the section was rotated the pressure went up to 1.5 to 2×10^{-6} mm Hg. These pressures are with differential pumping. The required pressure in the chamber is 1×10^{-7} mm Hg. The teflon cap seals were removed and reinstalled with larger-cross-section O rings. The pressure came down to 1×10^{-7} mm Hg with no change during rotation and no differential pumping; however, the loading on the rotating mechanism is greatly increased and the possibility of the O rings' stretching and bunching remains. A new design has been started which should solve these problems. Expected completion is by May 15.

Beta-Ray Experiment

J. Ralph Ullman

Two fast probes were assembled and bench tests were run. The shaft and seal scouring initially experienced was eliminated during the course of the seal run-in and testing. The seal arrangement is after Billett and Bishop,[2] but modified to improve reliability. Fluorosint, a filled teflon, has been substituted for half the teflon washers to reduce the cold flow rate. A Belleville spring stack was added to keep the washers loaded for periods compatible with the experiment.

Typically the probe can plunge or be retracted in 100 msec for a stroke of 14 in. when driven by an air cylinder 2.5 in. in diameter under 55 lb/in.^{2} of air pressure. The plunge time is small compared with the positron containment times. This cylinder has an adjustable split piston permitting presetting for a stroke between 5 and 16 in. Figure 23 shows the seal arrangement and a portion of the probe assembly.

The probes have been mounted in a catilever fashion on the north and south ports of the 44-in. -diameter vacuum tank. To date, the seals in their final assembly have experienced between 400 and 800 cycles. Plunging the probe in gives a pressure burst of 1×10^{-7} mm Hg. These probes in conjunction with hand probes will permit establishing plasma surfaces versus other parameters for the symmetric and asymmetric coil configuration.

Component Development

J. Ralph Ullman and Thomas H. Batzer

Parts for the bakeable hydrogen leak assembly have been received and the final welding assembly is being done. The leak will be mounted on liquid nitrogen circulating coil flange and will permit accurate and predetermined gas-flow rates in the Mopu No. 2 Tank.

Plans call for analyzing the residual gases in Mopu No. 2 Tank. Accordingly, an adapter for attaching the bakable mass spectrometer to the tank interchangeably with the hydrogen leak assembly has been designed.

Equipment is being designed and parts modified to provide for a rehabilitated surface-bombardment experiment. The chamber carrying silver evaporators, ion gauges, and a mass spectrometer port has been designed. A 1- to 2-in. -aperture gate valve, bakable to 200°C with closed conductances of less than 0.10 liter per second has yet to be designed. In addition, the structural support and bakeout muffle for the apparatus must be supplied. Target date for final assembly is July.

Parts for the 6-inch bakable gate valve have been completed by Nelson Specialty Company of San Leandro, California, and are being shipped. The layout has been started on a second-generation 10-inch bakable valve. This is to be installed beyond the west end of the ALICE reaction chamber, and will isolate the moly evaporator chamber from the 10-inch diffusion pumping

[2] E. A. Billett and J. Bishop, J. Sci. Instr. 35, 70 (1958).

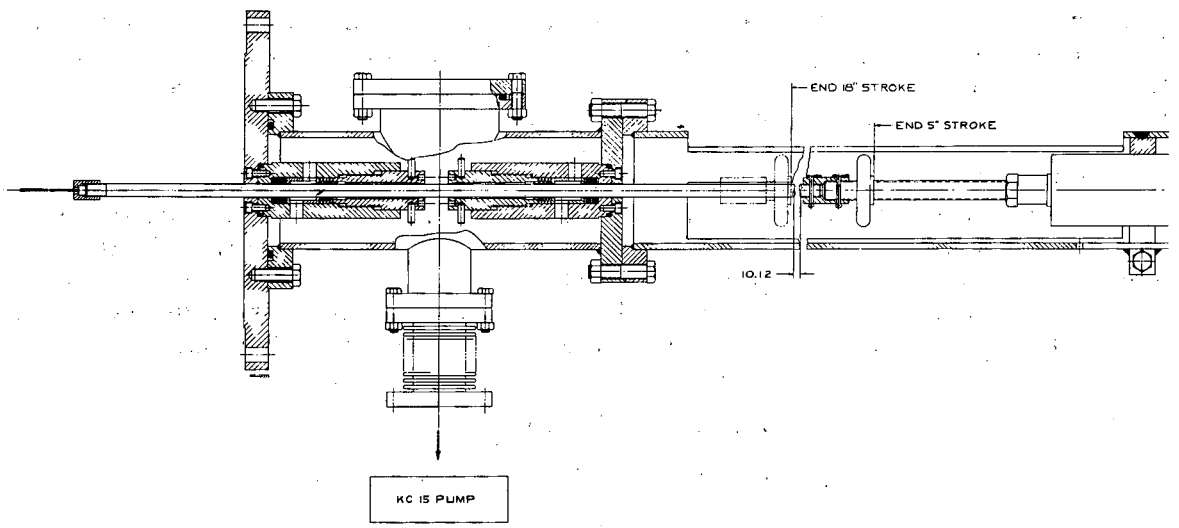

MU-23495

Fig. 23. Fast probe assembly.

unit. It will incorporate all the bakable valve improvements to date plus a simplified gate handle linkage permitting a shorter and lighter valve housing.

Successful completion of the bakeout tests on the ALICE pump box carrying five 15-in. single pinch seals indicate good reliability of the seals generally. An Engineering Note is on the way standardizing design details for the single- and double-seal configurations.

As a result of the test data described by Addiss, Pensak, and Scott[3] of RCA, the elastomer O-ring test was terminated and the system dismantled. Data presented indicate that vacua on the order of 10^{-9} mm Hg or less can be attained with Viton elastomers. Viton will withstand bakeout temperatures to 250°C.

As soon as all the parts are accumulated, the 3-inch bakable valve will be assembled with its bakeout shaft extension. Cupro-nickel and 321 stainless steel Conoseal gaskets are on hand for the valve seal. The valve and gaskets will be fully evaluated in a series of vacuum bakeout tests.

Some preliminary tests have been run to evaluate Monsanto's high-temperature functional fluid OS-124 as a diffusion pump fluid. The possibilities of this fluid for use in diffusion pumps were first noted by K. C. D. Hickman in a letter to Nature. The system consits of a P. M. C. 720 4-inch diffusion pump and a K. C. 5 Kinney pump. The system pumped consists of a brass cover plate bolted directly to the diffusion pump with a Viton A O ring. Hard-soldered into the brass plate is a 1.5-in. copper elbow, and welded to the other end of the copper elbow by a Kovar extension is a R. G. 75 Veeco ion gauge. Several turns of cooling-water tubes have been soft-soldered to the bend of the elbow. The original charge of 400 cc of Monsanto fluid has been running for approximately 8 weeks continuously. The average pressure reached has been 3×10^{-9} mm Hg, and the lowest pressure reached to date is 1.3×10^{-9} mm Hg. Future plans include replacing the cover plate and elbow with a sufficiently large tank to allow speed runs. The cover plate of this tank will contain connections for a nude ion gauge and the mass spectrometer.

Cryogenic Magnetic Coil Development

Clyde E. Taylor, Robert L. Nelson, and David C. Holten

The coil test facility is being assembled in the west end of Building 180. The iron and lead regenerators, the helium refrigeration chamber, and liquid nitrogen gas cooler have been delivered. Other major assemblies, including the sodium coil parts, valve boxes, and actuators are out for fabrication, and are due by April 14. The main helium compressor is now being run in on air. Outdoor piping is 75% completed. Fabrication of all other components, such as special low-temperature instrumentation, liquid nitrogen distribution systems, and valve interlock system, will run concurrently with assembly of the major components. The sodium coil mold is 75% complete.

[3] R. R. Addiss, Jr., L. Pensak, and Nancy J. Scott, Evaluation of a New Fluorelastomer as a Gasketing Material for High Vacuum Systems, R. C. A. Laboratories.

Laboratory measurements have demonstrated that sodium can be cast in copper tubing or extruded in air and wrapped in plastic tape, without impairment of the low-temperature resistivity by diffusion of impurities from the conductor surface.

A 100-kG 3-in. i. d. coil, using 1/4-in. square tape-coated sodium wire, is being designed.

3. ELECTRICAL ENGINEERING DEVELOPMENT

Vernon L. Smith

Pyrotron

David R. Branum

Table Top

The past three months have been spent in changing the experiment on this machine area.

A fast bank consisting of twelve 7.5-mf 20-kv "Green River" type capacitor-ignitron setups is being added to the experiment.

A three-channel source pulser (patterned after the type used at Toy Top III) is under construction.

Two 300-kw 2,000-amp dc supplies are being connected to the experimental area.

Toy Top III

The additional discharge banks have been added to the experiment. The new banks have been tested and pulsed for 2,000 shots to a level of 16 kv per section. The new "potted" type of transmission line seems to have ended the transmission-line problem. They are only 0.5 microhenrys and 0.5 milliohms each and are holding up satisfactorily.

The field decay on banks 3A and 3B (the final field banks) is 5.5 msec. These two banks are positive high-voltage banks.

The ejector bank No. 3C has a decay of 2.5 msec. It is a ± 20 kv bank.

All four new banks, 2, 3A, 3B, and 3C, are approximately 90+% efficient into a load coil of 21 μh self-inductance.

Fabrication parts for a future 50-channel source bank are under construction. A power supply to charge this bank every 15 sec is now under design.

A Marx type single-channel pulse bank is under construction. It is to be used in the large source development. The maximum output will be 32 kv out of a 7.5-mf bank capacitance.

Fabrication parts for an addition to the crowbar chains of bank No. 4 are being assembled. The new chains will be added early in March 1961.

Two sets of fast capacitors are on order for engineering tests for a new bank No. 1. The new "gate" bank will be faster than 6 μsec, and will be higher than a 40-kv bank. Capacitors will also be tested for a source bank. The source bank is a ringing service at a 10-kv level.

Two additional 300-kw 2,000-amp dc field supplies were connected to the experiment in February and are now in use. Toy Top III now has seven of these supplies connected to the experiment.

An ultrasonic delay-line generator is under development for a stable 10- to 400-μsec dual delay channel. This will be a "solid-state" delay generator.

A two-channel-phantastron type of delay generator is under development. This delay is very stable and has a range of 1 μsec to 1 msec. This is a "hard tube" delay generator.

Pyrotron--Miscellaneous

Hubert W. Van Ness and Alfred F. Waugh

ALICE

The dc power supply installation for the ALICE machine mirror field coils is now nearly complete. Four 300-kw Perkins supplies are in place, with provision for a fifth. The primary power connections are complete and the dc bus cables have been run from Bldg. 156 to Bldg. 180. The remote-control system design is complete. The 6,000-amp dc circuit breaker purchased from the I-T-E Circuit Breaker Company should arrive by March 15. The water-cooled thyrite installation is complete.

One of the pair of ALICE, liquid-nitrogen-cooled mirror coils, consisting of four modular sections, has been given preliminary tests. The coil was cycled from room temperature to liquid nitrogen temperature several times. About 30 pulses of current, charging the coil to 500 amp in 10 sec, were put through the coil, primarily for the purpose of making magnetic field measurements in the coil vicinity. The coil was then charged to 1,000 amp six times. Following this, while the coil was being charged to 1500 amp, an arc breakdown occurred between layers of the inside-diameter surface. The resultant heating and pressure rise of the confined liquid nitrogen vapor caused the modular coil sections to separate and fall off the support cradle. Three of the modular coil sections were badly damaged, and an attempt is being made to repair them.

The coil layer-to-layer series jumper bars are being redesigned to prevent recurrence of the above type of fault.

Source Development

The ion-source field coils are now being energized by the M G set in Bldg. 156. The remote-control chassis to be used with the J. C. Carter

rotating-coil fluxmeter for the field-regulating system is complete and will be installed soon. The fluxmeter purchase was delayed about a month by budget problems. Delivery is now expected by the end of March.

The acceleration high-voltage 20-kv 1-amp 0.2% regulator system has been completed. Considerable development and debugging was required. Initial operation is very satisfactory.

Pyrotron--Research and Development

Kristian Aaland, Bernard M. Loth, and Gilbert A. Reeser

Toy Top III

An investigation of the requirements needed to build a five-pulse train for the accelerating anode of the mass spectograph analyzer indicated that a feedback pulse-regulator system was not practical at this time.

The difficulty in building a pulse regulator at high power levels is the need for providing a stable high-voltage reference and comparator system. There is a device that appears to provide the answer to the problem. The field-emission diode, according to Dr. W. P. Dyke of Linfield College, could be used as a reference element in a feedback system. It will conduct a 10-amp pulse at 20 kv, voltage-regulate a factor of ten, and be stable to within 1% for 10 ampere-hours, and can be constructed to respond to a gigacycle frequency. Since this device is not yet commercial, no design has been based on using it; but it looks very promising.

Since a five-pulse regulated train at this power level (8 Mw) and pulse width (0.2 μsec) is still beyond the state of the art, a single pulse-line pulser was designed. It uses a triggered pressurized spark gap. This method of switching was decided upon after consultation with R. J. Thomas and D. B. Cummings. The rise and fall times are both 30 nsec into a 25-ohm load. The pulse top is controlled to -20 kv, ± 2%, in a simulated load. This unit is now being fabricated.

ALICE

Final checkout for the 20-kv regulated power supply was completed February 17, 1961. It was then turned over for trial operation on the ALICE machine. After some difficulties with transients and rf, the regulator was made stable and reliable, and is now being used by ALICE operations.

Description and instructions for the supply are now being written. This will include all the components of the regulator except the solid-state power supply. The regulator is presently being used on the Squash Bank S-4 supply in Bldg. 156 while a reliable silicon-diode-string supply is being constructed. (Limited to 25 kva.)

The following is a brief summary of the characteristics of the final regulator:

Output voltage	10 to 25 kv.
Output current	up to 3 or 4 amp.
Ripple	2 volts in 20 kv.
Noise	2 volts in 20 kv.
Corona	Fast spikes up to 20 v occur at 20 kv.
Drift	Not yet determined, but system has an internal gain of 10^5 and appears rock stable from panel meter readings.
Current interrupt	Regulator will cut off the output voltage at any desired load current level in 2 μsec. After staying off for several hundred μsec the unit will automatically reset to the original voltage. If the load current is still above the interrupt level, then cutoff will occur again within 5 μsec.

The adjustable reference supply in the ALICE console is a zener diode supply with built-in temperature control. It has been found that 0.1% stability is easily obtainable by this method and that 0.01% stability is extremely difficult to obtain.

A beam-position feedback loop may be added in the future.

P-4

The pulsed electron gun powering system as shown in Fig. 24 meets all specifications, which are as follows:

Pulse width	2 to 20 μsec
Output voltage	0 to 18 kv
Pulse current	50 amp
Bombardment voltage	2000 v (later increased to 2500) at 0.6 amp.

It is interesting to note that Mr. Wharton observed Bankhausen oscillations at 2 to 4 Gc. They were shifted to another tolerable frequency by changing the screen voltage on the output tubes, and were suppressed by shielding the pulser.

Pinch and Collapse

Hubert W. Van Ness

Gamma Bank Area

A 60-cycle core position-indicator system has been designed and partly constructed for the "Levitron" experiment. Operational tests of the gamma capacitor-bank facility are in progress. These tests will check the high-voltage insulation and the mechanical strength of the cabling within the bank room.

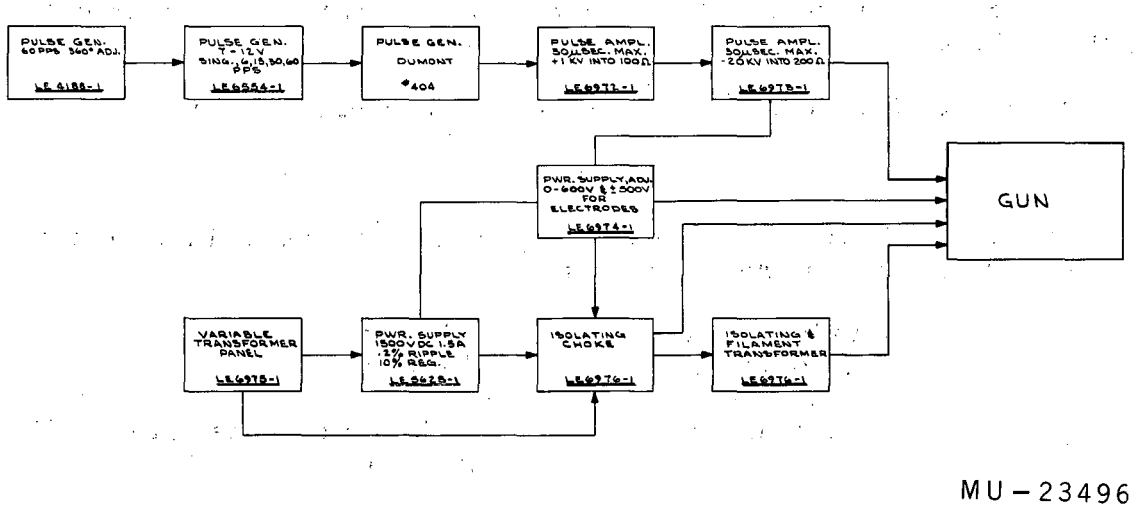

MU-23496

Fig. 24. Powering system for pulsed electron gun for P-4.

Fast-Scan Mass Spectrograph

Test and calibration of the hyperbolic-wave-form scanning system is complete. An additional "howler" circuit is being developed to make it possible to use the unit as a leak detector when desired.

Energy Storage System Investigation

The unipolar generator repair is nearly complete and it should be returned to the Laboratory around the first week in March. Injury suffered by a refrigeration technician, due to a NaK explosion in a valve being cleaned, has resulted in considerable delay. The hazards involved in the operation have been closely appraised, and a number of proposed changes in the pit design are under study. If these are all put into practice before the machine is reinstalled, a delay of several months may result.

Cryogenics Coil Experiment

The helium system compressor installation is essentially complete and is being checked. A redesign of the valve control system was found necessary because of mechanical problems involved. Some testing of this still has to be done.

Switch Development

David B. Cummings

Mechanical Switching

No further effort, because of the work load of the Mechanical Engineering Group.

Ignitron Development

Test Tubes

Tests of the submerged ignitor have shown that it will work. Several improvements are indicated to achieve the degree of reliability needed. These tests have also given a new understanding of the role of the support on a conventional ignitor. The characteristic drop in the voltage trace of an ignitor is due to the exposed support drawing an arc current through the gas.

New Designs

Two experimental ignitron designs have been ordered from Westinghouse. The first, the WX4564, is a short low-inductance tube with improved anode cooling. It has a short anode-cathode spacing for arc stabilization. A voltage rating of 15 kv is expected, and several may be stacked for higher voltages. The second, the WX4599, is a more conventional 2-in. tube with a vacuum-melted mild steel anode and a single glass pantleg. This $85 type is expected to be good for more than 20 kv and to perform as well as the $145 General Electric double-pantleg tube, which has a molybdenum anode. Delivery is expected on both orders in 2 to 3 weeks.

Cross-Section Experiment

David R. Branum

A counting system has been included in the detection of ions by this machine. The counting system includes a photomultiplier, a cathode follower, a linear amplifier, and two LRL-design scalers. The gate circuits of the counters are controlled by a reference signal detector, a time delay, a multivibrator, and a drive circuit. A signal integrator is used to provide front-panel indication of ion signal. The difference in counting rates is integrated and compared, then applied to an indicator for immediate observation of signal.

The reference-signal detection has been installed in the rack and is now in use.

Work on the pulse mass spectrometer has been completed. An operational unit can be constructed with existing information.

The rf oscillator has been received from the Model Shop and is at present under test.

Two "hot-wire preamplifier" chasis are under construction in the Model Shop. One of these units will be used in the calibration experiments and the other will be used to replace existing equipment on the main cross-section machine.

A 20-channel pulse-height analyzer has been installed in the racks. It will be used in the calibration work. Maintenance has tested the unit for satisfactory operation. The unit is now in operational condition.

Ion-source work has been concentrated on construction and testing of electrodes.

Microwave Diagnostic Development

Charles B. Wharton and Joseph E. Katz

Toy Top III

We are preparing to make electron temperature measurements on the compressed plasma with microwave radiometry. The compressed-plasma density will be quite high, corresponding to plasma frequencies as high as 100 to 200 Gc, and magnetic fields as high as 150 kG, corresponding to gyro-frequencies up to 400 Gc, will be present. Since we do not yet have reliable microwave equipment operating at frequencies above 90 Gc, we shall have to diagnose by using special transmission modes.

Left-hand circular polarization once was used successfully on Table Top, and we can try that mode here also, extending the measurable electron density upward by a factor of 4 or 5. In principle, by propagating at various angles in respect to the magnetic field lines, the gyro-resonances can be pushed up to 2 or 3 times ω_c, for densities of the magnitude expected here.

Unfortunately, these dispersion relations have not been well substantiated experimentally, owing to the lack of suitable laboratory plasmas (high density, high B field, low collision rate). We shall have to try out the new techniques on this experiment.

Radiometry requires transmission, reflection, and radiation measurements. However, since we have limited access to the plasma here, we can make only reflection and radiation measurements. Dielectric rod radiators will be tried. Supramica will be used as a first attempt, because of its good microwave properties and its resistance to the high-temperature plasma bombardment. It can be readily machined and has negligible vapor pressure in vacuum. Low-loss circular waveguide runs will be used from the measuring console to the machine. Mica, bonded in kovar with glass frit or epoxy, will be used for waveguide vacuum windows. Such windows can be baked out at 100° C if necessary.

Astron Electron Beam Equipment

New microwave components at 90 Gc and 100 Gc have been tried out on the bench. A 90-Gc interferometer, using a QK-673, has been assembled, but requires improvement before it can be used in a plasma experiment. The 140-Gc signal is being obtained by harmonic generation from a crystal. Using a video detector and 1,000-cps tuned amplifiers to detect a 1,000-cps modulated signal, we have 40 db of dynamic range. That is not good enough to hope to use in diagnostics of pulsed plasmas. For bench work and component development, however, the present signal strength should be adequate. A Raytheon klystron which oscillates at 110 Gc ($\omega_p \rightarrow 10^{14}$ electrons/cm^3; $\omega_c \rightarrow 30$ kG) is now available at $3,000. Several Raytheon-CSF Carcinotrons, oscillating in the 3-mm, 2-mm, and 1-mm ranges ($\omega_p \rightarrow$ up to 10^{15}/cm^3; $\omega_c \rightarrow$ up to 110 kg), are available at $4,000 to $12,000 each. Oki, of Japan, promises a klystron having an output frequency of 150 Gc in September. The price is unknown, but probably around $3,000.

We have looked into the possibility of using infrared techniques for plasma diagnostics. The recent successes in Lasers gives hope that intense ir sources at 100 μ to 1 mm may soon be feasible, allowing the construction of a "microwave-type" interferometer capable of diagnosing plasmas having densities of 10^{16}/cm^3. Short-response-time (< 10 μsec at λ = 2 mm) ir detectors of liquid-helium-cooled indium antomonide have been made in England. If the source had sufficient intensity, the sensitivity of the detector could be compromised and germanium or silicon photo transistors used. We shall continue to keep abreast of the state of the art.

P-4 Electron Beam Instabilities Experiment

The 20-kev electron gun has been operated with 10- to 20-μsec pulses at 30 pps up to 18 kev, the limit of the power supply. The cathode emission is low (2 amp instead of 5), for reasons unknown. Four hundred ma of pulsed current reaches a target near the source end of P-4, about 4 m from the gun. Ferrite-core current transformers are under construction to monitor the pulsed current at various locations along the column, when the plasma is on. Probes, etc. would be burned up immediately by the plasma bombardment. The attenuation of the electrons by the plasma can thus be determined.

A second method to measure the electron penetration into the plasma is to look at various optical ionization and excitation lines. No noticeable effect can be seen on the visible helium lines, such as λ 4686, λ 5015, etc., but that is not surprising, because of the low energy content of the electron beam compared with that of the plasma electrons. If a line whose threshold lies above the energy of the plasma electrons were viewed, such as O V impurity, etc., or if soft x rays from a probe were viewed, some effects might be observable. We plan to try some of these things. At present we can pick up pulsed currents on probes at the edges of the plasma, but it is not clear whether these are due to plasma waves excited by the electron pulses or due to the pulses themselves being received. Biasing these probes, to repel plasma electrons, should demonstrate which kind of electrons are being received, if ion effects can be eliminated. This will be tried soon.

Colossal bursts of microwave radiation at frequencies in the vicinity of ω_p are emitted when both the plasma and pulsed beam are present. These presumably are somewhat like the microwave "generation" seen in Stellarators occasionally--thought by some to be due to coupling between runaway electrons and the plasma. The relationships between radiation intensity, plasma density, beam energy, and beam current at various positions along the plasma column will next be investigated. We shall also look for coherence of these oscillations from point to point.

Small bursts of radiation at the electron gyrofrequency (≈ 3,500 Mc) also are seen, but these are difficult to distinguish from interference due to Barkhausen oscillations in the 4PR60 pulse-modulator tubes. We have shielded and decoupled the circuits until the two signals are of about the same magnitude.

Other plasma radiations at frequencies between 75 and 1500 Mc also seem to be present. These are monitored by a swept receiver (motor-driven quarter-wave resonator). The oscillations are picked up by a tungsten coaxial probe at the edge of the plasma column. The amplitudes and frequencies are very erratic, and a great deal of data taking will be necessary before we can make any sense of these. The amplitudes are very large compared with thermal radiations, some being of milliwatt intensity.

Astron--System Engineering

Clelland D. Nail and James D. Fahey

During the past three months our effort has been concentrated on the design of the electron accelerator for the Astron machine. Progress can be reported as follows.

Pulse-Forming Cables

The early decision to use large coaxial cable for energy storage and pulse formation was based on stringent requirements for pulse flatness and rapid rise times at 32-kv voltages. As some of these requirements have been de-emphasized, the possibility of using some other type of pulse-forming network has repeatedly been suggested. Various companies consulted have indicated a capability to provide "lumped-constant" networks with acceptable or nearly acceptable parameters. The cost has been estimated by these

vendors to be about equal to the cost of the cable type PFN's, particularly if the reels and supporting structures are included. The size and weight of "lumped lines" is, of course, only a fraction of that required by the use of large coaxial cable.

We have concluded, however, that the original decision is still sound, as based on the following facts:

(a) The reliability of RG-218/U cable at the required voltage has been experimentally verified.

(b) The pulse performance of cable is well known and exceeds the requirements, while the lumped-constant networks require design assumptions. Some development is certain to be necessary.

(c) The cable is already purchased and has been received. Moreover, it is a common type with re-use value, and was obtained at a good price because of the quantity.

The Switch Chassis

The Hydrogen Thyratron

The tests suggested by N. C. Christofilos on the 5949A or 7590 hydrogen thyratron have been completed. Results indicate it is considerably better suited to the switching requirements than the smaller type 6587. The tests with the 6587 were quite favorable, but the number of spontaneous firings observed makes simultaneous operation of 500 units extremely doubtful. In addition, the smaller tubes require careful aging, which is nearly eliminated with the bigger tube. Consequently, the larger tube will be used although it does appreciably increase some of the problems. For example, an 18-to-1 increase is required in the trigger energy to fire the tube. A trigger system to supply all units from a single source is under construction.

The higher trigger level also makes it uneconomical to vary the firing time of each chassis with commercial variable-delay networks. A compromise has been worked out using five selected lengths of coaxial cable which can be switched in or out. This will allow adjustment of the firing time over a 105-nsec range in 5-nsec steps.

The specification for connector and housing (L-468-1) has been withdrawn, since it applied to the smaller tube. A performance specification for the entire switch chassis (L-1477) is written. This, with a letter of inquiry, has been submitted to several vendors. Their estimates and proposals are now being received.

Charging Supply

A specification (L-1469) has been prepared, calling out special power supplies for charging the pulse-forming cables. These are to be either 50- or 100-kw units. A total capacity of 500 kw is needed to recharge 500 PFN's. This part of the system has been released to vendors for firm quotation, and proposals are being received for consideration.

Core-Excitation Winding

It has been decided that the initial gun section of the accelerator will be made with single exciting straps around each core. In the remaining accelerator sections, three parallel straps spaced 60 deg apart will be used.

Tests of strap design using corona-resistant mica sheets have shown no failures in more than 200 hr of continuous operation at 60 pps. This is the most promising design achieved so far.

Compensation

The problems of locating the compensating networks physically close to the cores have caused us to study ways to shape the pulse with networks located more remotely. Trial-and-error designs resulted in fairly good compensation at distances up to 10 ft. The ideal location, from the mechanical packaging viewpoint, is in the racks containing the switch chassis. The exact calculations of networks at this location are rather involved, and have been submitted to an analog computer group for solution.

There appears to be a reasonably good chance that a practical network will be developed for packaging at the switch.

Core Bias

The power necessary to reset all cores with dc amounts to about 500 kw continuous load, regardless of pulse-repetition rates. Tests show that bias currents of the same--or only slightly higher--peak values will reset the cores when pulsed on in a time such as 200 to 300 μsec. The total power needed by this method is computed to be less than 100 kw at 60 pps, and is proportionally less at slower trigger repetition rates. In addition, the large, heavy bias choke may be eliminated, since it is possible to introduce pulsed bias power through the isolating choke used for the trigger circuit.

Preliminary Tests On Three Cores

Tests have been made on three cores in a mock-up of the gun portion of the accelerator. These cores, which are larger than those in the subsequent accelerator sections, were assembled in a single cavity and placed in a tank pressurized to 30 psi of Freon-21 to simulate the atmosphere of the gun section.

The results from pulsing these cores indicate that the magnetic interaction between cores in the same cavity is very large. As a result, very little additive voltage was produced. When the arrangement was modified to include sheets of metal between each core, interaction was small and the voltages along the core axis were additive, about as calculated. This indicates that a change in the design of the gun sections will be necessary to include separate cavities for each core.

Construction Plans

The amount of electronic hardware needed for the entire accelerator

makes it necessary to construct an elevated storage facility for the PFN cables. A modification of the original design has been made which can be built in sections. The first quarter of this structure will be sufficient to contain all the electronics for the gun portion. When this has been checked, additional sections can be added without completely disrupting the existing arrangement. The construction of this facility is assigned to Plant Engineering and the Mechanical Engineering Department.

Astron--Research and Development

Kristian Aaland, Bernard M. Loth, and Gilbert A. Reeser

$\phi\pi$

The dry-run $\phi\pi$ supply is being changed from negative to positive output, and the voltage is being increased. This necessitated a new 35-kv reference supply (Fig. 25), also changing the transformer to a higher voltage (40 kv). Because of the increased voltage, a new silicon diode assembly is needed to avoid breakdown in the small cabinet space available.

Charging Supply

It has been shown that the least expensive and most efficient type of power supply for Astron is the $\phi\pi$ type of supply. The drawback to its otherwise great versatility is the necessity for line synchronization. Work is progressing on an approach that chops 60 cps to a higher frequency and thus overcomes this problem. A 25-kw scale model is being built for test, and a report will be written describing the results.

Trigger Distribution for Thyratron Pulser

A large single thyratron was specified for the power pulse. A complete trigger and solid-state powering system (2 kc, 20 kv) will be contained in a double rack.

To obtain a matched distribution over 50-ohm cables, a two-stage system of pulse transformers is being used (17 pulse transformers total).

Synchronization to line, power supplies, and clock pulses for any random start pulse will be handled by a solid-state digital computer.

Other Activities

The silicon diode evaluation report LE-442 will soon be available.

A silicon diode AIEE committee meeting, held in Los Angeles December 21, 1960, was attended by Kris Aaland.

Bernard Loth attended the AIEE Winter Meeting held in New York January 29 to February 3, 1961.

The paper on 30-nsec core tests by Gilbert Reeser was accepted for presentation at the SWIRECO Conference in Dallas, Texas, next April.

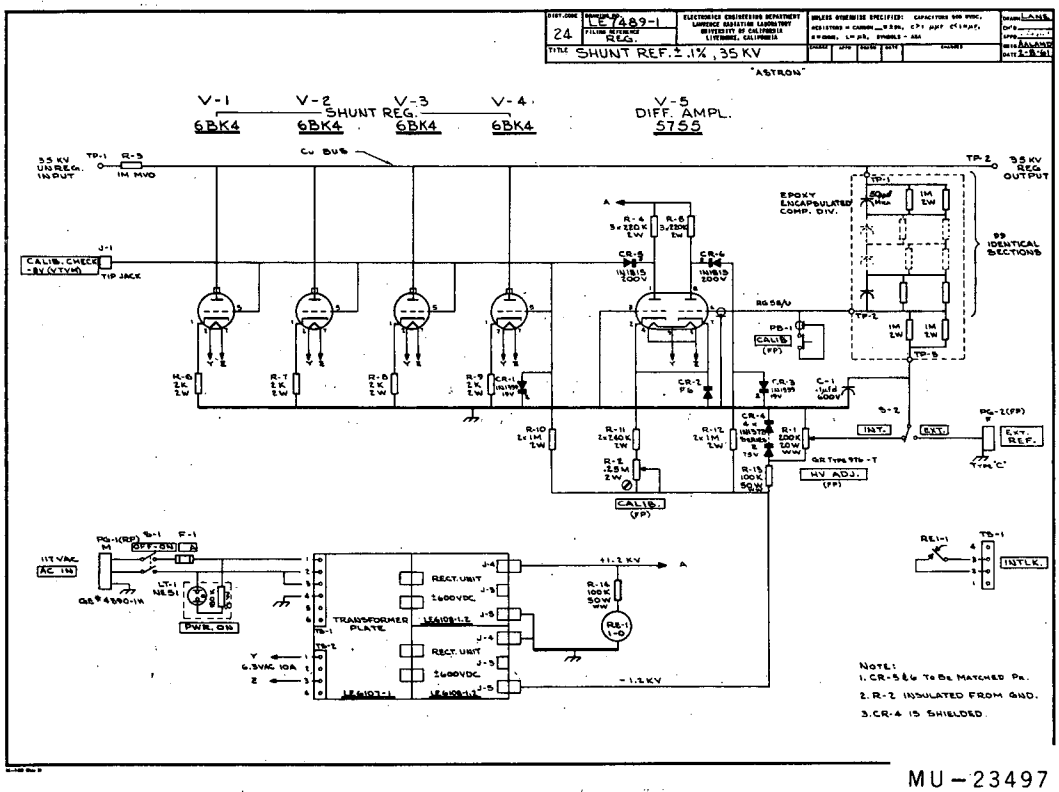

MU-23497

Fig. 25. Shunt Ref. ± .1%, 35 kv.

VII. TALKS AND PUBLICATIONS

Fifth Lockheed Symposium on Magnetohydrodynamics, Palo Alto, Calif., Dec. 16-17, 1960.

John M. Wilcox, Alan W. DeSilva, William S. Cooper III, and Forrest I. Boley, Experiments on Alfvén-Wave Propagation, UCRL-9482 Abst., Dec. 1960; and UCRL-9482, Nov. 1960.

1960 Winter Meeting of the American Physical Society, University of California, Berkeley, Calif., Dec. 29-31, 1960

R. F. Post and C. E. Taylor, An Effect of Thermal History on the Residual Resistivity of Sodium, UCRL-6181-T Abst., Oct. 11, 1960.

C. E. Taylor and R. F. Post, Transverse Magneto-Resistance Measurements on Large Sodium Conductors, UCRL-6182-T Abst., Oct. 20, 1960.

A. L. Hunt, C. C. Damm, and E. C. Popp, Attainment of Ultra-High Vacuum in an Unbaked System by Molybdenum Evaporation, UCRL-6183-T Abst., Oct. 12, 1960.

Second Nuclear Engineering Conference, Argonne National Laboratory, Chicago, Ill., Jan. 31, 1961

R. F. Post, Controlled Fusion Research, invited paper.

1961 Annual Meeting of the American Physical Society, New York, N. Y., Feb. 1-4, 1961

W. A. S. Lamb, Nuclear Measurements Related to Astrophysical Processes, invited paper.

H. P. Furth, Progress in High Magnetic Field Research, invited paper.

M. H. Mittleman and K. M. Watson, Scattering of Electrons by Heavy Atoms, UCRL-6216-T Abst., Nov. 7, 1960.

C. C. Chang and T. S. Lundgren, Equilibrium Solutions of Infinitely Long E-Layer in Astron, UCRL-6288-T Abst., January 1961.

General Atomic, Division of General Dynamics Corporation, San Diego, Calif., Colloquium held on Feb. 21, 1961

R. F. Post, Present Understanding of Plasma Confinement in a Mirror Machine, invited paper.

Publications

The Physical Review

R. E. Hester and W. A. S. Lamb, Radiative Capture of Protons in C^{13}, 121, 584 (1961).

The Physical Review Letters

R. F. Post and W. A. Perkins, Velocity Space Plasma Instabilities Observed in a Mirror Machine, 6, 85 (1961).

The Physics of Fluids

G. Ecker, Enhanced Interaction in the Positive Column, 4, 127 (1961).

Review of Scientific Instruments (Notes)

W. F. Cummins and D. R. Branum, A Stretcher for Short Counter Pulses, 31, 1247 (1960).

Information Division
sa

This report was prepared as an account of Government sponsored work. Neither the United States, nor the Commission, nor any person acting on behalf of the Commission:

A. Makes any warranty or representation, expressed or implied, with respect to the accuracy, completeness, or usefulness of the information contained in this report, or that the use of any information, apparatus, method, or process disclosed in this report may not infringe privately owned rights; or

B. Assumes any liabilities with respect to the use of, or for damages resulting from the use of any information, apparatus, method, or process disclosed in this report.

As used in the above, "person acting on behalf of the Commission" includes any employee or contractor of the Commission, or employee of such contractor, to the extent that such employee or contractor of the Commission, or employee of such contractor prepares, disseminates, or provides access to, any information pursuant to his employment or contract with the Commission, or his employment with such contractor.